LOUGHBOROUGH
UNIVERSITY OF TECHNOLOGY
LIBRARY

AUTHOR

SALIH O. F.

COPY NO. 081302/02

VOL NO. CLASS MARK

LOAN COPY

29 APR 93

27 JUN 1997

008 1302 02

TRANSFER FUNCTIONS OF THE 2-PHASE SERVOMOTOR

by

O. F. SALIH, B.Sc.

Master's Thesis
submitted in fulfilment of the requirements for
the award of Master of Science of Loughborough
University of Technology

March, 1976

Supervisor: Professor I. R. Smith

Department of Electronic and Electrical Engineering

© by O. F. Salih

Loughborough University
of Technology Library
Date July 1976
Class
Acc. No. 081302/02

ACKNOWLEDGEMENTS

I am deeply indebted to my supervisor Professor I. R. Smith for his help, guidance and valuable suggestions throughout this work.

I would also like to express my appreciation to Mrs J. M. Brown for her patient typing of this thesis.

I wish to acknowledge my gratitude to the Industrial Production Corporation of the Democratic Republic of the Sudan for its financial support of my studies at Loughborough University of Technology.

SYNOPSIS

One of the most common electromechanical positioning devices for low-power applications is the 2-phase servomotor, several different constructional forms being available.

When used in a control application, various transfer functions of the machine are important and these have been investigated by previous workers using analyses of varying validity. For example, in early studies, it was common to regard the speed-torque characteristics of the machine as straight lines, and also to neglect the electrical energy storage elements in comparison with those of the mechanical system. Quite sophisticated mathematical studies using, for example, symmetrical components, were based on these assumptions, but the results obtained are obviously highly suspect in view of the doubtful basis from which they are established. Experimental verification of the results of the analyses were confined to steady-state measurements, attention being devoted to establishing an equivalent circuit to provide steady-state characteristics. Recently, with the increasing use of powerful mathematical tools in engineering situations, several workers have attempted to obtain direct solutions of the non-linear equations characterising the operation of the servomotor. Thus, simulation and state transition methods, involving a step-by-step numerical solution, have attracted considerable interest. Although these approaches may provide useful numerical answers, they do not help in forming any understanding of the main factors affecting the transient performance of the machine. A recent paper used the complex convolution approach to provide analytical transfer functions, but unfortunately this

paper contains a fundamental error which completely invalidates the work. The same formal approach is followed in this thesis, with the complex convolution technique being used to find time-domain expressions for the variations in speed which follow step changes in either the torque or the magnitude or phase of the control-winding voltage. As in the previous work, attention is confined to the practically important range of speed much lower than synchronous speed. Results obtained from the analysis are compared with experimentally obtained results and with results provided by earlier analyses, and an assessment is made of the usefulness and limitations of the various techniques.

CONTENTS

page

LIST OF PRINCIPAL SYMBOLS

As several previous investigations are described during the course of this thesis, it is convenient to define the symbols used by earlier authors as they appear.

Only the more commonly occurring symbols are defined here.

ω = angular frequency of a.c. supply (rads/sec)

P = $\frac{d}{dt}$

t = time (seconds)

L = Laplace transform of

s = Laplace transform variable

$( )^*$ = conjugate

j = $\sqrt{-1}$

R_e = real part of

ρ_1 = number of pole pairs

R_1, R_2 = stator and rotor resistances (ohms)

L_1, L_2 = stator and rotor self inductances (henrys)

M = maximum mutual inductance between the stator and the rotor phase (henrys)

x_m = magnetising reactance, equal to ωM (ohms)

x_ℓ = leakage reactance (ohms)

R_1', L_1' = stator resistance (ohms) and inductance (henrys) at stall

Z_1' = magnitude of stall impedance of a stator phase, equal to $\sqrt{R_1'^2 + \omega^2 L_1'^2}$ (ohms)

$\phi\beta$ = equal to $\tan^{-1} \frac{\omega L_1'}{R_1'}$

T_1 = stator time constant at stall $(= \frac{L_1'}{R_1'})$ (seconds)

T_2 = rotor time constant $(= \frac{L_2}{R_2})$ (seconds)

$\omega_r(t)$ = angular speed of the rotor (rad.sec^{-1})

$\Delta\omega_r(t)$ = change in the angular speed of the rotor (rad.sec^{-1})

ω_s = synchronous speed (rad.sec^{-1})

$\theta_r(t)$ = angular displacement of rotor (radians)

v_D, v_Q = direct and quadrature axes stator phase voltages, taken as control and reference voltages

v_d, v_q = direct and quadrature axes rotor phase voltages

i_D, i_Q = currents flowing in control and refence stator phases

$i_{Do}(t)$, $i_{Qo}(t)$ = currents in control and reference windings at stall

i_d, i_q = direct and quadrature axes currents of the rotor windings

ϕ_D = angular phase shift between the two voltage signals

J = moment of inertia of armature and coupled load referred to rotor shaft (kg.m^2)

f = mechanical viscous-friction damping (Nm/rad.sec^{-1})

fa = average mechanical viscous-friction damping (Nm/rad.sec^{-1})

fe = effective damping when stalled (Nm/rad.sec^{-1})

T_m = mechanical time constant (= J/f) (seconds)

$T_\varepsilon(t)$ = electromagnetic torque (Nm)

$T_M(t)$ = load torque (Nm)

T_{MI} = step input load torque (Nm)

T_s = stall torque (Nm)

T_s' = modified stall torque to obtain effective damping (Nm)

S = slip

Z_p = input impedance per phase at angular frequency ω and slip S (ohms)

Z_n = input impedance per phase at angular frequency ω and slip 2-S (ohms

INTRODUCTION

In many control systems, a small 2-phase amplifier-driven servomotor is used as the output power unit. One phase winding of the motor (the reference winding) is connected to a constant voltage source, with the second phase (the control winding) fed with a signal obtained from the motor control loop. Control of the motor speed is achieved by changing either the magnitude or the phase of the control voltage. The 2-phase servomotor requires less associated electronic circuitry than any other polyphase machine, and this represents an important advantage in many practical applications. Since it does not require electrical connections, in the form of brushes and slip rings, friction is low and little maintenance is required.

Two-phase servo motors are extensively used in servomechanisms for instruments and computers, where relatively small torques are required. Large quantities of these machines are now used in military applications, where the environmental situations encountered may be extremely arduous. Servomotor loads are usually driven through a gear train, built integrally with the motor, which must be capable of accelerating the effective inertia against the frictional torque, at a sufficiently rapid rate to follow the input signal to the control winding. The servosystem designer must be able to provide an optimum motor for each application, and to specify the performance expected in each situation. For example, some medium-performance servomechanisms require a motor with high internal damping, since no additional external

damping can be added to the system, when the designer may become involved with magnetic and fluid damping.[1-6]

In machines in which a uniform torque and a minimum bearing friction are necessary, the drag-cup type of rotor construction is usually adopted, while viscous damping may be employed where relatively low output powers with high damping are required. However, where a continuously and rapidly varying input may be applied, and accurate following is essential, inertially damped servomotors are utilized.

In precision circuits requiring an accurate control of velocity, or the integration of an electrical signal, motor-generators are used. When a closed-loop feedback circuit is added, the machine may be used as a damping generator, producing an effective and flexible damping especially in high-gain positioning servomechanisms. However, the advantages of closed-loop operation are achieved at the expense of a higher initial cost, more complex wiring, greater physical length and a more sluggish response to changes in the input conditions.[5]

There are basically three types of servomotor rotor design, the squirrel cage, the drag-cup and the solid-iron rotor, although an additional rotating mass is often added to provide the required damping characteristics. The same type of stator assembly is equally suitable for all three types of rotor, with the 2-phase stator winding normally contained in closed slots in the stator punchings. To complete the magnetic circuit of the drag-cup arrangement, an additional central stationary cylinder is required, within the drag-cup and again made from steel punchings.

In some situations an inverted arrangement is adopted, with the rotor being mounted outside the central stator, although this makes no difference to any analysis made on the device.[3,5,7]

While the structure of a 2-phase servomotor is very simple, the phenomena that occur within it are very complicated, being combinations of electrical and mechanical effects. An adequate analysis of the behaviour of the motor is therefore difficult, although many attempts have been made to predict both the steady-state and the dynamic response. Since the 2-phase servomotor usually operates with unbalanced 2-phase voltages, the application of symmetrical component techniques is an obvious possibility. By this means, the currents and torques of the motor can be found, although in practice only for steady-state operation from sinusoidal input voltages obtained from a constant impedance source.[7-11] However, it has been suggested[11] that the application could be extended to nonsinusoidal input voltages, by the use of Fourier series and the principle of superposition. However, when a servomotor is used as a control-system element, it is frequently necessary to know various transfer functions of the device. Early studies of the transfer functions were a mixture of steady-state and transient considerations, and electrical transients in both the rotor and stator windings were frequently neglected. The torque/ speed curves of the machine were regarded as linear for different values of control voltage, and a very simple result was obtained.[12-14] Since the analyses based on the simple and idealized model of the motor, more detailed analyses have been presented. Several investigators

have interested themselves in the problem and they have approached it mainly theoretically, with no significant experimental work to verify their theoretically derived transfer functions. Based on different techniques for the approximate solution of the electrical (d, q) and mechanical (torque) differential equations of the machine several authors have produced motor transfer functions.[15-18] Nevertheless, in some of these approaches the transient and steady-state electrical conditions were considered as the same, which ensured that the result could not contain any electrical time constant and is therefore almost the same as that provided by the early idealized model .[15] However, some authors were convinced that an accurate transfer function must contain some electrical parameters, but they soon found that it was only practicable to obtain such a result under a restricted range of operating conditions. Thus, when the speed of the motor is low, such that rotational voltage terms within the motor can be neglected, the differential equations of the motor are in a form which allows an algebraic solution to be obtained. The equations contain a product-of-variable type nonlinearity, and in a recent paper [19] it has been shown how the complex convolution technique may be applied to these equations to provide an algebraic transfer function.

An alternative technique, which might be used to solve the full differential equations of the machine, is the state transition method, which is frequently encountered in modern control theory.[11,20] Although this provides a powerful tool for the numerical solution of linear differential equations, it is only suitable for a square-wave input signal because of the form of the numerical solution. Further, it does not allow the effects of the motor time constants

to be identified, and it is entirely unsuitable when the phase of the control voltage is varied.

Scope of the thesis:

The work described in this thesis is devoted to a study of the transfer functions of a 2-phase servomotor. A survey of the existing literature [1-19] reveals that although many authors have obtained transfer functions theoretically, most of the analyses are based on quite drastic idealising assumptions, which make the results of dubious reliability. It is shown in the thesis that a correct formulation of the problem leads to equations which it is entirely impracticable to solve in the general case. However, if the assumption is made that the speed of the motor is sufficiently low for the rotational voltage terms in the machine equations to be neglected a solution becomes possible, although even then the differential equations of the motor involve a product-of-variable type nonlinearity. When these equations are obtained complex convolution techniques[21-25] are used to find the Laplace transforms of the product-of-variable type nonlinearity. Transfer functions are thereby obtained relating speed to step changes in the magnitude and the phase of the control voltage and the load torque. Since the transfer function expressions are found to contain first-order poles only, a special form of complex convolution theorem[23], which does not require complex integration, is applied to find the necessary time-domain expressions in each case. The electrical and mechanical parameters arising in the transfer function are obtained from a series of tests on a 5 W, 50 Hz motor.

Mechanical viscous-friction damping is determined from the slope of the measured steady-state torque/speed characteristics of the motor [3], for various control voltages and the electrical parameters are obtained from no load and locked rotor tests.[26-28] These parameters are used to provide theoretical predictions of the transient response of the motor, for all the transfer functions derived. Similar predictions are made using earlier analyses [12,15] and a comparison is made with the experimental speed/time curves following step changes in either the magnitude or the phase of the control voltage and load torque of the test motor. An assessment is made of the usefulness and limitations of the various approaches.

CHAPTER I Constructional features of a Servomotor

The stator frames of a.c. servomotors are all constructed in essentially the same way, although motors made by different manufacturers have external differences and various mounting styles. Since the high acceleration conditions sometimes encountered require the rotor to be of small diameter, the stator coils are often machine wound in closed stator slots.

A closed slot construction has a higher inductance at low flux densities than a conventional stator, and sufficient control voltage to saturate the slot bridge must be applied before the motor will start. This reduces the accuracy of a servosystem at low voltage, although when the control voltage is high and the slot bridges are saturated the performance is little different from that of a machine with open stator slots. The closed slot construction reduces irregularities in the airgap, and by smoothing out the airgap flux density it reduces the stray losses of the motor. A further advantage is that the effective length of the airgap is reduced, which reduces the no load current and the stator copper losses. In general, closed slot motors run quietly and smoothly with a faster response and a higher efficiency than open slot motors. The stators have a standard distributed winding, suitably arranged to improve the spacial variation of flux density in the airgap and thereby to reduce harmonic effects in the motor and to minimise irregularities in the torque/speed curves[3,5].

Motors are designed for various supply frequencies and for different numbers of poles. The reference phase is usually a winding with two

leads fed directly from a fixed voltage source. The control phase may be a 2-lead winding similar to that of the reference winding, or a centre-tapped 3-lead winding, or even a 4-lead winding in two separate sections. In use, a servomotor often receives most of its power through the reference winding, and only a small portion of the total through the control winding. The control winding is often fed directly from the output of a control amplifier, although sometimes a transformer is interposed.

1.1 Rotor Construction

The different requirements for servomotors arising in various areas of application have resulted in three basically different forms of rotor design. These are the squirrel-cage rotor, the drag-cup rotor and the solid iron rotor.[3,5,7]

1.1.1 Squirrel-cage rotor

To obtain the form of torque-speed curve desirable in servomotors, a high rotor resistance is required, and in the typical squirrel-cage construction shown in Fig. (1.1) the diameter is small compared with the length. The low moment of inertia associated with the small diameter produces the high torque-to-inertia ratio required for a fast response at high speeds. The possible presence of slots on both sides of the airgap results in a magnetic slot locking phenomenon, particularly when operating at low speeds. This leads to a minimum break-away voltage which is defined as the minimum control voltage that will just cause rotation with rated voltage applied to the reference winding.[4] Slot locking effects and bearing friction clearly degrade the motor performance, and in a control application the system sensitivity will be reduced by the voltage that the error detecting device must develop to overcome their presence. The slot effect may be minimised by a proper choice of the

number of stator and rotor slots, and by using skewed rotor slots. Closed stator and rotor slots may also help, although their use will increase the effective airgap of the machine.

Skewing the slots of a squirrel-cage reduces the rotor sensitivity to the various stator harmonics that may be generated, and prevents the possibility of the rotor becoming locked. Skewing may either be used to cancel the effect of a particular harmonic, such as the third or fifth, or to minimise the effect of a significant group[6,7]. The third harmonic is often the most troublesome in small 2-phase servomotors, and to eliminate its effects the rotor needs to be designed with a skew of two 3rd-harmonic pole pitches. Elimination of the third harmonic will also normally reduce the fifth harmonic to a level with which the servomotor will have entirely acceptable characteristics. However, a little care is necessary in design, since too great a physical angle of skew may unduly increase both the leakage reactance and the resistance of the rotor and may lead to a significant loss of output torque. Increasing the number of poles in a servomotor leads to a decrease in the winding inductance and to an increase in the losses, and to overcome this it is necessary that the airgap should be as small as possible. In practice it may be as short as 0.025 mm, and it is clear that both manufacturing tolerances and the matching of the coefficients of expansion of the materials of the servomotor are important considerations. The best servomotors available today possess good mechanical rigidity and strength and/a very efficient cooling system for heat conduction from the windings. Advanced machining techniques and precision bearings have resulted in servomotors with as many as eight poles in a frame size of under one inch. Non-corrosive high-nickel magnetic alloys are substituted for the usual silicon steel, to prevent corrosion in the

narrow airgap. Class H insulations (such as Teflon and silicone varnishes) and bearing greases, have resulted in motors capable of operating at ambient temperature of 160°C. The majority of a.c. servomotors are under 100 watts in size and operate from either 50 Hz or 400 Hz supplies. Above 10 watts, cooling is provided by a separate motor-driven blower, included in the same stator housing as the control motor.[6]

1.1.2 The drag-cup type:

For some applications the squirrel-cage construction is inferior to other types of rotor configuration. For example, the drag-cup type servomotor is adopted when uniformity of developed torque with rotor angular position is important, and it also offers the advantages of freedom from cogging and low bearing friction, resulting from the absence of radial airgap forces on the nonmagnetic rotor. As shown in Fig (1.2) the stator of a drag-cup machine has the usual stator punchings and windings but the slotted rotor laminations of the squirrel-cage construction are replaced by a set of stationary iron-ring laminations that provide a low reluctance path for the magnetic flux. It may be regarded as derived from a squirrel-cage rotor, by removing the squirrel-cage assembly from the rotor slots and forming this into a drag-cup of nonmagnetic, but conducting material, such as copper or copper alloy. The drag-cup fits between the windings and a stationary iron cylinder, and the airgap is kept as small as possible by using very small clearances between the cup and the two adjacent surfaces. The drag-cup rotor has clearly a very low moment of inertia, and consequently the torque-to-inertia ratio compares favourably with that of the squirrel-cage rotor. The drag-cup has a very high sensitivity

to supply voltage changes, typical starting voltages being of the order of ½% rated voltage.[3] If aluminium is considered for use as the cup material, then since the conductivity of aluminium is lower than that of copper, a greater cup thickness is required. This effectively results in a larger airgap and higher stator copper losses, so that in practice copper is always used as the basic rotor material. Manufacturing tolerances limit the smallest gap length which can be employed to about 0.03 inches, and due to this restriction small drag-cup machines have a low ratio of torque developed to power input.[5-7]

1.1.3 The solid iron rotor:

The solid iron rotor is similar in external appearance to a squirrel cage rotor, with a slender and non-slotted cylindrical rotor. Its characteristics are a compromise between the high performance of the squirrel cage rotor and the uniformity of the drag-cup rotor. The iron used in the rotor must have good magnetic and electrical properties, so that sufficient rotor current can be produced. Since there are no slots, there is no cogging effect, and although some rotor nonuniformity will exist due to grain effects in the iron, this can be minimised by careful annealing. Since the structure is simple, the solid-rotor motor is strong mechanically, and it is suitable for applications involving frequent starting and stopping operations.

Space harmonics can be generated in small-size servomotors having a limited stator-winding distribution and a large number of poles, and in constrast to the skewed squirrel-cage rotor, these will produce losses in the solid-iron rotor. Moreover, the pattern of the rotor flux distribution will also result in somewhat less developed torque.

Although the overall torque per watt input may be 20% less than that for the squirrel-cage, this is unimportant in comparison with the gain in smoothness of performance, low starting voltage and reduced manufacturing costs.[5]

Although the magnetic and electric circuits of a squirrel-cage rotor can be clearly separated for analytical purposes, no simple separation is possible in the case of the solid iron rotor. A full analysis of a machine with this type of rotor is an extremely complicated undertaking.

1.2 Servomotor damping:

The measured torque/speed characteristics of a servomotor, supplied by a fixed control voltage, shows a decrease of torque with speed, as if a viscous drag was applied to the shaft. For successful operation of a control system the motor must respond quickly to changes in the control voltage, and it must not oscillate or overshoot.[1-2] The required rapid response is achieved by a high torque-to-inertia ratio, and the overshooting is minimised and stability achieved by the use of different forms of retarding torques that increase with rotational speed

Usually, a damping torque exerts no effect at standstill, and a motor will have a high initial acceleration. However, as the speed rises and the damping torque gets progressively higher, the acceleration correspondingly decreases. If the control phase voltage is reduced, the stalled torque decreases faster than does the no-load speed, so that the internal damping coefficient of the motor is also reduced and the system is inherently less stable.

If the internal damping of a motor is inadequate for the stabilization of a closed loop, additional viscous friction can be added. A vane on

the motor shaft rotating in a viscous fluid or a drag-cup rotating in a magnetic field can be used for this purpose. Although the driven load can sometimes supply viscous damping, in many applications the gear arrangement is such that the contribution of the load to the system dynamics is negligible.

While viscous friction that varies linearly with speed is most desirable, cost factors sometimes dictate the use of nonlinear coulomb friction which is independent of the speed. Typically this is obtained through the pressure of an oiled felt pad on a metal braking surface on the motor shaft.

Damping is also sometimes obtained by feeding a direct current proportional to the system error through the motor control winding, but although this is both effective and cheap it results in a considerable reduction in both torque and efficiency.

Dampers that rely on the properties of a fluid are obviously sensitive to temperature variation, although materials enabling satisfactory operation over a temperature range of 50^{o}C are now available. Magnetic damper arrangements are inherently insensitive to temperature changes, although second-order effects may result from changes in the drag-cup conductivity.

All of the above damping methods add viscous or coulomb frictional drag to the internal damping characteristics of the machine. Although these methods are effective, they subtract from either the speed or the available shaft power. In applications requiring this reduction to be minimal, inertially or tachometer-damped servomotors are used.[3-7]

1.2.1 Inertial dampers

An inertially-damped motor has a double shaft extension, with one of these carrying a special drag-cup assembly. As shown in Fig (1.3), the end of one of the extensions carries a "frictionless" bearing, on which is mounted a ring-shaped permanent magnet with the drag cup located in an annular ring cut in the magnet.

During steady-state operation, interaction between the magnet and the drag cup causes the magnet to rotate at a speed slightly below that of the motor, and there is very little reduction in the speed of the motor. During a transient condition increased viscous damping is generated as a result of the increased relative motion between the drag-cup and the relatively massive structure of the magnet. Although inertial damping of the type shown by Fig (1.3) is superior to viscous damping in not affecting the steady-state performance of the motor, it does introduce substantial errors during acceleration, and it is utilised mainly for servomechanisms in which the acceleration conditions are not very arduous.

1.2.2 Tachometer damping

An alternative to inertial damping is provided by tachometer damping, in which the drag cup and the flywheel of Fig (1.3) are replaced by an additional machine. This takes the form of a permanent magnet generator, constructed on the same shaft as the servomotor, and used to provide a voltage proportional to the motor speed for feeding back to the input of the control-winding amplifier. By reducing the control amplifier input by an amount proportional to the speed, the torque developed in the motor is reduced by an amount also proportional to the

speed. Although this is precisely the same result as is achieved using viscous damping, the tachometer enables almost the full power capacity of the servomotor to be utilized. Although tachometer damping results in a sluggish response, and is costly, it is used extensively in high-gain positioning servomechanisms.

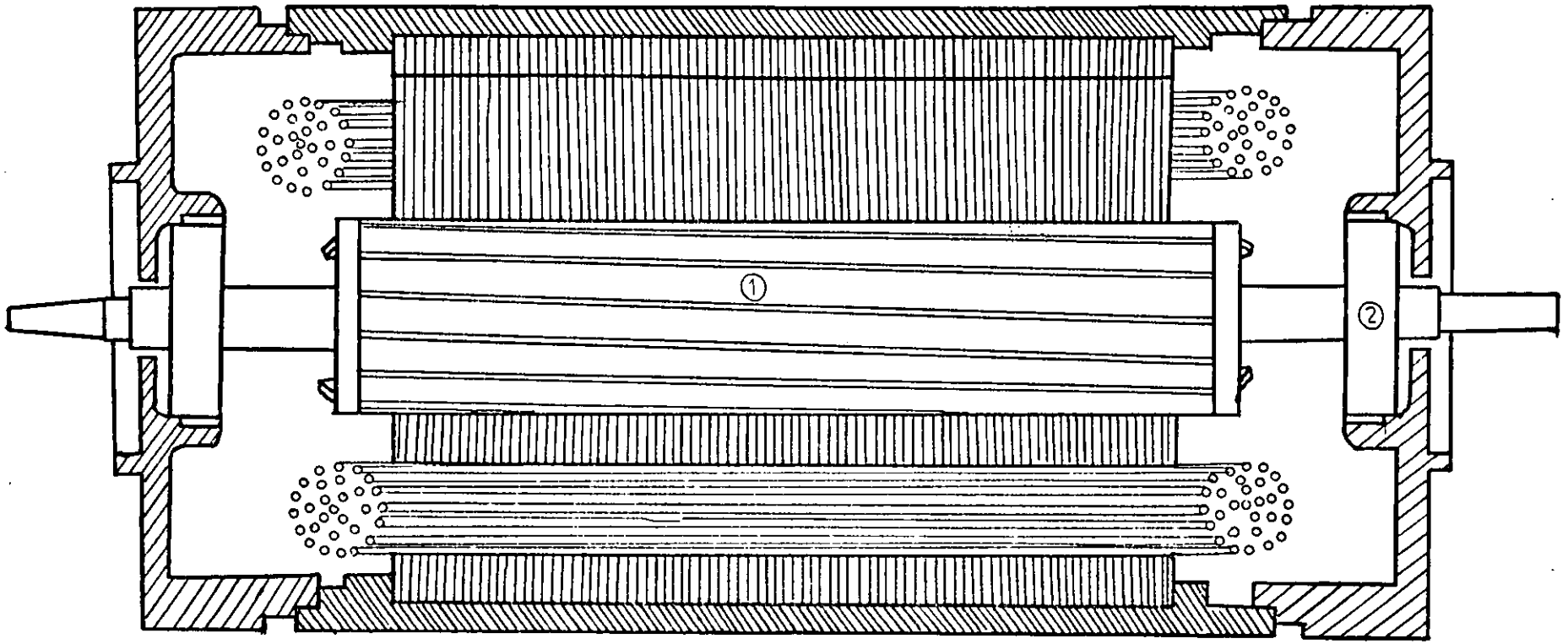

Fig.1.1 Cut away view of a.c. squirrel-cage rotor servomotor

① Long slim design and skewed rotor slots

② Ball bearing

Fig. 1.2. Internal construction of a drag-cup type servomotor

① Drag cup ② Central stator core ③ Outer stator core ④ Stator winding ⑤ Shaft
⑥ Bearing retainer ⑦ End bell ⑧ Motor frame ⑨ Retaining nut

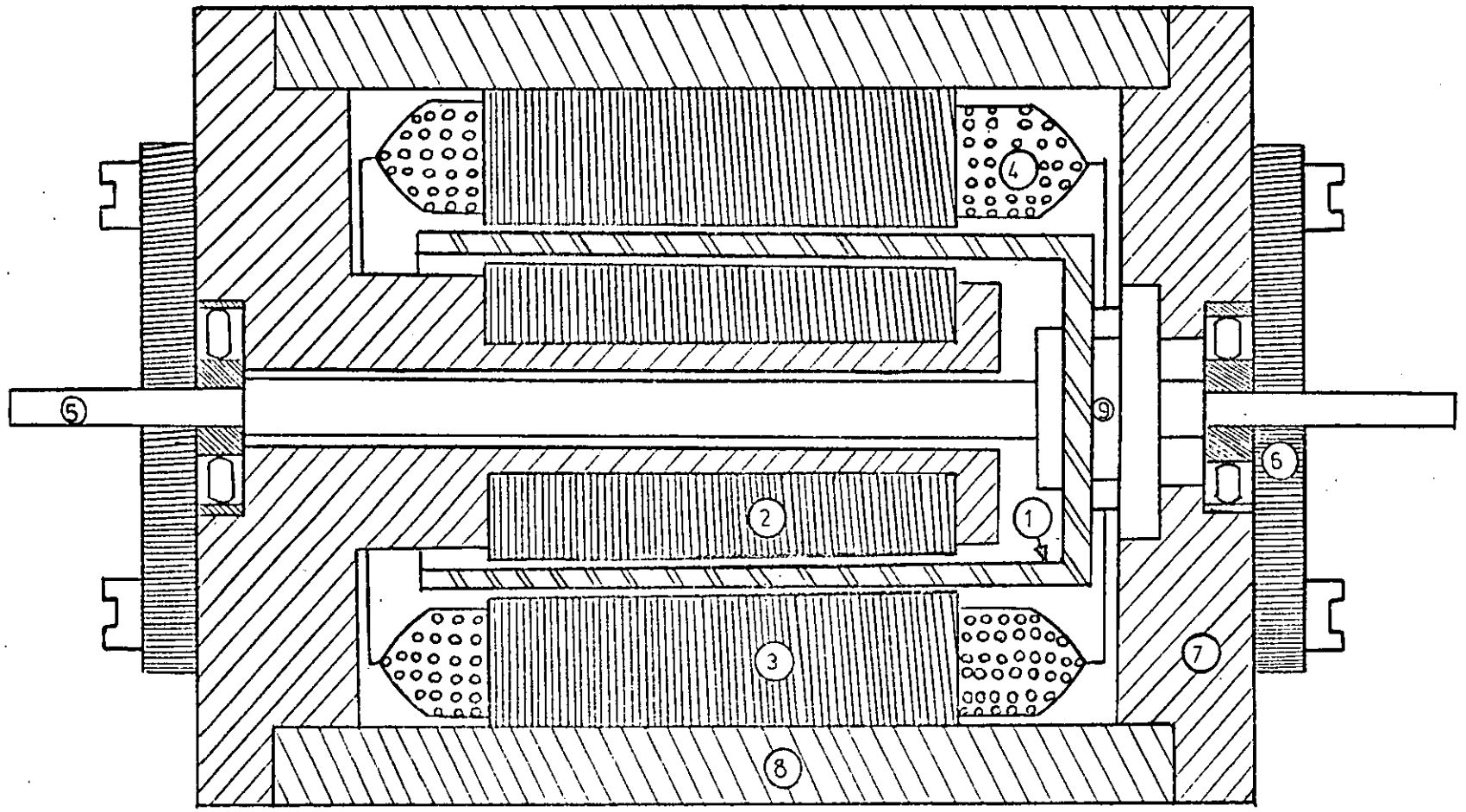

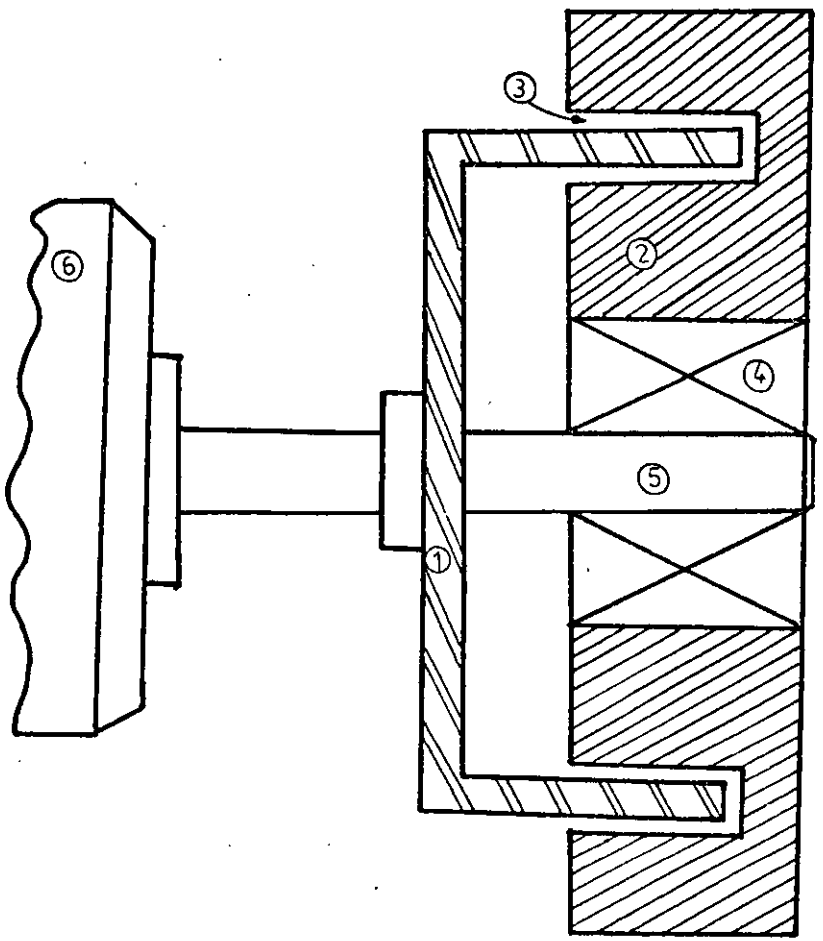

Fig.1.3 Viscous coupled, flywheel oscillation damper

① Drag cup rigidly connected to the motor ② Flywheel magnet ③ Air gap

④ High quality ball bearing ⑤ Motor shaft ⑥ Servomotor

Chapter 2: Steady-state calculation of servomotor performance

2.1 Symmetrical component method

As explained in the introduction, a 2-phase servomotor usually contains two windings in quadrature on the stator, with the rotor being often of the squirrel-cage type. One phase winding is fed from a reference a.c. voltage and the other from a variable control voltage.

The operation of a servomotor differs from that of a conventional induction motor, primarily because the voltages supplied do not usually constitute a balanced polyphase set. During steady-state operation the behaviour may be investigated using the method of symmetrical components [7-11]. Two different situations were considered by Koopman[8]. In the first of these both sources were of negligible impedance, but in the second the control source was assumed to have a resistance approximately equal to the motor impedance.

Generally, the unbalanced supply voltages are converted into two sets of balanced 2-phase voltages of opposite phase sequence, a positive-sequence set and a negative-sequence set. The positive-sequence set produces only positive-sequence currents and the negative-sequence set only negative-sequence currents. The total current and torque are found by the principle of superposition. Alternatively, the servomotor can be considered as equivalent to a system consisting of two identical motors mechanically coupled, one supplied by the positive-sequence voltages and the other by the negative-sequence voltages.

In practice the principle of symmetrical component analysis has been successful in providing theoretical results which are in good agreement with experimental observations, for machines operating with quite widely varying degrees of unbalance [8,10].

2.1.1 2-phase symmetrical component

An unbalanced 2-phase system of voltages is essentially a special case of the unbalanced but symmetrical 4-phase system[9]. The unbalanced phase voltages $\overline{V}_A$, $\overline{V}_B$, $\overline{V}_C$ and $\overline{V}_D$ of the 4-phase system can be expressed mathematically as

$$\begin{vmatrix} \overline{V}_A \\ \overline{V}_B \\ \overline{V}_C \\ \overline{V}_D \end{vmatrix} = \begin{vmatrix} 1 & 1 & 1 & 1 \\ -j & j & -1 & 1 \\ -1 & -1 & 1 & 1 \\ j & -j & -1 & 1 \end{vmatrix} \cdot \begin{vmatrix} \overline{V}_{a1} \\ \overline{V}_{a2} \\ \overline{V}_{a3} \\ \overline{V}_o \end{vmatrix} \qquad \ldots (2.1)$$

where

$\overline{V}_{a1}$ = balanced positive-sequence component

$\overline{V}_{a2}$ = balanced negative-sequence component

$\overline{V}_{a3}$ = single-phase component $j = \sqrt{-1}$

$\overline{V}_o$ = zero-sequence component

but in the unbalanced but symmetrical 2-phase case, both $\overline{V}_{a3}$ and $\overline{V}_o$ are zero, since two sets of balanced voltages are sufficient to define the unbalanced 2-phase supply voltages. Thus, in the case of the servomotor, the reference and control voltages v_r and v_c are resolved into positive and negative sequence components v_{r1} and v_{r2} by

$$v_{r1} = \frac{1}{2}(v_r + jv_c) \qquad \ldots (2.2)$$

$$v_{r2} = \frac{1}{2}(v_r - jv_c) \qquad \ldots (2.3)$$

2.1.2 Determination of net torque

When the voltages v_{r1} and v_{r2} are applied to two identical motors on a common shaft, the resultant torque can be calculated from the equivalent circuit of Fig. (4.1c), noting that when the positive-sequence motor has a slip S, that of the negative-sequence motor is 2-S. It is normally assumed that the two windings are identical, and hence that the equivalent circuits for positive and negative sequence operation differ only in the value of the slip. However, if the windings are not identical the use of a suitable transformer can bring about a balanced condition.

When the stator windings are not electrically balanced, it is assumed that the windings of the motor each produce a sinusoidal distribution of magnetomotive force. Thus, if $K_{\omega r}$ and $K_{\omega c}$ are the winding factors of the reference and control windings respectively, and N_r and N_c are the corresponding numbers of turns, then $I_r.K_{\omega r}.N_r$ and $I_c.K_{\omega c}.N_c$ are the ampere-turns of the main and control windings.

Assuming uniform permeance in the magnetic circuit, the flux waves produced by the two windings will be equal when

$$\frac{I_r}{I_c} = \frac{K_{\omega c} \cdot N_c}{K_{\omega r} \cdot N_r} = \bar{c} \qquad \ldots (2.4)$$

or $v_c^2 = c^2 v_r^2$. When an ideal transformer of turns ratio c is introduced before the control winding, and equal voltages are applied to both windings, $v_c = c\, v_r$ and $I_c = cI_r$, which satisfies equation (2.4). Usually taking c as the ratio of the rated voltages of the two windings is adequate. The servomotor/transformer combination may then be regarded as having the terminal characteristics of a motor with balanced stator windings.

The airgap power associated with the positive-sequence rotating field is

$$P_{g1} = 2 |I_{21}|^2 \frac{R_2}{S} \quad \ldots (2.5)$$

and that with the negative-sequence field is

$$P_{g2} = 2 |I_{22}|^2 \frac{R_2}{2-S} \quad \ldots (2.6)$$

so that the resultant torque is

$$T_\varepsilon = 2 R_2 \left(\frac{|I_{21}|^2}{S} - \frac{|I_{22}|^2}{2-S} \right) . \frac{1}{\omega} \text{ Nm} \quad \ldots (2.7)$$

where

ω = synchronous angular frequency (rad.sec^{-1})

I_{21} = positive-sequence current in the rotor

I_{22} = negative-sequence current in the rotor

With positive- and negative-sequence input impedances of Z_p, Z_n the corresponding sequence currents in the reference phase are:

$$I_{r1} = \frac{v_{r1}}{Z_p} \quad \ldots (2.8)$$

$$I_{r2} = \frac{v_{r2}}{Z_n} \quad \ldots (2.9)$$

where

$$Z_p = R_1 + \frac{\omega^2 \frac{M^2}{R_2} \cdot \frac{1}{S}}{\frac{1}{S^2} + \frac{\omega^2 L_2}{R_2^2}} + j\omega \left(L_1 - \frac{\omega^3 \frac{M^2}{R_2} \cdot \frac{L_2}{R_2}}{\frac{1}{S^2} + \frac{\omega^2 L_2^2}{R_2^2}} \right) \quad \ldots (2.10)$$

and Z_n is obtained by replacing S in equation (2.10) by (2-S). The rotor currents produced by the action of the positive and negative-sequence rotating fields are

$$I_{21} = I_{r1} \cdot \frac{Z(S)}{\frac{R_2}{S} + jx_2} \qquad \ldots (2.11)$$

$$I_{22} = I_{r2} \cdot \frac{Z(2-S)}{\frac{R_2}{(2-S)} + jx_2} \qquad \ldots (2.12)$$

where

$$Z(S) = \frac{jx_m \left(\frac{R_2}{S} + jx_2 \right)}{R_2/S + j(x_2 + x_m)}$$

and $Z(2-S)$ is obtained by replacing S by (2-S) in the expression for $Z(S)$.

$$x_m = \omega M$$

$$x_2 = \omega(L_2 - M)$$

On substituting for I_{r1} and I_{r2} from equations (2.8) and (2.9), $|I_{21}|$ and $|I_{22}|$ become

$$|I_{21}| = \left| \frac{\nu_{r1}}{Z_p} \cdot \frac{Z(S)}{\frac{R_2}{S} + jx_2} \right| \qquad \ldots (2.13)$$

$$|I_{22}| = \left| \frac{\nu_{r2}}{Z_n} \cdot \frac{Z(2-S)}{\frac{R_2}{2-S} + jx_2} \right| \qquad \ldots (2.14)$$

leading to

$$P_{g1} = 2 \left| \frac{\nu_{r1}}{Z_p} \cdot \frac{Z(S)}{\frac{R_2}{S} + jx_2} \right|^2 \cdot \frac{R_2}{S} \qquad \ldots (2.15)$$

$$P_{g2} = 2 \left| \frac{\nu_{r2}}{Z_n} \cdot \frac{Z(2-S)}{\frac{R_2}{2-S} + jx_2} \right|^2 \cdot \frac{R_2}{2-S} \qquad \ldots (2.16)$$

On the other hand, when the motor is operated with balanced 2-phase voltages (i.e. $v_r = v_c \angle -90^\circ$) the phase current is

$$I_r = \frac{v_r}{Z_p} \qquad \ldots (2.17)$$

the rotor current is

$$I_2 = I_r \cdot \frac{Z(S)}{\frac{R_2}{S} + jx_2} \qquad \ldots (2.18)$$

and the gap power is

$$P_g(S) = 2 |I_2|^2 \cdot \frac{R_2}{S} \qquad \ldots (2.19)$$

$$= 2 \left| \frac{v_r}{Z_p} \cdot \frac{Z(S)}{\frac{R_2}{S} + jx_2} \right|^2 \cdot \frac{R_2}{S} \qquad \ldots (2.20)$$

As before, the gap power for operation at a slip 2-S is obtained by replacing S by (2-S) in equation (2.20). By formulating the ratio of equation (2.15) to equation (2.20),

$$P_{g1} = \left| \frac{v_{r1}}{v_r} \right|^2 \cdot P_g(S)$$

and by proceeding in a similar manner

$$P_{g2} = \left| \frac{v_{r2}}{v_r} \right|^2 \cdot P_g(2 - S)$$

the net gap power is obtained as

$$P_{net} = P_{g1} - P_{g2}$$

or

$$P_{net} = \left| \frac{v_{r1}}{v_r} \right|^2 \cdot P_g(S) - \left| \frac{v_{r2}}{v_r} \right|^2 P_g(2 - S) \qquad \ldots (2.21)$$

Generally, torque is expressed in terms of power by

$$T_\varepsilon = \frac{P}{\omega} \quad \text{Nm.}$$

or from (2.21) as

$$T_\varepsilon = T_{Eb}(S) \cdot \left|\frac{\nu_{r1}}{\nu_r}\right|^2 - T_{Eb}(2 - S) \cdot \left|\frac{\nu_{r2}}{\nu_r}\right|^2 \quad \ldots (2.22)$$

where

$T_{Eb}(S)$ and $T_{Eb}(2-S)$ are the torques for balanced operation at rated voltage and slips of S and 2-S. Thus, the resultant torque at any slip and any condition of unbalanced voltages may be obtained in terms of that for balanced operation at rated voltage. Hence, using equation (2.22), the torque/speed characteristics for various values of the control winding voltage can be determined without resorting to the equivalent circuit.

2.1.3 Electromagnetic torque expression when the angle between the control and reference voltages is ϕ°.

The torque produced by the servomotor is different in direction depending on whether the control voltage leads or lags the reference voltage. In equation (2.22) we need to find the positive and negative sequence voltages ν_{r1} and ν_{r2} to establish the general expression for this torque.

(1) If ν_c lags ν_r by ϕ° ($|\phi| < 90^\circ$) then from symmetrical component analysis.

$$\nu_c = \nu_{c1} + \nu_{c2} \quad \ldots (2.23)$$

$$\nu_r = \nu_{r1} + \nu_{r2} \quad \ldots (2.24)$$

Assuming that

$$\nu_c = \nu_r \; k \angle -\phi \qquad \ldots (2.25)$$

then

$$\nu_{c1} = -j\nu_{r1} \qquad \ldots (2.26)$$

$$\nu_{c2} = j\nu_{r2} \qquad \ldots (2.27)$$

From equations (2.23), (2.24), (2.26) and (2.27)

$$\nu_{r1} = \frac{1}{2} (\nu_r + j\nu_c)$$

and using equation (2.25)

$$\nu_{r1} = \frac{\nu_r}{2} (1 + jk \angle -\phi)$$

$$\nu_{r1} = \frac{\nu_r}{2} (1 + k \angle 90 - \phi)$$

$$\nu_{r1} = \frac{\nu_r}{2} (1 + k(\sin\phi + j \cos\phi)) \qquad \ldots (2.28)$$

Similarly, it can be shown that

$$\nu_{r2} = \frac{\nu_r}{2} (1 - k \angle 90 - \phi)$$

$$\nu_{r2} = \frac{\nu_r}{2} (1 - k (\sin\phi + j \cos\phi)) \qquad \ldots (2.29)$$

From equations (2.28) and (2.29) it now follows that

$$\left| \frac{\nu_{r1}}{\nu_r} \right|^2 = \frac{1}{4} (1 + 2 k \sin\phi + k^2) \qquad \ldots (2.30)$$

and

$$\left| \frac{\nu_{r2}}{\nu_r} \right|^2 = \frac{1}{4} (1 - 2k \sin\phi + k^2)$$

substituting in equation (2.22)

$$T_\varepsilon = \frac{1}{4} (T_{Eb}(S) \cdot (1 + 2k \sin\phi + k^2) - T_{Eb}(2 - S) \cdot (1 - 2k \sin\phi + k^2)) \qquad \ldots (2.31)$$

when k = 1

$$T_{\varepsilon} = \frac{1}{2} (T_{Eb}(S).(1 + \sin\phi) - T_{Eb}(2-S).(1 - \sin\phi)) \quad \ldots (2.32)$$

(2) If ν_c leads ν_r by ϕ^{o}, then

$$\nu_{c1} = j\nu_{r1} \quad \ldots (2.33)$$

$$\nu_{c2} = -j\nu_{r2} \quad \ldots (2.34)$$

$$\nu_c = k\,\nu_r \angle\phi \quad \ldots (2.35)$$

and if $|\phi| < 90$

$$\nu_{r1} = \frac{\nu_r}{2} (1 - k \angle 90 + \phi)$$

$$\nu_{r1} = \frac{\nu_r}{2} (1 + k(\sin\phi - j\cos\phi)) \quad \ldots (2.36)$$

and similarly

$$\nu_{r2} = \frac{\nu_r}{2} (1 - k (\sin\phi - j\cos\phi)) \quad \ldots (2.37)$$

from which

$$\left|\frac{\nu_{r1}}{\nu_r}\right|^2 = \frac{1}{4} (1 + 2k \sin\phi + k^2)$$

and

$$\left|\frac{\nu_{r2}}{\nu_r}\right|^2 = \frac{1}{4} (1 - 2 k \sin\phi + k^2)$$

2.1.4 Analysis of the machine performance for finite impedance source

The control voltage is applied to the control winding through a series resistance approximately equal to the average magnitude of the motor impedance[8]. This is equivalent to supplying the winding from a power amplifier matched to the motor winding through an impedance matching transformer. The control voltage v_c is represented in terms of the voltage drop across the series impedance $I_c Z_c$ and the source voltage E_c as

$$E_c = v_c + I_c Z_c \qquad \ldots (2.38)$$

If the control voltage leads the reference voltage, rotation will be in one direction, if it lags then it will be in the opposite direction as before. Koopman assumed that

$$E_c = - jk\, v_r \qquad \ldots (2.39)$$

where

$$k = \left| \frac{E_c}{v_r} \right|$$

and is chosen according to the requirements of the control system.

From equations (2.23), (2.26) and (2.27)

$$I_c = -j \frac{v_{r1}}{z_n} + j \frac{v_{r2}}{z_p} \qquad \ldots (2.40)$$

Using equation (2.39), (2.40) and (2.38), the control and reference voltages are given as

$$v_c = - jkv_r - (-j \frac{v_{r1}}{z_p} + j \frac{v_{r2}}{z_n}) Z_c \quad \ldots (2.41)$$

From equations (2.2) and (2.41)

$$2 v_{r1} = v_r + j(-jkv_r + (j \frac{v_{r1}}{z_p} - j\frac{v_{r2}}{z_n}) Z_c) \qquad \ldots (2.42)$$

and from equations (2.3) and (2.41)

$$2v_{r2} = v_r - j(-jkv_r + (j \frac{v_{r1}}{z_p} - j \frac{v_{r2}}{z_n}) Z_c) \qquad \ldots (2.43)$$

so that

$$v_{r1} = \frac{1}{2} \cdot v_r \cdot \frac{1 + k + \frac{Z_c}{Z_n}}{1 + \frac{Z_c}{2}\left(\frac{1}{Z_p} + \frac{1}{Z_n}\right)} \quad \ldots (2.44)$$

$$v_{r2} = \frac{1}{2} \cdot v_r \cdot \frac{1 - k + \frac{Z_c}{Z_p}}{1 + \frac{Z_c}{2}\left(\frac{1}{Z_p} + \frac{1}{Z_n}\right)} \quad \ldots (2.45)$$

The expressions for v_{r1} and v_{r2} can be found for all control voltages, and the corresponding torque/speed characteristics can be computed using equation (2.22).

2.1.5 Analysis of the machine performance for low impedance source

When the control voltage is applied directly to the control winding, Z_c becomes zero in equation (2.44) and (2.45), i.e.

$$v_{r1} = \frac{v_r}{2}(1 + k) \quad \ldots (2.46)$$

$$v_{r2} = \frac{v_r}{2}(1 - k) \quad \ldots (2.47)$$

and the analysis continues as before.

2.1.6 Theoretical and measured steady-state characteristics

Many authors[3,4,8-11] have used the analytical approach described above to investigate the steady-state performance of a 2-phase servomotor. Although their analyses differ in detail, they originate from the same basic principle and provide fundamentally the same results. The principle concern of the authors has been the steady-state torque/speed

characteristics of the machine, and the validity of their analyses has been established experimentally by many workers. Reasonable agreement has been obtained between the theoretical and measured results when the supply voltages are both balanced and unbalanced. Advance reference to Fig. (5.5) shows the nonlinear characteristics of a 5 W motor, and these are typical of many similar results presented in the literature. The general shape of these curves should be kept in mind when the idealizing assumptions given in section (3.1.1) are read.

2.2 State transition method

The work described in this thesis is restricted to machines fed with sinusoidal reference and control voltages, and the analysis of the performance when the motor is driven by nonsinusoidal voltages is beyond the scope of the present contribution. The only nonsinusoidal voltage supply likely to be encountered in practice is rectangular in form, as provided by the output of many inverter circuits. This situation is mathematically more complex than that of the sine-wave supply, and one author[11] has used the state-transition technique as the basis of an analytical method for calculating the performance characteristics. The state-transition technique is used commonly in modern control theory to solve linear differential equations, and it has been found to be especially useful in the analysis of discrete time systems.

In applying the state-transition technique to the servomotor, the d-q axis differential equations of the stator and the rotor are first

transformed into instantaneous symmetrical component form. In this reference frame the positive and negative-sequence quantities are conjugate pairs, so that only the positive-sequence set is needed to form the state vector of the state-transition equation. The net effect of the voltages fed to the servomotor during a supply cycle is conveniently divided into four stages, transition between the stages occurring at 90° intervals, as either of the supply voltages changes in direction. Each of the 90° intervals is regarded as a sampling period, and the symmetrical components of the motor voltages are obtained during these periods on the assumption that the speed remains constant. The differential equations of the motor are represented in Z-transform notation, which enables the currents and torque during the sampling instants to be calculated.

Although the theory has been worked out fully, predictions of the motor performance have only been made for one sampling period, and no attempt at all has been made at experimental verification of the analysis.

CHAPTER 3. EARLY ANALYSES OF THE TRANSFER FUNCTION OF 2-PHASE SERVOMOTORS

The transfer function of a control system element is defined as the ratio of the output response to the input excitation. If the output is linearly related to the input, the transfer function is normally expressed as the ratio of the Laplace transform of the output to that of the input, with the initial conditions assumed zero.

The use of the Laplace transform provides a convenient method of handling in a systematic algebraic manner the differential equations of the element, and the transfer function of the element is the same for both open and closed loop operation. However, the transfer function of different control elements can have different dimensions (e.g. the output of a position transducer may be in volts and the input in radians, whereas the output of a sensitive servocontrol valve is in m^3/sec and the input in radians) or they may be dimensionless. As a transfer function is the ratio of two Laplace transforms, it will be an algebraic function of the Laplace complex variable s. The symbol G(s) is normally used in control theory to denote the transfer function of a forward path, and the symbol H(s) that of a feedback path. Since the conditions for the validity of a transfer function stem from its definition as the ratio of the Laplace transforms of initially inert system, a system not directly transformable has no valid transfer function. Although strictly this eliminates systems

with non-constant coefficients, such as nonlinear systems, various techniques (such as the use of the describing function) enable approximate results to be obtained for certain nonlinear situations. In many instances, the generalised transfer function of a nonlinear element is composed of a frequency-independent non-linear term, which is the describing function of the element, followed by a linear term in the form of a low-pass filter. Using the conditions for the limit-cycle oscillation of the system, the describing function is modified in terms of the linear filter, and various convenient graphical techniques are available to enable such relations to be used in analysis and design.

The input/output (or excitation/response) relationships of many systems and system elements will contain product-of-variable type nonlinearities, and this is found to be the case in a rigorous analysis of the 2-phase servomotor. All early analyses neglected this effect, but it is clearly necessary to overcome this and include it when a rigorous analysis is attempted.

3.1 Comparison of different early approaches to the machine transfer function

Among many authors who have studied the behaviour, properties and characteristics of the 2-phase servomotor, several have considered the transient response and have attempted to establish valid transfer functions for the machine. The following sections provide a summary

of the different approaches which have been followed, and attempt to show the need for the rigorous analysis of Chapter 4.

3.1.1 Analyses based on a simplified model of the servomotor

The most elementary approach to the transfer function of the 2-phase servomotor assumes linear torque/speed characteristics, equally spaced for equal changes in the control voltage and parallel [12] as shown in Fig (3.1). A further assumption involved is that both the stator and the rotor windings have negligible time constants, so that the control current is proportional to the error signal. During the analysis, torque is taken as a function of both speed and control voltage, and only the first terms in a Taylor expansion for the electromechanical torque are retained:

$$\text{i.e.} \quad dT_E = K_1 \, d\omega_r + K_2 \, dV_c \qquad \ldots.(3.1)$$

where

K_1 = (change in torque)/(change in speed) for constant input signal

K_2 = (change in torque/(change in signal voltage) for constant speed

V_c = control voltage

To obtain the transfer function, equation (3.1) is expressed in Laplace transform notation, and equated to the dynamic equation for the mechanical system, also expressed in Laplace transform notation, i.e.

$$T_M = Js^2 \theta_r(s) + fs \, \theta_r(s) \qquad \ldots. \ (3.2)$$

where θ_r is angular displacement of the rotor in radians, and J and f

are respectively the moment of inertia and the coefficient of viscous friction damping. By this means, the transfer function between the output shaft position and the control voltage is obtained as

$$G_1(s) = \frac{\theta_r(s)}{V_c(s)} = \frac{K_3}{s(1 + sT_m)} \quad \ldots\ (3.3)$$

where $K_3 = \frac{K_2}{f - K_1}$

and $T_m = \frac{J}{f - K_1}$

In a second and quite similar elementary study, it was assumed that the control winding of the motor was energised from a power source that provided a control current proportional to an error signal ε [13]. Thus

$$G_2(s) = \frac{\theta_r(s)}{\varepsilon(s)} = \frac{K_v}{s(1 + T_m s)} \quad \ldots\ (3.4)$$

where

$K_v = \frac{\partial \omega_r}{\partial I_c} \cdot \frac{\partial I_c}{\partial \varepsilon}$

I_c = control phase current

$T_m = J/\frac{\partial T}{\partial \omega_r} = J/K_1$

= mechanical time constant at no load.

The above transfer functions, $G_1(s)$ and $G_2(s)$, indicate that the frequency response of a servomotor contains only the single time constant of the mechanical system, and that the phase shift of 90° at low frequency increases to 180° as the frequency is raised.

To verify this, Hopkins [15] obtained experimental transient responses resulting from various step input amplitudes applied to the control winding, with various values of reference field voltage. The response was drawn as log (final velocity - instantaneous velocity) versus time and a straight line would be expected. However, considerable curvature was observed in the early-time domain, and this was accounted for as the result of a second exponential term, caused by the electrical time delays in the motor winding neglected in the theoretical analysis. Without any further basis, it was proposed that the transfer function should be written as

$$G_1(s) = \frac{K}{s(1 + T_m s)(1 + T_e s)} \qquad \ldots\ (3.5)$$

where T_e is an electrical time constant. Although the transfer functions given in equations (3.3) and (3.4) are attractive for their simplicity and are intellectually interesting, they rely on basic assumptions which are far from valid. Although they are likely to provide results much different from the actual situation, no direct comparison appears to have so far been made.

In 1951, L. O. Brown [14] published a slightly more detailed solution for the transfer function of the servomotor, although he still assumed the transient and steady state torques to be equal. By considering the interactions between the distributions of flux density and current following a step change in the control voltage, he obtained an expression for the electromechanical torque of the motor. Equating

this to the rotor and load requirements, he produced the equation

$$J \frac{d\omega_r}{dt} + f\omega_r = K_1 e^{-\frac{R_2}{L_2} t} \cos(\omega t - \alpha) + K_2 A_1 \quad \ldots\ (3.6)$$

where A_1 = amplitude of the inphase component of the rotor current as a function of the instantaneous rotor velocity

K_1, K_2 = constants

α = angle between the stator and rotor reference lines ~~as a function of time~~

Numerical examination of the first term on the right-hand side of equation (3.6), which contains typical machine parameters, shows that the exponential term decays very rapidly in comparison with the decay of the cosine term, which can therefore, be regarded as approximately constant and equal to unity for the duration of the exponential. The equation relating the inphase and quadrature components of the rotor current (of amplitudes A_1 and A_2 respectively) is

$$L_2 \frac{dA_1}{dt} + R_2 A_1 = (A_2 L_2 - \frac{P_c I_m}{2}) (\omega - \omega_r) \quad \ldots\ (3.7)$$

P_c = proportionality constant between the stator magnetizing current and the flux density

I_m = magnitude of magnitizing current in either phase.

An examination of the right-hand side of equation (3.7) from the standpoint of the initial and final values for various final velocities, will show that it remains nearly constant over a wide range. The

equation can then be written approximately as

$$L_2 \frac{dA_1}{dt} + R_2 A_1 = K_3$$

which leads to an approximate expression for the instantaneous angular velocity as

$$\omega_r(t) = M_1 + M_2 e^{-J/f t} + M_3 e^{-\frac{R_2}{L_2} t} \quad \ldots\ (3.8)$$

where M_1 = steady state torque divided by the coefficient of friction for the system

From the initial conditions of zero acceleration and velocity, the coefficients of the exponential terms (M_2 and M_3) can be evaluated in terms of the constant M_1. By taking the Laplace transform of each term, and then collecting the terms over a common denominator, Brown obtained the transfer function for the motor as

$$G_1(s) = \frac{\theta_r}{V_c}(s) = \frac{A}{s(1 + T_m s)(1 + T_e s)} \quad \ldots\ (3.9)$$

where A is a combination of various electrical and mechanical parameters of the motor. It will be noted that equation (3.9) has precisely the same form as that proposed by Hopkins (equation (3.5))

With the excitation voltage to the control winding considered as amplitude modulated by a low frequency signal, the amplitudes and phase of the frequency response of a typical 25 W motor was predicted from equation (3.9), and compared with an experimentally obtained result.

Although a reasonably high level of agreement was obtained, this is very surprising in view of the assumptions involved in the analysis and the doubtful nature of the mathematical treatments. It cannot therefore be regarded as establishing any widespread validity of the result.

3.1.2 More detailed early analyses

In the first attempt at a more than superficial analysis, Hopkins [15] used the method of symmetrical components, to separate the unbalanced supply voltages into two balanced sets. He no longer regarded the torque/speed characteristics of the motor as parallel straight lines, and expressed the characteristic for balanced steady-state operation at rated voltage by the expression

$$T = \text{constant} \times \text{reference voltage} \times \text{control voltage} \times \text{slip} \quad \ldots (3.10)$$

when unbalanced voltages are fed to the motor windings, the techniques of symmetrical component analysis may be used to determine the corresponding steady-state torque of the motor. If the assumptions involved in the previous section still apply, the steady-state and the transient torques are the same at any given speed, and Hopkins thereby obtained an expression for the electromechanical torque as

$$T_\varepsilon = K \left[V_c(t) \cdot V_r - \frac{V_c^2(t) + V_r^2}{2} \cdot \frac{\omega_r}{\omega_s} \right] \quad \ldots (3.11)$$

where

V_r = amplitude of constant reference voltage, $v_r = \sqrt{2}\, V_r \sin\omega t$

$V_c(t)$ = amplitude of time varying control voltage, $v_c = \sqrt{2}\, V_c(t) \cos\omega t$

ω_s = synchronous speed

With equal steady state and transient torques, the differential equation which relates the electromechanical torque to the parameters of the mechanical system is

$$\frac{d\omega_r}{dt} + \frac{K(V_c^2(t) + V_r^2) + 2f\omega_s}{2\omega_s J}\omega_r = \frac{K V_c(t) V_r - a}{J} \quad \ldots\ (3.12)$$

where J, a and f are, respectively, the moment of inertia and the coefficients of Coulomb and viscous friction. Although equation (3.12) can be solved for any specific form of time variation of the control voltage amplitude, numerical or graphical integration may be necessary for some forms of variation. The solution for the case of step change is similar to that for a linear system, except that the time constant is now a function of the step voltage amplitude. Thus, the corresponding speed response is

$$\omega_r = \omega_{ss}(1 - e^{-t/T}) \quad \ldots\ (3.13)$$

where

$$T = \frac{2 J \omega_s}{K(V_c^2 + V_r^2) + 2f\omega_s} = \text{effective time constant}$$

$$\omega_{ss} = \frac{2\omega_s (K V_c V_r - a)}{K(V_c^2 + V_r^2) + 2f\omega_s}$$

Since only one time constant exists in this result, the transfer function resembles that obtained previously in equation (3.3). If the control voltage amplitude is time varying the theory of small oscillations may be used, provided that the amplitude variations are sufficiently small, but this results in an extremely complicated expression for the speed variations.

Hopkins was unable to continue his analysis and obtain a solution for the case of large amplitude variations, and although he set out

to solve completely the nonlinear differential equations of the motor he ended up by deducing from experimental observations the same result as that arrived at by previous workers.

In an analysis based on an approximate solution of the differential equations of the machine, Kutvinov [16] presented a further improved solution. As with Hopkins he no longer maintained the restrictive assumptions of early authors concerning the linear form of the torque/speed characteristics, but unlike Hopkins he conducted a fundamental study. By writing loop equations for the steady-state currents in the conventional equivalent circuit of the motor and substituting these in the expression for the torque, he obtained the ratio of the motor torque at a speed ω_r to the stalled torque $\frac{T}{T_s}$ as

$$\frac{T}{T_s} = \alpha\beta\sin\theta - \frac{\gamma(K_1 + \alpha^2\beta^2K_2) - \gamma^2\alpha\beta\sin\theta\left(4K_1K_2 - \frac{R_2^2\cos(\phi_c - \phi_e)}{Z_{rc}\cdot Z_{re}}\right)}{1 - \gamma^2\left(1 + 4K_1K_2 - \frac{2R_2^2\cos(\phi_c - \phi_e)}{Z_{re}\cdot Z_{rc}}\right) + \gamma^4\left(2K_1 - \frac{R_2^2}{Z_{rc}^2}\right)\left(2K_2 - \frac{R_2^2}{Z_{re}^2}\right)}$$

$$- \frac{\gamma^3\left(\frac{R_2^2}{2Z_{rc}^2} - K_1 + \alpha^2\beta^2\left(\frac{R_2^2}{2Z_{re}} - K_2\right)\right) + \gamma^4\left(2K_1 - \frac{R_2^2}{Z_{rc}^2}\right)\left(2K_2 - \frac{R_2^2}{Z_{re}^2}\right)}{1 - \gamma^2\left(1 + 4K_1K_2 - \frac{2R_2^2\cos(\phi_c - \phi_e)}{Z_{re}\cdot Z_{rc}}\right) + \gamma^4\left(2K_1 - \frac{R_2^2}{Z_{rc}^2}\right)\left(2K_2 - \frac{R_2^2}{Z_{re}^2}\right)} \quad \ldots (3.14)$$

where $\alpha e^{j\phi} = \frac{\dot{V}_c}{\dot{V}_r}$, $\gamma = \frac{\omega_r}{\omega_s}$, $\beta e^{j\phi_1} = \frac{\dot{Z}_{ke}}{\dot{Z}_{kc}}$, $\theta = \phi + \phi_1$

$$K_1 = \frac{R_2 \cos \phi_c}{Z_{rc}} - \frac{1}{2} \qquad K_2 = \frac{R_2 \cos \phi_e}{Z_{re}} - \frac{1}{2}$$

$\dot{Z}_{kc}$ and $\dot{Z}_{ke}$ are defined by Kutvinov as the transmission impedances of the control and reference circuits, with the rotor locked.

θ is the phase difference of the currents in the stator windings with locked rotor

$\dot{Z}_{re}$, $\dot{Z}_{rc}$ are the moduli of the reference and control circuit impedances measured on the rotor side.

$$\dot{Z}_{re} = \dot{Z}_2 + \frac{\dot{Z}_m \dot{Z}_e}{\dot{Z}_m + \dot{Z}_e} \qquad \dot{Z}_{rc} = \dot{Z}_2 + \frac{\dot{Z}_m \dot{Z}_c}{\dot{Z}_m + \dot{Z}_c}$$

$$\dot{Z}_m = j\omega M \qquad \dot{Z}_2 = R_2 + j\omega L_2 \qquad \dot{Z}_e = \dot{Z}_{ie} + R_1 + j\omega L_1$$

$$\dot{Z}_c = \dot{Z}_{ic} + R_1 + j\omega L_1$$

$\dot{Z}_{ie}$, $\dot{Z}_{ic}$ are the internal impedances of the equivalent generators of the control and excitation circuits.

Assuming the rotor resistance to be greater than one half that of the stator, and a speed range between 0 and 80% of synchronous speed, the above torque equation, expressed in series form, is

$$\frac{T}{T_s} = \alpha\beta\sin\theta - \gamma(K_1 + \alpha^2\beta^2 K_2) - \gamma^2 n_2 - \gamma^3 n_3 \qquad \ldots (3.15)$$

Kutvinov assumed that the general solution for the motor current obtained from the differential equations describing the machine could also be given as a power series in γ, but since $\gamma < 1$, and for any small changes in speed, $\Delta\gamma << 1$, it is clear that $\gamma\Delta\gamma$, $(\Delta\gamma)^2$ etc. are all approximately zero. The general solution for the transient response

thus leads to an equation which differs from equation (3.15) only in the coefficients of the zero and first powers of γ. Kutvinov therefore limited his equation (3.15) to the first power of γ, and sought a solution by setting the average speed change equal to zero for the cases of both amplitude modulated and frequency modulated methods of control. After much algebraic manipulation of the differential equations of the circuit, a transfer function relating the instantaneous changes in speed to the changes in an amplitude modulated signal was obtained as

$$\frac{\Delta\omega_r}{\Delta E_m}(P) = \frac{\omega_o}{E_o P_1} \cdot \frac{\beta K_o \sin\theta\, A(P)}{(a + P\frac{\tau\omega_o}{P_1})\, D(P) + K_1 N(P)} \qquad \ldots\ (3.16)$$

and the transfer function relating the changes in speed to the changes in the phase in a frequency modulated input signal as

$$\frac{\Delta\omega_r}{\Delta\phi} = \frac{\omega_o}{P_1} \cdot \frac{\alpha\beta \sin\theta_f\, A(P)}{D(P)(a + P\frac{\tau\omega_o}{P_1}) + K_1 N(P)} \qquad \ldots\ (3.17)$$

where $P = j\omega_m$ (ω_m being the modulating frequency)

$\theta_f = \theta - \pi/2$

$a = \dfrac{f\omega_o}{T_s P_1}$, $\omega_s = \dfrac{\omega_o}{P_1}$,

$\tau = J/T_s$; P_1 = number of pole pairs

E_o = reference voltage amplitude

The denominators of both equations (3.16) and (3.17) contain two different functions of the operator P, D(P) and N(P). To avoid complication these two functions were assumed approximately equal, although this was said to lead to an error of only 5% to 7% in the

determination of the transfer function, which is not beyond the limits of engineering accuracy. As a result of this approximation the transfer functions were rewritten as

$$\frac{\Delta\omega_r}{\Delta E_m}(P) = \frac{\omega_o}{E_o P_1} \cdot \frac{\beta K_o \sin\theta}{(a + K_1 + \frac{P\tau\omega_o}{P_1})} \cdot \frac{A(P)}{D(P)} \quad \ldots\ (3.18)$$

and

$$\frac{\Delta\omega_r}{\Delta\phi}(P) = \frac{\omega_o}{P_1} \frac{\alpha\ \beta\ \sin\theta_f}{(a + K_1 + \frac{P\tau\omega_o}{P_1})} \cdot \frac{A(P)}{D(P)} \quad \ldots\ (3.19)$$

which now contain the single operator $\frac{A(P)}{D(P)}$.

A full statement of the functions involved in equations (3.16) - (3.19) is

$$A(P) = Re\ \frac{1}{2}\ [\ \frac{\dot{K}_N^*\ e^{j\theta}(\dot{Z}_2 + \dot{Z}_m)}{\dot{K}_o \sin\theta} \cdot \frac{s}{\omega_o} \cdot \frac{\dot{Z}_q + qM}{\dot{Z}_c + \dot{Z}_m} \cdots \frac{\dot{Z}_{qr}}{\dot{Z}_{rc}}$$

$$- j\ \frac{\dot{K}_e}{\dot{K}_o}\ \frac{e^{-j\theta}}{\sin\theta}\ (\dot{Z}_{2q} + qM) \left(\frac{\dot{Z}_s + sM}{\dot{Z}_c + \dot{Z}_m}\right)^* \cdot \left(\frac{\dot{Z}_{sr}}{\dot{Z}_{rc}}\right)^*\ ] \quad \ldots\ (3.20)$$

$$D(P) = \left(\frac{\dot{Z}_{sr}}{\dot{Z}_{rc}}\right)^*\ \frac{\dot{Z}_{qr}}{\dot{Z}_{rc}}\ \left(\frac{\dot{Z}_s + sM}{\dot{Z}_c + \dot{Z}_m}\right)^* \cdot \frac{\dot{Z}_q + qM}{\dot{Z}_c + \dot{Z}_m} \quad \ldots\ (3.21)$$

and

$$N(P) = Re\ \frac{1}{2K_1}\ [\ \frac{\dot{Z}_m^{\,2}}{\dot{Z}_{rc}(\dot{Z}_c + \dot{Z}_m)}\ \frac{q}{j\omega_o}\ \left(\frac{\dot{Z}_{sr}}{\dot{Z}_{rc}}\right)^*\ \left(\frac{\dot{Z}_s + sM}{\dot{Z}_c + \dot{Z}_m}\right)^*$$

$$+ \frac{\dot{Z}_2 + \dot{Z}_m}{\dot{Z}_{rc}^*} \cdot \frac{\dot{Z}_{qr}}{\dot{Z}_{rc}}\ \left(\frac{\dot{Z}_s + sM}{\dot{Z}_c + \dot{Z}_m}\right)^* \cdot \frac{\dot{Z}_q + qM}{\dot{Z}_c + \dot{Z}_m}\ ] \quad \ldots\ (3.22)$$

where R_e is the real part with respect to P, $\dot{K}_N = K_N e^{j\phi_N}$, $\dot{K}_o = K_o e^{j\phi_o}$ and $\dot{K}_e = K_e e^{j\phi_e}$ are the complex transmission factors of amplifier and modulator for frequencies $\omega - \omega_m$, ω and $\omega + \omega_m$.

$$s = j(\omega - \omega_m), \quad q = j(\omega + \omega_m)$$

$\dot{Z}_s$ and $\dot{Z}_q$ stator winding control supply impedances at frequencies $\omega - \omega_m$ and $\omega + \omega_m$

$\dot{Z}_{sr}$ and $\dot{Z}_{qr}$ are motor control circuit impedances measured on the rotor side at frequencies $\omega - \omega_m$ and $\omega + \omega_m$.

$\dot{Z}_{2q} = R_2 + j(\omega + \omega_m) L_2$

The above expressions for the transfer functions are difficult to use in any practical computations, since the direct calculation of the coefficients necessitates the carrying out of lengthy mathematical transformations. However, Kutvinov showed that an approximate transfer function could be obtained in the case of amplitude modulated control by using graphical techniques based on the frequency response characteristics of the motor. Even so, a considerable volume of calculation is required. It is perhaps not surprising that Kutvinov presents an entirely theoretical paper in which he neither evaluates the transfer function for a given machine nor attempts any correlation with the practical results.

In a general method of solution suggested by Vlasov [17], the servomotor is a component of a carrier type automatic control system operating on a.c., and Vlasov attempts to describe the overall system by linear

differential equations with periodic coefficients. In his approach, the torque equation of the servomotor is linearised, by the assumption that the control winding flux linkage is much less than that of the reference winding. The coefficient in the torque equation thereby becomes periodic at the supply frequency. Vlasov considered a system comprising a modulator, a quadripole, and a motor, with the inputs to these stages being respectively $x(t)$, $x(t)Um\cos(\omega t - \phi)$ and $L^{-1}(Y(s).\ L(x(t).\ Um\cos(\omega t + \phi)))$

where Um = control voltage amplitude

ω = supply frequency

The Laplace transform of the quadripole is

$$Uy(s') = Y(s').\ U_x(s')$$

where $U_x(s') = L(x(t).\ Um\cos(\omega t + \phi))$ and $s' = \frac{s}{\omega}$

Neglecting terms modulated at twice supply frequency, since the motor acts as a low pass filter, this approach leads to an overall transfer function relating the motor output to the modulator input as

$$G_1(s') = \frac{\theta_2(s')}{x(s')} = \frac{1}{c_2 s'(c_1 s' + 1)}\left(\frac{s' - 2j}{s' - j}\,Y(s' - j)e^{j\delta} + \frac{s' + 2j}{s' + j}\,Y(s' + j)\,e^{j\delta}\right) \quad \ldots\ (3.23)$$

where c_1 and c_2 are dimensionless constants. With the quadripole designed to operate at supply frequency with a gain K_o, equation (3.23) becomes

$$G_1(s') = \frac{2K_o\,((s'^2 + 2)\cos\delta + s'\sin\delta)}{c_2 s'(c_1 s' + 1)((s')^2 + 1)}$$

where $\delta = \psi - \phi$ $\qquad V_r = U_{2m}\sin(\omega t + \psi)$

The transfer function is simplified still further if we set $\partial = 0$ and $s'^2 << 1$. Then

$$G_1(s') = \frac{4 K_o}{c_2 s' (1 + c_1 s')}$$

which can be written as

$$G_1(s) = \frac{K}{s(1 + T_m s)} \qquad \ldots\ (3.24)$$

where $K = \frac{4\omega K_o}{c_2}$, $T_m = \frac{c_1}{\omega}$

which resembles the result obtained by Brown and Campbell[13], although the basic requirement that the differential equations should be linear with periodic coefficients is quite restrictive and the gain and time constant factors ($\frac{4K_o\omega}{c_2}$ and $\frac{c_1}{\omega}$) are quite different. As in the approach of Brown[14], the development of equation (3.23) requires the equating of the electromagnetic torque developed by the motor with the mechanical torque required by the load, and it is in the solution of this equation that the linerization process is used.

In an approach broadly similar to that of Kutvinov, Mikhail and Fett[18] established from the differential equations of the motor the general form of the torque/speed equation, in terms of the 2-phase currents of the motor. At an important stage of their analysis, the authors attempt to solve the torque equation before linearisation, by the use of Laplace transform. However, they made a fundamental mistake by simply replacing the differential operator by the Laplace operator when finding the Laplace transform of the product of two time functions,

a process which completely invalidates their result. The result of their study is a transfer function relating the speed to the modulating signal, given as

$$G(s) = \frac{2\omega I}{\frac{f R_2}{KM^3}(1 + T_e s)(1 + T_m s) + (I^2 + g^2)} \quad \ldots\ (3.25)$$

where I = r.m.s. value of the current in the reference phase

g = r.m.s. value of the modulating function $g(t)$

K = constant

T_e = electrical time constant

T_m = mechanical time constant

$$G(s) = \frac{A}{(1 + sT_a)(1 + sT_b)} \quad \ldots\ (3.26)$$

where $A = \frac{2\omega K M^3 I}{f R_2 T_m T_e} T_a T_b$

$$T_a = \frac{1}{s_1} \qquad T_b = \frac{1}{s_2}$$

where

$$s_{1,2} = -\frac{1}{2}\left(\frac{1}{T_e} + \frac{1}{T_m}\right) \pm \sqrt{\left(\frac{1}{2}\left(\frac{1}{T_e} + \frac{1}{T_m}\right)\right)^2 - \frac{K M^3 (g^2 + I^2)}{f R_2 T_e T_m}}$$

although resembling in form the result of L.O. Brown, the terms of the equation are quite different. Neither Vlasov nor Mikail and Fett give more in their papers than the mathematical statements of the transfer functions.

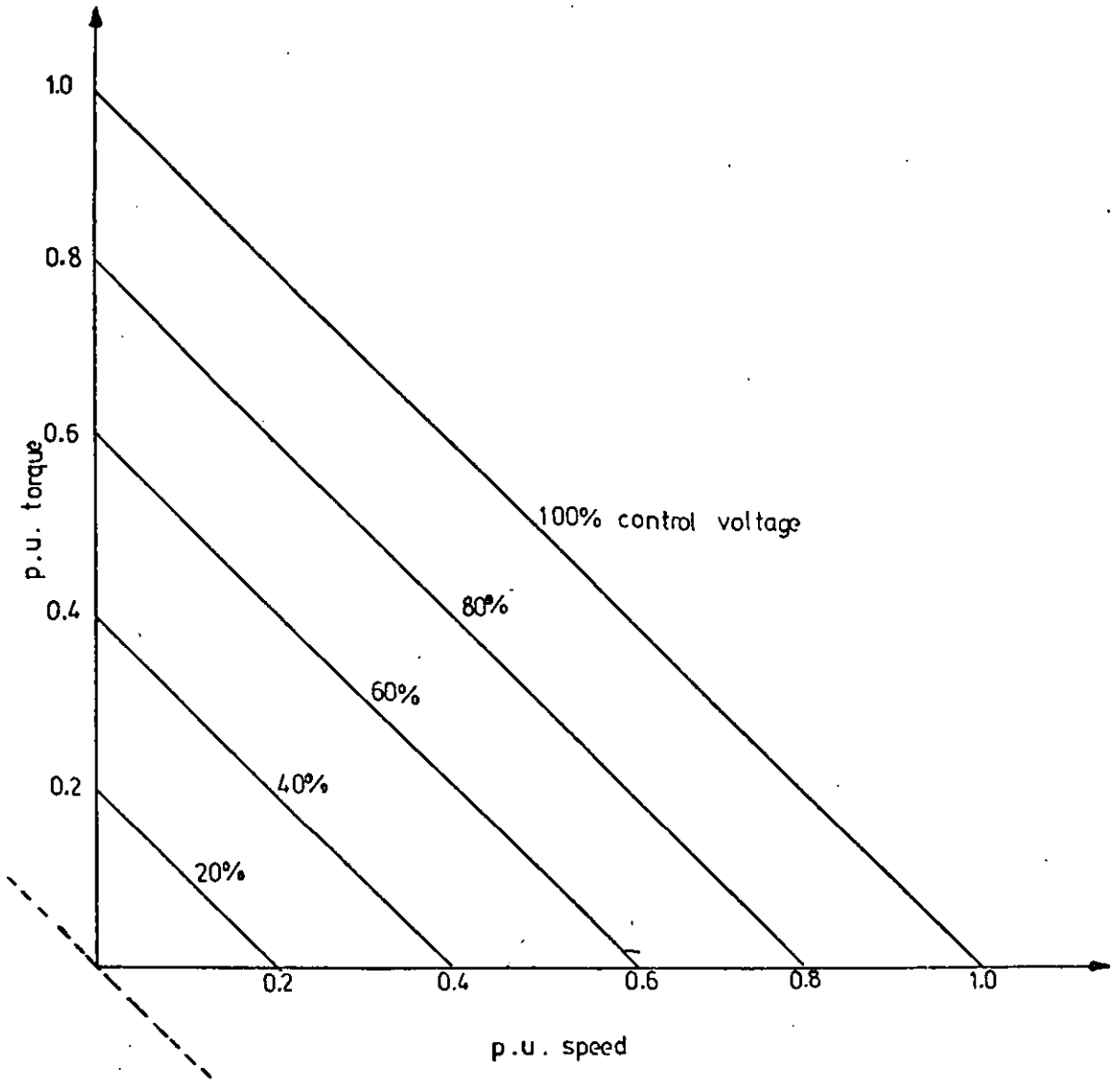

Fig 3.1 Linear torque/speed characteristics of idealised 2-phase servomotor

Reference voltage = 100%

CHAPTER 4. TRANSFER FUNCTIONS OF 2-PHASE SERVOMOTOR USING COMPLEX CONVOLUTION APPROACH

The early analyses described in the previous chapter of the thesis, were either based on a machine model assuming a linear torque-speed characteristic, and the same behaviour during both steady state and transient conditions, or on a solution of the machine equations in which quite drastic approximations were made. Both approaches may lead eventually to a transfer function of the same general form, although these differ in the magnitudes of the gain and time constants involved. To establish correctly a transfer function for the servomotor containing the time constants associated with all the electrical energy storage elements of the motor, besides that of the mechanical system, necessitates an algebraic solution of the nonlinear equations involved. The product of variables nonlinearity which arises in this solution can most conveniently be dealt with by the use of the Complex Convolution technique (see Appendix 8.1.4) which enables the Laplace transform of the product of two time functions to be briefly expressed as follows.[21-24] If $f_1(t)$ and $f_2(t)$ are Laplace transformable functions, having the Laplace transforms of $F_1(s)$ and $F_2(s)$, and if $F_1(s) = \frac{A}{B}\frac{(s)}{(s)}$ is a rational fraction with q first order poles only, then

$$L\,(f_1(t).\ f_2(t)) = \sum_{k=1}^{k=q} \frac{A\,(s)}{B'(s)}\ F_2(s - s_K) \qquad \ldots\ (4.1a)$$

where $B'(s) = \left| \frac{d}{ds}\ B(s) \right|_{s = s_K}$

The inverse of a transfer function given by a general rational proper fraction is

$$L^{-1}\left(\frac{A(s)}{s\,B_1(s)}\right) = \frac{A(0)}{B_1(0)} + \sum_{k=2}^{k=q} \frac{A(s_K)}{s_K\,B_1'(s_K)}\, e^{s_K t} \qquad \ldots (4.1b)$$

where $B_1'(s) = \left|\frac{d}{ds}\,(B_1(s))\right|_{s = s_K}$

4.1 D-Q axis equation of a 2-phase servomotor

The idealized 2-phase induction motor provides a very convenient starting point for the study of the dynamic bahaviour of the 2-phase servomotor. This model is shown in Fig. 4.1a, while Fig. 4.1b shows the stationary axis equivalent produced by the application of Park's transformation. The idealised machine is assumed to possess

(1) negligible saturation, hysteresis and eddy currents

(2) a uniform airgap, and rotor and stator inductances which are independent of the rotor position

(3) conductors and coils so distributed that the mutual inductance between a rotor phase and a stator phase is a cosinusoidal function of their relative displacement.

Based on these assumptions the familiar d, q equations of the machine may be obtained as:

$$\begin{bmatrix} \nu_D \\ \nu_Q \\ \nu_d \\ \nu_q \end{bmatrix} = \begin{bmatrix} R_1 + L_1 p & 0 & Mp & 0 \\ 0 & R_1 + L_1 p & 0 & Mp \\ Mp & M\omega_r & R_2 + L_2 p & L_2\omega_r \\ -M\omega_r & Mp & -L_2\omega_r & R_2 + L_2 p \end{bmatrix} \begin{bmatrix} i_D \\ i_Q \\ i_d \\ i_q \end{bmatrix} \qquad \ldots (4.$$

$$\text{or } [\nu] = [Z][i]$$

where $[Z]$ is the impedance matrix of the machine. The conventional equivalent circuit of the induction machine, which can be derived from equation (4.2) is shown in Fig.(4.1c).

In equation(4.2) the upper-case symbols D and Q refer to the stator windings while the lower-case symbols d and q refer to the rotor windings, and normally $v_d = v_q = 0$.

The electromechanical torque produced by the motor is normally obtained from

$$T_\varepsilon = [i_t][G][i]$$

$$= \rho_1 M (i_Q i_d - i_D i_q) \quad \ldots\ (4.3)$$

where $[G]$ is a matrix found from the coefficients of ω_r in $[z]$ and ρ_1 is the number of pairs of poles in the machine.

The first stage in the development of the transfer function is to obtain equations from (4.2) for i_d and i_q, as

$$i_d = \frac{-M\left((R_2 + L_2 p)(\rho_1 \omega_r i_Q + p i_D) + \rho_1 \omega_r L_2 (\rho_1 \omega_r i_D - p i_Q)\right)}{(R_2 + L_2 p)^2 + \rho_1^2 \omega_r^2 L_2^2} \quad \ldots(4.4)$$

and

$$i_q = \frac{M\left((R_2 + L_2 p)(\rho_1 \omega_r i_D - p i_Q) - \rho_1 \omega_r L_2 (\rho_1 \omega_r i_Q + p i_D)\right)}{(R_2 + L_2 p)^2 + \rho_1^2 \omega_r^2 L_2^2} \quad \ldots\ (4.5$$

and to substitute these in equation (4.3) to give the electromechanical torque equation as

$$T_\varepsilon = \frac{\rho_1 M}{(R_2 + L_2 \rho)^2 + \rho_1^2 \omega_r^2 L_2^2} \left(- (R_2 + L_2 p)(\rho_1 \omega_r (i_D^2 + i_Q^2) + i_Q p i_D - i_D p i_Q \right.$$

$$\left. + \rho_1 \omega_r L_2 (i_D p i_D + i_Q p i_Q) \right) \quad \ldots\ (4.6)$$

During normal operation a servomotor will be operating at speeds very much below synchronous, and under these conditions it is reasonable to neglect all the terms in equation(4.6) which involve ω_r.[19]

With the introduction of the rotor time constant $T_2 (= \frac{L_2}{R_2})$, equation (4.6) may then be rewritten as

$$T_\varepsilon = \frac{\rho_1 M^2}{R_2 (1 + T_2 p)} (i_D pi_Q - i_Q pi_D) \quad .... (4.7)$$

A further useful simplification is now to introduce the stalled stator impedances of the machine, which may be written as

$$i_{Do}(t) = \frac{\nu_D(t)}{R_1' + L_1' p} \quad .... (4.8a)$$

$$i_{Qo}(t) = \frac{\nu_Q(t)}{R_1' + L_1' p} \quad .... (4.8b)$$

where R_1' and L_1' are the input resistance and inductance respectively, given by

$$R_1' = R_1 + \frac{\omega^2 \frac{M^2}{R_2}}{1 + (\omega T_2)^2} \quad .... (4.9a)$$

$$L_1' = L_1 - \frac{(\omega M)^2 T_2}{R_2 (1 + \omega^2 T_2^2)} \quad .... (4.9b)$$

4.2 Transfer function for amplitude modulated control

When the control of the servomotor is by amplitude modulation of the control winding voltages, the mutual phase shift between the control and reference voltages remains always at 90^{o}.

If a fixed reference voltage $v_Q(t) = V_Q \sin\omega t$ is applied to the Q axis winding and a control voltage $v_D(t) = V_D(t) \sin(\omega t + \pi/2)$ to the D-axis winding then

$$i_{Qo}(t) = \frac{V_Q e^{-j\phi\beta}}{|Z_1'|} \sin \omega t \qquad \ldots (4.10)$$

$$pi_{Qo}(t) = \frac{\omega V_Q e^{-j\phi\beta}}{|Z_1'|} \cos \omega t \qquad \ldots (4.11)$$

where $|Z_1'| e^{+j\phi\beta} = R_1' + j\omega L_1'$

It is at this stage that the analysis of the present author departs from that of the only previous solution of (4.10) using complex conjugate techniques. In equation (17) of his paper, D. R. Wilson[19] applied this technique incorrectly, and his equation for the reference phase current

$$i_{Qo}(t) = \frac{V_M}{Z_1} \sin(\omega t + \phi_1 - \phi_Q) \begin{cases} v_Q(t) = V_M \sin(\omega t + \phi_1) \\ \phi_1 = \text{phase at } t = 0 \\ \phi_Q = \tan^{-1} \dfrac{\omega L_1}{R_1} \end{cases}$$

is accordingly in error. This error is maintained throughout his analysis, and leads to expressions considerably different from those in the present study. A further mistake which appears in the analysis of Wilson is that the stalled impedance of the motor is taken simply as the stator winding impedance $R_1 + pL_1$.

Since the control voltage ν_D is a function of both $V_D(t)$ and $\sin(\omega t + \pi/2)$, we need to use complex convolution in determining the Laplace transform. Thus, if we let $f_1(t) = \cos \omega t$ and $f_2(t) = V_D(t)$, then

$$L\ f_1(t) = \frac{s}{s^2 + \omega^2}$$

$$= \frac{A(s)}{B(s)} \qquad \text{with}$$

first order poles $s_1, s_2 = \pm j\omega$ and

$$L\{f_2(t)\} = V_D(s)$$

substituting in equation (4.1a) and noting that

$$B'(s) = \frac{d}{ds} B(s)$$

$$= 2s \qquad \text{we obtain}$$

$$\nu_D(s) = L(V_D(t) \cos\omega t) = \frac{(+j\omega)}{2(+j\omega)} V_D(s - j\omega) + \frac{(-j\omega)}{2(-j\omega)} V_D(s + j\omega)$$

$$\nu_D(s) = \frac{V_D(s + j\omega) + V_D(s - j\omega)}{2} \qquad \ldots (4.12)$$

The Laplace transforms of the reference and control winding currents are given by equations (4.8a and b) as

$$i_{Qo}(s) = \frac{\nu_Q(s)}{R_1' + L_1's}$$

and

$$i_{Do}(s) = \frac{\nu_D(s)}{R_1' + L_1's}$$

$$= \frac{V_D(s + j\omega) + V_D(s - j\omega)}{2\, Z_1'(s)} \qquad \ldots\ (4.13)$$

From equation (4.13), two currents $i_{Do}(s + j\omega)$ and $i_{Do}(s - j\omega)$, which arise later in the analysis, may be defined as

$$i_{Do}(s + j\omega) = \frac{V_D(s) + V_D(s + 2j\omega)}{2\, Z_1'(s + j\omega)}$$

$$i_{Do}(s - j\omega) = \frac{V_D(s) + V_D(s - 2j\omega)}{2\, Z_1'(s - j\omega)}$$

It is reasonable to assume that the twice supply frequency terms in these equations cannot give rise to shaft oscillations at that frequency,[19,28] and with these components of the currents neglected

$$i_{Do}(s + j\omega) = \frac{V_D(s)}{2Z_1'(s + j\omega)} \qquad \ldots\ (4.14)$$

$$i_{Do}(s - j\omega) = \frac{V_D(s)}{2Z_1'(s - j\omega)} \qquad \ldots\ (4.15)$$

Substituting $i_{Qo}(t)$ and $p\, i_{Qo}(t)$ in equation (4.7) we obtain for the torque of the motor

$$T_\varepsilon(t) = \frac{\rho_1 M^2 V_Q}{|Z_1'|}\, e^{-j\phi\beta}\left[\omega \frac{i_{Do}(t)}{Z_2(p)} \cos\omega t - \frac{p\, i_{Do}(t)}{Z_2(p)} \sin\omega t\right] \qquad \ldots\ (4.16)$$

and it is clearly necessary to apply complex convolution to each term in the square bracket. Thus, for the first term

$$f_1(t) = \cos\omega t \qquad f_2(t) = \frac{i_{Do}(t)}{Z_2(p)}$$

$$F_1(s) = \frac{s}{s^2 + \omega^2} = \frac{A_1(s)}{B_1(s)}, \quad F_2(s) = \frac{i_{D_o}(s)}{Z_2(s)}$$

$$B_1'(s) = 2s \quad \text{and } s_1, s_2 = \pm j\omega$$

and $$L\left(\frac{\omega i_{D_o}(t)}{Z_2(p)} \cos \omega t\right) = \frac{\omega}{2}\left(\frac{i_{D_o}(s + j\omega)}{Z_2(s + j\omega)} + \frac{i_{D_o}(s - j\omega)}{Z_2(s - j\omega)}\right) \quad \ldots\ (4.17)$$

and similarly for the second term in the bracket

$$L\left(\frac{p\, i_{D_o}(t)}{Z_2(p)} \cdot \sin \omega t\right) = \frac{1}{2j}\left(\frac{(s - j\omega)\, i_{D_o}(s - j\omega)}{Z_2(s - j\omega)} + \frac{(s + j\omega)\, i_{D_o}(s + j\omega)}{Z_2(s + j\omega)}\right)$$

$$\ldots\ (4.18)$$

From equation (4.16) the Laplace transform of the motor torque is therefore,

$$T_\varepsilon(s) = \frac{p_1 M^2}{2|Z_1'|} V_Q e^{-j\phi\beta}\left(\frac{i_{D_o}(s + j\omega)}{Z_2(s + j\omega)}(2\omega - js) + \frac{i_{D_o}(s - j\omega)}{Z_2(s - j\omega)}(2\omega + js)\right) \quad \ldots\ (4.19)$$

and on substituting for $i_{D_o}(s + j\omega)$ and $i_{D_o}(s - j\omega)$ from equations (4.14) and (4.15)

$$T_\varepsilon(s) = \frac{p_1}{4|Z_1'|} M^2 V_Q V_D(s) e^{-j\phi\beta} \frac{Z_1'(+) \cdot Z_2(+)(2\omega + js) + Z_1'(-)(2\omega - js) Z_2(-)}{Z_1'(+) Z_2(+) \cdot Z_1'(-) Z_2(-)}$$

$$\ldots\ (4.20)$$

where $$Z_1'(\pm) = Z_1'(s \pm j\omega) = R_1' + (s \pm j\omega) L_1'$$

$$= R_1'(1 + (s \pm j\omega) T_1)$$

$$Z_2(\pm) = Z_2(s \pm j\omega)$$

$$= R_2 (1 + (s \pm j\omega) T_2)$$

$$T_1 = \frac{L_1'}{R_1'} \quad \text{and} \quad T_2 = \frac{L_2}{R_2}$$

Evaluating the complex conjugate pairs in equation (4.20)

$$Z_1'(+) . Z_2(+) = R_1' R_2 (1 + (s + j\omega) T_1)(1 + (s + j\omega) T_2)$$

$$= R_1' R_2 (1 + s(T_1 + T_2) + (s^2 - \omega^2)T_1T_2$$

$$+ j\omega (T_1 + T_2 + 2sT_1T_2)) \quad .... (4.21)$$

and

$$Z_1'(-) Z_2(-) = R_1' R_2 (1 + s(T_1 + T_2) + (s^2 - \omega^2) T_1T_2$$

$$- j\omega(T_1 + T_2 + 2s T_1T_2))$$

Further, since $Z_1'(+) . Z_2(+) (2\omega + js)$ and $Z_1'(-) Z_2(-) (2\omega - js)$ are also complex conjugates, their sum is twice the real part of either, i.e.

$$\text{since} \quad R_e (Z_1'(+) Z_2(+) (2\omega + js))$$

$$= \omega R_1' R_2 (2(1 - \omega^2T_1T_2) + s (T_1 + T_2)) \quad .... (4.22)$$

then

$$Z_1'(+) . Z_2 (+)(2\omega + js) + Z_1'(-) . Z_2(-)(2\omega - js)$$

$$= 2\omega R_1' R_2 (2 (1 - \omega^2T_1T_2) + s(T_1 + T_2)) \quad .... (4.23)$$

Thus the final equation for the electromagnetic motor torque becomes

$$T_e(s) = \frac{\rho_1}{2|Z_1'|} e^{-j\phi\beta} . \frac{M^2}{R_2} \frac{V_Q}{R_1'} V_D(s)\omega \frac{2.(1 - \omega^2T_1T_2) + s(T_1 + T_2)}{((1 + sT_1)^2 + \omega^2T_1^2) ((1 + sT_2)^2+\omega^2T_2^2)}$$

.... (4.24)

4.2.1 Transfer function relating speed and control voltage

The equation for the mechanical system is

$$\text{mechanical torque} = \text{inertia torque} + \text{frictional torque}$$

$$\text{or } T_M(s) = (Js + f)\,\omega_r(s) \qquad \ldots\ (4.25)$$

where $\omega_r(s) = s\,\theta_r(s)$

The required transfer function can now be obtained by equating the electromagnetic torque given by equation (4.24) to the mechanical torque requirement of equation (4.25), leading to

$$\frac{\omega_r}{V_D}(s) = \frac{\rho_1 \omega}{2|Z_1'|} \cdot \frac{M^2}{R_2} \cdot \frac{V_Q}{R_1'} \cdot \frac{e^{-j\phi\beta}}{f} \cdot \frac{2(1 - \omega^2 T_1 T_2) + s(T_1 + T_2)}{((1 + sT_1)^2 + \omega^2 T_1^2)((1 + sT_2)^2 + \omega^2 T_2^2)(1 + T_m s)} \qquad \ldots\ (4.26)$$

after a considerable amount of algebraic manipulation.

A particular case of interest is the speed response following a step change in the control voltage. Replacing V_D by $\frac{V_D}{s}$ in equation (4.26) leads to a speed repsonse of the form

$$\omega_r(s) = H.V_D \cdot \frac{2(1 - \omega^2 T_1 T_2) + s(T_1 + T_2)}{s(s + \frac{1}{T_m})((s + \frac{1}{T_1})^2 + \omega^2)((s + \frac{1}{T_2})^2 + \omega^2)} \qquad \ldots\ (4.27)$$

where

$$H = \frac{\rho_1 \omega}{2 J T_1^2 T_2^2} \cdot \frac{V_Q}{R_1'} \cdot \frac{M^2}{R_2} \cdot \frac{e^{-j\phi\beta}}{|Z_1'|}$$

Obtaining the inverse Laplace transform of equation (4.27), to provide the required time response of speed, is an extensive task necessitating a further application of the complex convolution technique.

If equation (4.27) is written as

$$\frac{\omega_r}{HV_D} = \frac{A(s)}{s\ B_1(s)} \qquad \ldots\ (4.28)$$

the demoninator has the form

$$(s - s_1)(s - s_2)\ \ldots\ldots\ (s - s_6)$$

where $s_1 = 0 \qquad s_2 = -\frac{1}{T_m}$

$$s_3\ ,\ s_4 = -\left(\frac{1}{T_1} \pm j\omega\right)$$

$$s_5\ ,\ s_6 = -\left(\frac{1}{T_2} \pm j\omega\right)$$

The term which corresponds to the zero first order pole is the first term on the right-hand side of equation (4.1b), and is obtained by substituting s = 0 in s times equation (4.28), as

$$\frac{A(o)}{B_1(o)} = \frac{2(1 - \omega^2 T_1 T_2)\ T_m\ T_1^{\,2}\ T_2^{\,2}}{(1 + \omega^2 T_1^{\,2})(1 + \omega^2 T_2^{\,2})}$$

Equation (4.1b) requires also the evaluation of both $A(s_K)$ and $s_K\ B_1'(s_K)$, for all the five non-zero roots of the denominator, thus

$$A(s_2) = 2(1 - \omega^2 T_1 T_2) - (T_1 + T_2)\ s_2$$

$$A(s_3) = 2(1 - \omega^2 T_1 T_2) - (T_1 + T_2)\ s_3$$

$$A(s_4) = 2(1 - \omega^2 T_1 T_2) - (T_1 + T_2)\ s_4 \qquad \Big\} \text{ a conjugate pair}$$

$$A(s_5) = 2(1 - \omega^2 T_1 T_2) - (T_1 + T_2)\ s_5$$

$$A(s_6) = 2(1 - \omega^2 T_1 T_2) - (T_1 + T_2)\ s_6 \qquad \Big\} \text{ a conjugate pair}$$

$$s_2\ B_1'(s_2) = s_2(s_2 - s_3)(s_2 - s_4)(s_2 - s_5)(s_2 - s_6) \qquad \ldots\ (4.29)$$

$$s_3\ B_1'(s_3) = s_3(s_3 - s_2)(s_3 - s_4)(s_3 - s_5)(s_3 - s_6) \qquad \ldots\ (4.30)$$

$$s_4\ B_1'(s_4) = s_4(s_4 - s_2)(s_4 - s_3)(s_4 - s_5)(s_4 - s_6) \qquad \ldots\ (4.31)$$

$$= (s_3\ B_1'(s_3))^*$$

$$s_5 B_1'(s_5) = s_5(s_5 - s_2)(s_5 - s_3)(s_5 - s_4)(s_5 - s_6) \quad \ldots\ (4.32)$$

$$s_6 B_1'(s_6) = s_6(s_6 - s_2)(s_6 - s_3)(s_6 - s_4)(s_6 - s_5) \quad \ldots\ (4.33)$$

$$= (s_5 B_1'(s_5))^*$$

On obtaining the summation of equation (4.1b), after adding together terms corresponding to conjugate poles, and performing a considerable amount of algebraic manipulations, we obtain

$$\frac{A(s_2)}{s_2 B_1'(s_2)} e^{s_2 t} = - \frac{(2(1 - \omega^2 T_1 T_2) - \frac{T_1 + T_2}{T_m}) T_m^5 T_1^2 T_2^2 \cdot e^{-\frac{1}{T_m} t}}{((T_m - T_1)^2 + \omega^2 T_1^2 T_m^2)((T_m - T_2)^2 + \omega^2 T_2^2 T_m^2)}$$

$$\frac{A(s_3) e^{s_3 t}}{s_3 B_1'(s_3)} + \frac{A(s_4) e^{s_4 t}}{s_4 B_1'(s_4)} =$$

$$\frac{2 \cdot e^{-\frac{1}{T_1} t}}{x_1^2 + y_1^2} ((x_1 \lambda - \omega T y_1) \cos \omega t - (y_1 \lambda + \omega T x_1) \sin \omega t)$$

$$\frac{A(s_5) e^{s_5 t}}{s_5 B_1'(s_5)} + \frac{A(s_6) e^{s_6 t}}{s_6 B_1'(s_6)}$$

$$= \frac{2 e^{-\frac{1}{T_2} t}}{x_2^2 + y_2^2} ((x_2 \lambda' - \omega T y_2) \cos \omega t - (y_2 \lambda' + \omega T x_2) \sin \omega t)$$

$$\ldots\ (4.34)$$

where

$$x_1 = 2\omega^2 \cdot \frac{T_1 - T_2}{T_1 T_2} \left(2 \left(\frac{T_1 - T_m}{T_1^2 T_m} + \omega^2\right) - \frac{T_1 - T_2}{T_1 T_2} \cdot \frac{T_1 - 2 T_m}{T_1 T_m}\right)$$

$$x_2 = 2\omega^2 \cdot \frac{T_2 - T_1}{T_1 T_2} \cdot \left(2\left(\frac{T_2 - T_m}{T_2^2\, T_m} + \omega^2\right) - \frac{T_2 - T_1}{T_1 T_2} \cdot \frac{T_2 - 2\,T_m}{T_2\, T_m}\right)$$

$$y_1 = 2\omega \frac{T_1 - T_2}{T_1 T_2} \left(2\omega^2 \cdot \frac{T_1 - 2\,T_m}{T_1\, T_m} + \frac{T_1 - T_2}{T_1 T_2}\left(\frac{T_1 - T_m}{T_1^2\, T_m} + \omega^2\right)\right)$$

$$y_2 = 2\omega \frac{T_2 - T_1}{T_1 T_2} \left(2\omega^2 \cdot \frac{T_2 - 2\,T_m}{T_2\, T_m} + \frac{T_2 - T_1}{T_1 T_2} \cdot \left(\frac{T_2 - T_m}{T_2^2\, T_m} + \omega^2\right)\right)$$

$$T = T_1 + T_2$$

$$\lambda = 2\,(1 - \omega^2 T_1 T_2) - \frac{T}{T_1}$$

$$\lambda' = 2\,(1 - \omega^2\, T_1 T_2) - \frac{T}{T_2}$$

Adding together all the above terms, we obtain the required speed response as

$$\omega_r(t) = V_D H \left[\frac{2(1 - \omega^2 T_1 T_2)\; T_m\, T_2^2\, T_1^2}{(1 + \omega^2\, T_1^2)(1 + \omega^2\, T_2^2)} - \right.$$

$$\frac{\left(2\,(1 - \omega^2 T_1 T_2) - \dfrac{T_1 + T_2}{T_m}\right)\; T_1^2\, T_2^2\, T_m^5}{\left((T_m - T_1)^2 + \omega^2\, T_1^2\, T_m^2\right)\left((T_m - T_2)^2 + \omega^2\, T_2^2 T_m^2\right)} \cdot e^{-\frac{1}{T_m} t} +$$

$$\frac{2\, e^{-\frac{1}{T_1} t}}{x_1^2 + y_1^2} \left((x_1\lambda - \omega T y_1)\cos\omega t - (y_1\lambda + \omega T x_1)\sin\omega t\right)$$

$$\left. + \frac{2\, e^{-\frac{1}{T_2} t}}{x_2^2 + y_2^2} \left((x_2\lambda' - \omega T y_2)\cos\omega t - (y_2\lambda' + \omega T x_2)\sin\omega t\right)\right] \qquad \ldots (4.35)$$

4.3 Transfer function for phase modulated control

As was stated in the previous section, the stator currents of the servomotor are governed essentially by the stalled impedance of the stator, so that

$$i_{Do}(t) = \frac{\nu_D(t)}{R_1' + pL_1'}$$

$$i_{Qo}(t) = \frac{\nu_Q(t)}{R_1' + pL_1'}$$

For phase-modulation control, the constant voltage applied to the reference winding will again be assumed as

$$\nu_Q(t) = V_Q \sin \omega t$$

but the voltage applied to the control winding now has the form

$$\begin{aligned} \nu_D(t) &= V_D \sin (\omega t + \phi_D(t)) \\ &= A_1(t)\cos\omega t + A_2(t) \sin\omega t \qquad \ldots\ (4.36) \end{aligned}$$

where

$$A_1(t) = V_D \sin \phi_D(t)$$

$$A_2(t) = V_D \cos \phi_D(t)$$

In the analysis of the previous section, the voltage applied to the control winding had precisely the same form as the first term of equation (4.36), so that the electromagnetic torque caused by this voltage is given directly from equation (4.24) as

$$T_{el}(s) = \frac{\rho_1 \omega}{2|Z_1'|} \cdot \frac{M^2}{R_2} \cdot \frac{V_Q}{R_1'} \cdot e^{-j\phi\beta} \cdot A_1(s) \frac{2(1-\omega^2 T_1 T_2) + s(T_1+T_2)}{(1+sT_1)^2+\omega^2 T_1^2)((1+sT_2)^2+\omega^2 T_2^2)}$$

$\ldots\ (4.37)$

The torque produced by the second term of equations (4.36) is obtained by the same technique used in Section (4.2), differences being introduced by the sine term which has replaced the cosine term. Thus, the two components of the control winding currents are now

$$i_{Do}(s + j\omega) = \frac{A_2(s)}{2j\ Z_1'(s + j\omega)}$$

$$i_{Do}(s - j\omega) = -\frac{A_2(s)}{2j\ Z_1'(s - j\omega)}$$

and on substituting these in equation (4.19),

$$T_{e2}(s) = -\frac{\rho_1 M^2}{4|Z_1'|} \cdot V_Q.e.^{-j\phi\beta} \cdot A_2(s) \frac{Z_1'(-)Z_2(-)(s+j2\omega) + Z_1'(+)Z_2(+)(s-j2\omega)}{Z_1'(+).Z_1'(-).\ Z_2(+)Z_2(-)} \quad \ldots\ (4.38)$$

Since the numerator of equation (4.38) is the sum of two conjugate quantities, its sum is twice the real part of either or

$$2\ R_e\ (Z_1'(-).Z_2(-)\ (s+2j\omega)) = 2R_1'R_2\ (s^3T_1T_2 + s^2(T_1+T_2) + s(1+3\omega^2T_1T_2)+2\omega^2(T_1+T_2)$$

which gives

$$T_{e2}(s) = -\frac{\rho_1 M^2}{2|Z_1'|} \cdot \frac{e^{-j\phi\beta}.A_2(s)}{R_1'R_2} \cdot \frac{s^3T_1T_2+s^2(T_1+T_2)+s(1+3\omega^2T_1T_2) + 2\omega^2(T_1+T_2)}{((1+sT_1)^2 + \omega^2T_1^2)((1+sT_2)^2+\omega^2T_2^2)} \quad \ldots(4.39)$$

and on adding equations (4.37) and (4.39), the total electromagnetic torque is

$$T_\varepsilon(s) = \frac{\rho_1}{2} \cdot \frac{V_Q}{R_1'} \cdot \frac{M^2}{R_2} \cdot \frac{e^{-j\phi\beta}}{|Z_1'|} \left(\frac{\omega A_1(s)(2(1-\omega^2T_1T_2) + s(T_1+T_2))}{((1+sT_1)^2+\omega^2T_1^2)((1+sT_2)^2+\omega^2T_2^2)} - \frac{A_2(s)\ (s^3T_1T_2 + s^2(T_1+T_2) + s(3\omega^2T_1T_2 + 1) + 2\omega^2(T_1+T_2))}{((1+sT_1)^2+\omega^2T_1^2)((1+sT_2)^2+\omega^2T_2^2)}\right) \quad \ldots\ (4.40)$$

where

$$A_1(s) = L\, V_D \sin \phi_D(t)$$

$$A_2(s) = L\, V_D \cos \phi_D(t)$$

4.3.1 Transfer function relating change in speed to a step change in the phase shift

The electromagnetic torque given by equation (4.40) is equated to the mechanical torque requirement of equation (4.25), leading to

$$\omega_r(s) = H_1 \left(\frac{\omega A_1(s) \left(2(1 - \omega^2 T_1 T_2) + s(T_1+T_2)\right)}{(s + \frac{1}{T_m})\left((s+\frac{1}{T_1})^2 + \omega^2\right)\left((s+\frac{1}{T_2})^2 + \omega^2\right)} \right.$$

$$\left. - \frac{A_2(s)\ (s^3 T_1 T_2 + s^2(T_1+T_2) + s(3\omega^2 T_1 T_2 + 1) + 2\omega^2(T_1 + T_2))}{(s + \frac{1}{T_m})\ \left((s + \frac{1}{T_1})^2 + \omega^2\right)\ \left((s+ \frac{1}{T_2})^2 + \omega^2\right)} \right) \quad \ldots (4.41)$$

where $H_1 = \frac{H}{\omega}$

For a step change in the phase between the control and reference voltages from an initial angle ϕ_2 to a final angle ϕ_1

$$A_1(s) = V_D \cdot \frac{\sin\phi_2 - \sin\phi_1}{s}$$

$$A_2(s) = V_D \cdot \frac{\cos\phi_2 - \cos\phi_1}{s}$$

from which it follows that

$$\Delta\omega_r(s) = V_D\, H_1 \left[\frac{\omega C_{11}\left(2\ (1 - \omega^2 T_1 T_2) + s(T_1 + T_2)\right)}{s(s + \frac{1}{T_m})\left((s + \frac{1}{T_1})^2 + \omega^2\right)\left((s+ \frac{1}{T_2})^2 + \omega^2\right)} - \right.$$

$$\left. \frac{C_{22}\ (s^3 T_1 T_2 + s^2(T_1 + T_2) + s(3\omega^2 T_1 T_2 + 1) + 2\omega^2(T_1 + T_2))}{s(s + \frac{1}{T_m})\ \left((s + \frac{1}{T_1})^2 + \omega^2\right)\ \left((s + \frac{1}{T_2})^2 + \omega^2\right)} \right] \quad \ldots (4.42)$$

where

$$C_{11} = \sin\phi_2 - \sin\phi_1$$

$$C_{22} = \cos\phi_2 - \cos\phi_1$$

The first term in the square bracket is exactly that for which the speed response was obtained in section (4.2.1). In investigating by the same procedure the second term, it is found that

$$\frac{A(o)}{B_1(o)} = \frac{2\omega^2(T_1 + T_2)\, T_m\, T_1^2\, T_2^2}{(1 + \omega^2 T_1^2)(1 + \omega^2 T_2^2)}$$

$$A(s) = s^3 T_1 T_2 + s^2(T_1 + T_2) + s(3\omega^2 T_1 T_2 + 1) + 2\omega^2(T_1 + T_2)$$

$$s_2 = -\frac{1}{T_m}$$

$$A(s_2) = \frac{-T_1 T_2 + T_m(T_1 + T_2) - T_m^2(3\omega^2 T_1 T_2 + 1) + T_m^3\, 2\omega^2(T_1 + T_2)}{T_m^3}$$

$$A(s_3) = -(\frac{1}{T_1} + j\omega)^3 T_1 T_2 + (\frac{1}{T_1} + j\omega)^2(T_1 + T_2) - (\frac{1}{T_1} + j\omega)(3\omega^2 T_1 T_2 + 1) + 2\omega^2(T_1 + T_2)$$

$$A(s_3) = \omega^2(T_1 + T_2) + j\omega(1 - 2\omega^2 T_1 T_2 - \frac{T_2}{T_1}) = a_3 + jb_3$$

$$A(s_4) = \omega^2(T_1 + T_2) - j\omega(1 - 2\omega^2 T_1 T_2 - \frac{T_2}{T_1}) = a_3 - jb_3$$

} a conjugate pair

Similarly

$$A(s_5) = -(\frac{1}{T_2} + j\omega)^3 T_1 T_2 + (\frac{1}{T_2} + j\omega)^2 (T_1 + T_2) - (\frac{1}{T_2} + j\omega)(3\omega^2 T_1 T_2 + 1) + 2\omega^2(T_1 + T_2)$$

$$= \omega^2(T_1 + T_2) + j\omega(1 - 2\omega^2 T_1 T_2 - \frac{T_1}{T_2}) = a_5 + jb_5$$

Since s_5 and s_6 are conjugate, it follows that

$$A(s_6) = \omega^2(T_1 + T_2) - j\omega(1 - 2\omega^2 T_1 T_2 - \frac{T_1}{T_2}) = a_5 - jb_5$$

$s_2 B_1'(s_2)$, $s_3 B_1'(s_3)$, $s_4 B_1'(s_4)$, $s_5 B_1'(s_5)$ and $s_6 B_1'(s_6)$ are all as before.

On obtaining the summation of equation (4.1b)

$$\Delta\omega_r(t) = H V_D C_{11} \left[\frac{2(1 - \omega^2 T_1 T_2) T_m\, T_1^2 T_2^2}{(1 + \omega^2 T_1^2)(1 + \omega^2 T_2^2)} \right.$$

$$- \frac{(2(1 - \omega^2 T_1 T_2) - \frac{T_1 + T_2}{T_m}) T_m^5 T_1^2 T_2^2}{((T_m - T_1)^2 + \omega^2 T_1^2 T_m^2)((T_m - T_2)^2 + \omega^2 T_2^2 T_m^2)} \cdot e^{-\frac{1}{T_m} t}$$

$$+ 2 \left(e^{-\frac{1}{T_1} t} \cdot \frac{x_1 \lambda - \omega T y_1}{x_1^2 + y_1^2} + e^{-\frac{1}{T_2} t} \cdot \frac{x_2 \lambda' - \omega T y_2}{x_2^2 + y_2^2}\right) \cos \omega t$$

$$- 2 \left(e^{-\frac{1}{T_1} t} \cdot \frac{y_1 \lambda + \omega T x_1}{x_1^2 + y_1^2} + e^{-\frac{1}{T_2} t} \cdot \frac{y_2 \lambda' + \omega T x_2}{x_2^2 + y_2^2}\right) \sin \omega t \Bigg]$$

$$- V_D \frac{H}{\omega} C_{22} \Bigg[\frac{2\omega^2 (T_1 + T_2) T_m T_1^2 T_2^2}{(1 + \omega^2 T_1^2)(1 + \omega^2 T_2^2)} -$$

$$(T_m T_1 T_2)^2 \cdot \frac{- T_1 T_2 + T_m (T_1 + T_2) - T_m^2 (3\omega^2 T_1 T_2 + 1) + 2 T_m^3 \omega^2 (T_1 + T_2)}{((T_m - T_1)^2 + (\omega T_1 T_m)^2)((T_m - T_2)^2 + (\omega T_2 T_m)^2)} e^{-\frac{1}{T_m} t}$$

$$+ 2 \left(e^{-\frac{1}{T_1} t} \cdot \frac{a_3 x_1 + b_3 y_1}{x_1^2 + y_1^2} + e^{-\frac{1}{T_2} t} \cdot \frac{a_5 x_2 + b_5 y_2}{x_2^2 + y_2^2} \right) \cos \omega t$$

$$+ 2 \left(e^{-\frac{1}{T_1} t} \cdot \frac{b_3 x_1 - a_3 y_1}{x_1^2 + y_1^2} + e^{-\frac{1}{T_2} t} \cdot \frac{b_5 x_2 - a_5 y_2}{x_2^2 + y_2^2} \right) \sin \omega t \Bigg] \quad \ldots (4.43)$$

where $a_3 = a_5 = \omega^2 (T_1 + T_2)$

$$b_3 = \omega \left(1 - 2\omega^2 T_1 T_2 - \frac{T_2}{T_1}\right)$$

$$b_5 = \omega \left(1 - 2\omega^2 T_1 T_2 - \frac{T_1}{T_2}\right)$$

x_1, x_2, , y_1, y_2, T, λ, λ' and H are as before.

4.4 Transfer function relating speed and torque

The equation for the mechanical system is

mechanical torque = inertia torque + frictional torque

$$\text{i.e.} \quad T_M(s) = (Js + f)\,\omega_r(s)$$

$$= f(1 + T_m s)\omega_r(s)$$

$$\text{or} \quad \omega_r(s) = \frac{T_M(s)}{f(1 + sT_m)}$$

On replacing $T_M(s)$ by $\frac{T_{MI}}{s}$, the speed response following a step change in the mechanical torque is given as

$$\omega_{rl}(s) = \frac{T_{MI}}{f} \cdot \frac{\frac{1}{T_m}}{s(s + \frac{1}{T_m})} \qquad \ldots\ldots (4.44)$$

The required time response of the speed is provided by obtaining the inverse Laplace transform of equation (4.44). From standard Laplace transformations, this can be written as

$$\omega_{rl}(t) = \frac{T_{MI}}{f}\left(1 - e^{-\frac{1}{T_m}t}\right) \qquad \ldots\ldots (4.45)$$

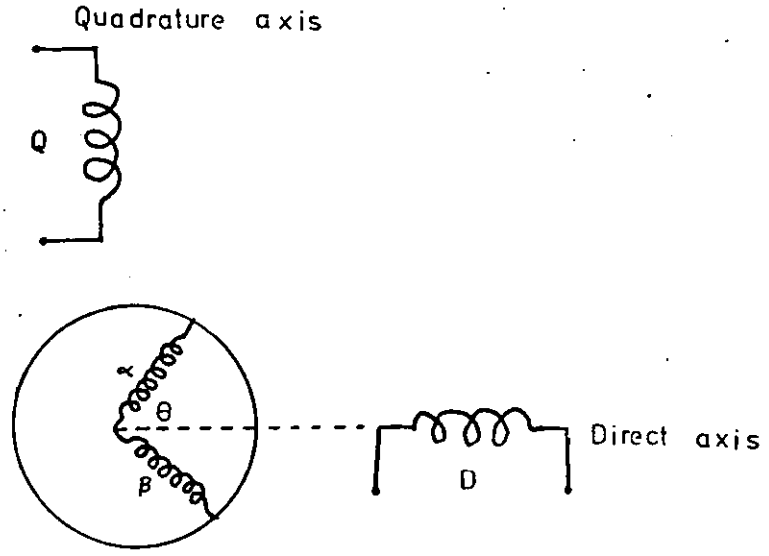

Fig. 4.1a A two pole 2-phase symmetrical machine

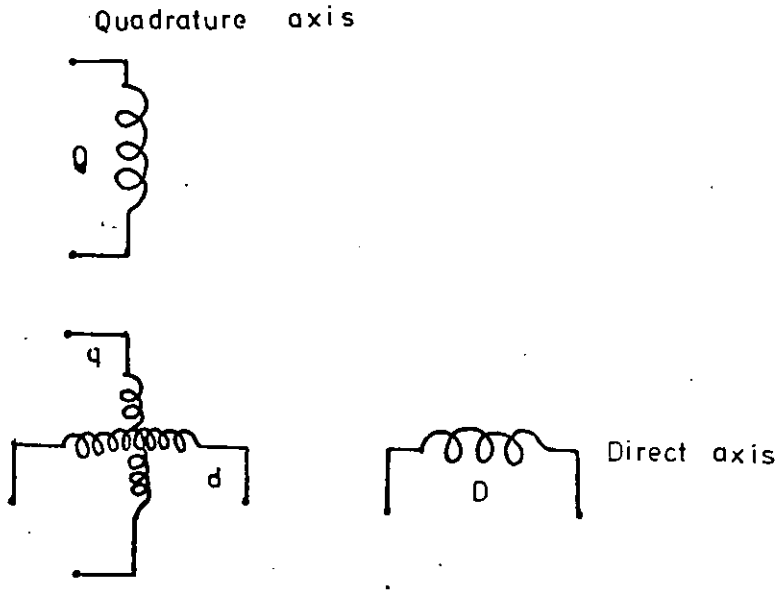

Fig. 4.1b Stationary axis equivalent of the 2-phase servomotor

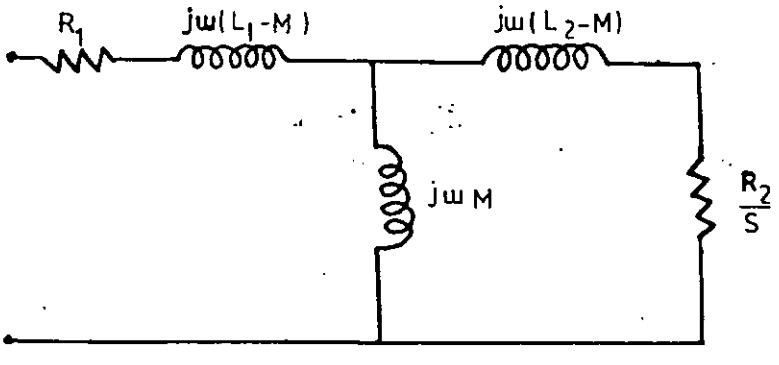

Fig. 4.1c Equivalent circuit per phase

CHAPTER 5. EXPERIMENTAL PROCEDURE AND COMPARISON OF RESULTS

In order to compare the transient behaviour of the servomotor, as predicted by the results of the previous chapter, with its experimental performance, it is clearly necessary for an accurate measurement of the machine parameters to be made. The two techniques most commonly used for this purpose are described below, and the measured parameters of a typical servomotor are given.

5.1 The use of an a.c. impedance circle diagram

The use of an a.c. impedance circle for determining servomotor parameters was first described by Rekoffyr [26,27]. The technique neglects any core loss in the motor and assumes that the control and reference windings are identical, as are the stator and rotor leakage reactances.

Test data is obtained by connecting the servomotor to a 2-phase source of rated machine voltage, and measuring the impedance of one of the windings at two known values of slip (conveniently $S_1 = 0$ and $S_2 = 1$). As shown in the impedance circle diagram of Fig. (5.1), the impedance data of the two slips is plotted on a graph, with an ordinate of inductive reactance x and an abscissa of resistance R. A semicircle is then drawn through the two points, wih its centre on a line parallel to the x axis and passing through the data point at zero slip. A perpendicular bisector to the chord between the data points, $S = 0$ and $S = 1$, cuts the vertical line through $S = 0$ at the centre of the circle. The semicircle can then be drawn as shown, and extended by the horizontal lines which cut the ordinate at δ and β. A horizontal line through $S = 1$ cuts this axis at γ.

With the construction as shown, a vertical line through $S = 0$ obviously intersects the abscissa at the value of the stator resistance R_1 and a horizontal line at the value of

$$\delta = x_m + x_\ell \qquad \ldots\ (5.1)$$

where x_m and x_ℓ are the mutual and leakage reactances. The intersection on the ordinate at β is the value of the input reactance at $S = \infty$, and is thus

$$\beta = x_\ell + \frac{x_m x_\ell}{x_m + x_\ell} \qquad \ldots\ (5.2)$$

Hence

$$x_m = \sqrt{\delta^2 - \delta\beta} \qquad \ldots\ (5.3)$$

and

$$x_\ell = \delta - x_m$$

Similarly, the projection on the ordinate of $S = 1$ gives

$$\gamma = x_\ell + \frac{x_m R_2^2 + x_m x_\ell (x_m + x_\ell)}{R_2^2 + (x_m + x_\ell)^2} \qquad \ldots\ (5.4)$$

from which

$$R_2 = \sqrt{\frac{x_m x_\ell \delta - (\gamma - x_\ell)\delta^2}{\gamma - (x_m + x_\ell)}}$$

and all the impedances of the motor can be obtained.

5.2 Alternative interpretation of measured data

Some of the limitations in the technique described in the previous section are removed when the measured data is analysed as suggested by Hughes [28]. The stator and rotor leakage reactances are no longer assumed equal, and the analysis provides values of R_1, L_1, $\frac{M^2}{R_2}$ and $\frac{L_2}{R_2}$, which, as the previous chapter has shown, is sufficient to enable the transfer functions of the motor to be evaluated.

From Fig. 4.1(c), the input impedance per phase at frequency ω and slip S is

$$Z_p = R_1 + \frac{\frac{1}{S}\omega^2 \cdot \frac{M^2}{R_2}}{\frac{1}{S^2} + \frac{\omega^2 L_2^2}{R_2^2}} + j\left(\omega L_1 - \frac{\omega^3 \frac{M^2}{R_2} \cdot \frac{L_2}{R_2}}{\frac{1}{S^2} + \frac{\omega^2 \cdot L_2^2}{R_2^2}}\right) \quad \ldots\ (5.5)$$

If the input impedance at the no-load slip of s_o is $Z_o e^{j\phi_o}$ and that at the locked-rotor slip of S = 1 is $Z_1' e^{j\phi_\beta}$, then on separating the real and imaginary parts of equation (5.5), we obtain

$$Z_1' \cos\phi_\beta = R_1 + \frac{\omega^2 \frac{M^2}{R_2}}{1 + \omega^2 T_2^2} \quad \ldots\ (5.6)$$

$$Z_1' \sin\phi_\beta = \omega\left(L_1 - \frac{\omega^2 \cdot \frac{M^2}{R_2} \cdot T_2}{1 + \omega^2 T_2^2}\right) \quad \ldots\ (5.7)$$

and

$$Z_o \cos\phi_o = R_1 + \frac{1}{s_o} \cdot \frac{\omega^2 \frac{M^2}{R_2}}{\frac{1}{s_o^2} + \omega^2 T_2^2} \quad \ldots\ (5.8)$$

$$Z_o \sin\phi_o = \omega\left(L_1 - \frac{T_2 \cdot \omega^2 \frac{M^2}{R_2}}{\frac{1}{s_o^2} + \omega^2 T_2^2}\right) \quad \ldots\ (5.9)$$

On subtracting equation (5.9) from equation (5.7) and rearranging we obtain

$$\frac{M^2}{R_2} = \frac{(Z_o \sin\phi_o - Z_1' \sin\phi_\beta)(1 + \omega^2 T_2^2)(\frac{1}{s_o^2} + \omega^2 T_2^2)}{(\frac{1}{s_o^2} - 1)\omega^3 T_2} \quad \ldots\ (5.10)$$

and on substituting this result in equations (5.6) and (5.7) the stator resistance and inductance are obtained as

$$R_1 = Z_1' \cos\phi_\beta - \frac{(Z_o \sin\phi_o - Z_1' \sin\phi_\beta)(\frac{1}{s_o^2} + \omega^2 T_2^2)}{(\frac{1}{s_o^2} - 1)\ \omega T_2} \quad \ldots\ (5.11)$$

$$L_1 = \frac{Z_1' \sin\phi_\beta}{\omega} + \frac{(Z_o \sin\phi_o - Z_1' \sin\phi_\beta)(\frac{1}{s_o^2} + \omega^2 T_2^2)}{\omega(\frac{1}{s_o^2} - 1)} \quad \ldots\ (5.12)$$

After subtracting equations (5.9) and (5.7) and also equations (5.6) and (5.8), and then dividing the first result by the second, the rotor time constant $\frac{L_2}{R_2}$ can be obtained from the resulting equation.

$$\frac{Z_o \sin\phi_o - Z_1' \sin\phi_\beta}{Z_1' \cos\phi_\beta - Z_o \cos\phi_o} = \frac{\omega T_2 (1 + \frac{1}{s_o})}{\frac{1}{s_o} - \omega^2 T_2^2} \quad \ldots\ (5.13)$$

5.3 Experimental motor

The tests described in the previous sections were carried out on a servomotor with the following manufacturer's data, quoted at a motor temperature of approximately 65°C.

Type FAF102/H_3	5.3 watts, 50 Hz, 115 volts, identical stator windings
starting torque	= 540 gm cm
	= 540×10^{-5} kg m
rotor moment of inertia	= 58.6 gm cm^2
	= 0.586×10^{-5} kg m^2
initial acceleration	= 9050 rad/sec^2
static friction	= 5.8×10^{-5} kgm
single phasing torque at 50 Hz	= 21.6 gm cm
motor stalled input per phase at rated voltage	= 15.0 watts
	= 17.5 VA
stalled impedance per phase	= 830 ohms
stalled power factor	= 0.86
number of pole pairs	= 1
nominal d.c. resistance per phase	= 185 ohms
plain shaft diameter	= 6.35 mm
overall weight	= 1100 gms

5.3.1 No load and locked rotor test results

With the reference phase of the experimental servomotor supplied at rated voltage, the control voltage was varied from 0 to 130 volts (i.e. 113% of rated voltage). Both open and short circuit characteristics were measured, as shown in Fig. (5.2) and (5.3).

At rated control voltage, the no load test data obtained for the reference and control phases is:

reference phase current = 127 mA

power factor $= \frac{4.9}{14.6}$

$= 0.3356$

Hence, input impedance of the reference phase = $905.51 \angle 70.39^{\circ}$ ohms

control phase current = 127 mA

power factor $= \frac{4.5}{14.6}$

$= 0.3082$

Hence, input impedance of control phase = $905.51 \angle 72.05$ ohms

no load speed = 2940 r.p.m.

Similarly, from the rated voltage, locked rotor results shown in Fig. (5.3)

reference phase current = 160 mA

power factor $= \frac{16.125}{18.4}$

$= 0.8764$

Hence, input impedance of reference phase

= $718.75 \angle 28.79$ ohms

control phase current = 160 mA

power factor $= \frac{16}{18.4}$

$= 0.8696$

Hence, input impedance of the control phase = $718.75 \angle 29.59$ ohms

5.3.2 Calculation of servomotor parameters using a.c. impedance circle diagram

Following the constructional procedure outlined in section (5.1), we obtain the scales for the a.c. impedance circle diagram of Fig (5.1), from which δ = 857.51 ohms, β = 125 ohms, γ = 350.75 ohms, α = 291.5 ohms.

From this data and the equations given in section (5.1) , the equivalent circuit impedances are found as

$R_1 = \alpha$ = 291.5 ohms

R_2 = 572.36 "

X_m = 792.56 "

X_ℓ = 64.95 "

Hence $M = \frac{X_m}{\omega}$

= 2.52 henrys

$\ell = \frac{X_\ell}{\omega}$ "

= 0.21 "

$L_1 = L_2$

$= M + \ell$

= 2.73 henrys

$T_2 = \frac{L_2}{R_2}$

= 4.77 m sec

$\frac{M^2}{R_2}$ = 0.01109

When the test results are analysed by the method outlined in section (5.2), the motor parameter terms required in equations (4.35) and (4.43) are

$$Z'_1 \cos \phi_\beta = 627.467 \quad \text{ohms}$$

$$Z'_1 \sin \phi_\beta = 350.750 \quad "$$

$$Z_o \cos \phi_o = 291.574 \quad "$$

$$Z_o \sin \phi_o = 857.518 \quad "$$

and since

$$s_o = 0.02$$

it follows that

$$R_1 = 270.157 \text{ ohms}$$

$$L_1 = 2.7315 \text{ henrys}$$

$$T_2 = L_2/R_2$$

$$= 4.52 \text{ m sec}$$

$$\frac{M^2}{R_2} = 0.0109202 \quad (\text{henry})^2/\text{ohm}$$

which all agree closely with the results obtained from the circle diagram. The stalled resistance, inductance and time constant of the stator required in equations (4.35) and (4.43) are given by equations (4.9a) and (4.9b) as

$$R'_1 = 627.467 \text{ ohms}$$

$$L'_1 = 1.12 \text{ henrys}$$

5.4 Steady state torque-speed characteristics at various control voltages

In addition to the no-load and stalled tests, the steady-state torque-speed characteristics of the servomotor were established with the reference winding supplied at rated voltage with the control winding voltage varied in 20% steps from zero to the rated value. The motor was loaded as shown in Fig (5.4) and the experimentally obtained torque/speed characteristics are shown in Fig (5.5). These curves resemble closely corresponding curves provided by the manufacturers and are similar to results obtained by previous workers on different machines.[8,11,15]

5.5 Determination of various parameters affecting the dynamic characteristics

5.5.1 Determination of the mechanical viscous-friction damping

Determination of the coefficients in the speed response equations for the servomotor (see sections (4.2.1) and (4.3.1)), for step changes in either the magnitude or the phase of the control winding voltage, necessitates that the mechanical viscous damping should be known under stalled conditions. Damping is generally defined as the slope of the torque/speed characteristics of the motor, and Fig. (5.5) shows that this decreases in a nonlinear manner with the control voltage. In a position servo, internal damping of the motor is utilized in producing a stable control system. The operating point at stall, with zero control voltage, is thus particularly important, since it is here that secondary effects such as backlash tend to cause trouble. As Fig. (5.3) shows, even in a practical motor, with a nonlinear torque-speed characteristics, the stall torque is almost proportional to the control voltage.

It has been well established by previous workers that, for small servomotors, the damping at zero speed and zero control voltage is about half the slope of the torque/speed curve for balanced operation. The curve relating stalled damping to control winding voltage has been regarded as roughly parabolic, with the minimum damping at zero control voltage [3]. A reasonably accurate estimate of the effective stalled damping can be obtained.

From Fig. (5.5), by extending the straight portion of the torque-speed curve near no load speed to meet the torque axis at T_s', when [3]

$$\text{effective stalled damping } (f_e) = \text{Average damping } \left(1 - 2\left(\frac{T_s' - T_s}{T_s'}\right)\right) \quad \ldots (5.14)$$

where

$$\text{Average damping } (f_a) = \frac{\text{actual stalled torque } (T_s)}{\text{no load speed}}$$

Calculations based merely on the average damping (in which the term in the brackets is ignored) have been shown to be in error by factors of three or more [3]. For the experimental motor, the effective and average damping coefficients obtained from Fig. (5.5) are given in Table (5.1).

When a series of step changes was made in the control winding voltage, the experimentally obtained changes in speed are as given in Table (5.1). The Table also shows the changes in speed found from the two values of the damping coefficients, and the necessity for the corrected value is clear. The Table indicates that although a parabolic variation of damping with the control winding voltage is a reasonable assumption above 25% voltage, the damping coefficient of the machine tested may conveniently be assumed constant below this voltage.

5.5.2 Determination of the Coulomb friction:

The servomotor was run at no load with rated voltages applied to both control and reference windings. The tachogenerator output was fed to the u.v recorder, through the complex-matching circuit shown in Fig. (5.6). The supplies to both windings were switched off, and the speed/time characteristic was recorded as the motor ran down to standstill. The deceleration at different speeds was obtained by finding the gradient of the curve at the appropriate speed. From a knowledge of the moment of inertia, the curve in Fig. (5.7), showing the variation in deceleration torque with speed, was then obtained. The figure thereby

obtained should not be confused with the curve of electromagnetically-produced torque against speed shown in Fig. (5.5). Since frictional torque was assumed to vary linearly with speed (see Section 4.4), the best straight-line fit to Fig (5.7) was obtained using the method of least squares, and the Coulomb friction (i.e. the frictional torque at zero speed) thus obtained as 2.3 gm cm.

Although for the experimental machine the Coulomb friction is very small in comparison with the stalled torque under balanced conditions of 585 gm cm (see Fig. (5.5)), some previous workers [15] have taken it into consideration when establishing curves of the speed response following step changes in the control voltage.

5.5.3 Determination of best linearity of tachogenerator output

With the tachgenerator terminated in loads of 2 kΩ, 5 kΩ and 10 kΩ , the output voltage was measured over the full range of servomotor speed. The voltage/speed characteristics thus obtained are shown in Fig. (5.8) and they establish that the most linear relationship between the quantities is obtained with the output terminated in a 5 kΩ load.

5.6 Transient speed response

The speed response of the servomotor following a step change in the input conditions was obtained from measurements of the output of the tachogenerator (the coefficient of mechanical viscous damping measured before included the contribution provided by this machine), terminated in a 5 kΩ load. Since this is too high a source impedance for the electromagnetically damped galvanometers used, it was necessary to use the damping circuit shown in Fig. (5.6).

Before performing any experiments, the overall linearity of the tachogenerator and ultra-violet recorder was determined, with the resulting characteristics as shown in Fig. (5.9). From this graph, the overall measurement sensitivity is

$$\frac{\text{peak to peak galvanometer deflection (cm)}}{\text{speed (r.p.m.)}} = 0.0046153 \text{ cm/r.p.m.}$$

or

$$\frac{\text{speed (r.p.m.)}}{\text{peak to peak galvanometer deflection}} = 216.667 \text{ r.p.m.}$$

5.7 Speed response following a step change in the control voltage:

With the reference winding of the servomotor supplied at rated voltage from phase A to the neutral of the laboratory supply, the motor control winding was supplied from the line voltage between phases B and C, to provide the necessary 90^{o} phase shift. The motor control voltage was chosen to lead the reference winding voltage by 90^{o}, the resulting direction of rotation being counter-clockwise when viewed from the drive end. The line voltage V_{BC} was controlled to any desired value by a variac. A series of tests was performed, in which step function changes were made in the control winding voltage, from an initial value of zero, and the speed response was obtained from the tachogenerator output. The height of the step change was varied from a very small value to rated value, and the results obtained are as shown in Fig. (5.10).

5.7.1 Computed speed/time curves using ideal servomotor model

The early analyses which assumed linear torque/speed characteristics (see section 3.1.1)) led to a transfer function as given in equation (3.3).

From this it follows that, for a step change in the control voltage,

$$\omega_r(s) = V_D \frac{K_2}{f - k_1} \cdot \frac{1}{s} \cdot \frac{1}{1 + T_m s}$$

and thus that the corresponding speed response is

$$\omega_r(t) = V_D \cdot \frac{K_2}{f - k_1} (1 - e^{-\frac{1}{T_m} t}) \qquad \ldots (5.15)$$

The viscous damping coefficient (f) in this equation is defined by Balmer and Lewis [12] as the slope of the straight-line torque/speed characteristics of the idealised machine. Since the actual torque/speed curves depart somewhat from this ideal situation, an estimate of (f) was obtained for each of the curves of Fig. (5.5), as the average slope between zero speed and zero torque. The parameters required for the calculation of the speed response are:

V_D (volts)	115	92	69	50	30	15	5	2.6
$K_1 \times 10^5$ (Nm rad sec^{-1})	-18.64	-16.4	-12.6	-9.55	-7.26	-6.04	-5.80	-5.66
$K_2 \times 10^5$ (Nm/volt)	49.90	53.32	52.60	51.012	50.685	50.69	49.05	47.16
$f \times 10^5$ (Nm/rad sec^{-1})	18.64	16.4	12.6	9.55	7.26	6.04	5.80	5.66
T_m (msec) ($J = 0.586 \times 10^{-5}$ Kg m^2)	15.72	17.9	23.3	30.7	40.4	48.51	50.52	51.8

V_Q = 115 volts

Using this information the corresponding speed/time curves were calculated from equation (5.15) and added in Fig. (5.10).

5.7.2 Speed/time curves based on more detailed early analyses:

The approximate solution of the servomotor differential equation, given by Hopkins [15], was also used to compute the speed variation with time of the experimental motor, following a step change in the control voltage magnitude.

In equation (3.13) of section (3.1.2)

$$\omega_r = \omega_{ss}\left(1 - e^{-\frac{1}{T}t}\right) \qquad \ldots\ (5.16)$$

where

$$T = \frac{2 J \omega_s}{K(V_r^2 + V_c^2) + 2 f\omega_s}$$

$$\omega_{ss} = \frac{2 \omega_s(K V_r V_c - a)}{K (V_r^2 + V_c^2) + 2 f\omega_s}$$

The torque constant K for balanced operation

$$K = \frac{T_\varepsilon}{V^2\left(1 - \frac{\omega_r}{\omega_s}\right)} \qquad V = V_c = V_r$$

where its value at a speed 2860 r.p.m. is obtained from Fig. (5.5) as

$$K = 0.3974 \times 10^{-5} \quad \text{Nm/volt}^2$$

The stalled value is obtained from the same figure as

$$K_s = 0.4339 \times 10^{-5} \text{ Nm/volt}^2$$

and is assumed constant over the entire range of control winding voltage.

Together with data obtained in the previous section, this enabled the speed/time curve to be calculated from equation (5.16) and the results obtained are also included in Fig. (5.10).

5.7.3 Speed/time curves obtained by complex convolution approach

Equation (4.35) from Section (4.2.1) was used to compute speed/time curves for the experimental motor, following step changes in the control voltages ofthe same magnitude as in the previous two sections, using values of the rotor and stator time constants given in sections (5.3.1) and (5.3.2). For the nonlinear torque/speed curves of Fig. (5.5) the effective mechanical viscous damping (f) for each control voltage was obtained as described in section (5.5.1)as

V_D (volts) r.m.s.	115	92	69	50	30	23	15	5	2.6
f x 10^5 Nm/rad sec^{-1}	10.28	8.6	6.98	5.48	4.04	3.23	3.23	3.23	3.23

V_Q (r.m.s.) = 115

From a knowledge of the moment of inertia, the time constant (T_m) for the mechanical system at each control voltage was then obtained, and the speed/time curves were computed, and added to Fig. (5.10). The computer programme is shown in appendix (8.2.a).

5.7.4 Comparison of results

Generally, the experimental speed/time curves obtained are of approximately exponential form, with a time constant that increases with a decreasing magnitude of the control voltage step. Curves computed on the basis of the ideal model of the servomotor and the approximate solution of the differential equations of the motor agree reasonably closely, as is expected from the similar forms of the transfer functions given in equations (3.3) and (3.13). A very

obvious feature of the graphs is that the curves computed from the complex-convolution approach are much closer to the experimental curves than are results obtained from either of the other theoretical approaches, especially when the control voltage is low. Computed results using the complex-convolution approach become closer to the experimental curves at very low speeds, validating the simplifications made by introducing the stalled stator terms of the machine, as given in section (4.1).

Using both early approaches, the computed steady-state speeds, over the whole range of voltages, are much lower than those given by the complex-convolution approach, which are also much closer to the experimental.

Although Hopkins attempted to analyse the unbalanced operation using symmetrical components, his results include a torque constant which applies for balanced steady-state operation at rated voltage. The values of torque constant at stall and at a high speed, given in Section (5.7.2), result in two values of steady-state speed. It is clear from equation (5.16) that the speed/time curves obtained using the stalled value of the torque constant gives results closer to the experimental than the value for high speeds. This case is taken to give the best possible results that can be obtained using Hopkins approach.

Taking values of mechanical damping of Section (5.7.1), the steady state speeds following the same step changes in control voltage were calculated using the complex convolution approach. The results obtained are given in Table (5.1) and can be seen to be closer to the experimental results than the corresponding results obtained by previous workers.

5.8 Speed responses following step changes in the angle between control and reference voltages

The circuit diagram shown in Fig. (5.11) was used to obtain a step change of 60^{o} in the phase of the control winding voltage. The primary sides of two single-phase transformers were fed from phases A and B of the supply, and the secondaries were connected in series to give rated voltage. This was fed to the control winding of the experimental machine and the reference winding was supplied directly from the phase A voltage. With the switch S_1 open the motor was run at rated steady-state speed. When the switch S_1 was closed, fuse F_1 was blown, and a step change from $+120^{o}$ to $+60^{o}$ was made in the phase angle between the reference and control winding voltages. Similarly, a step change of from -30^{o} to $+30^{o}$ was obtained from the circuit shown in Fig. (5.12).

5.8.1 Computation of speed/time curves following step changes in the phase angle:

Equation (4.43) of Section (4.3.1) for the change in speed following a step change in the phase shift of the control voltage can be rewritten as

$$\Delta\omega_r(t) = A_1 A(t) - B_1 B(t) \qquad \ldots\ldots (5.17)$$

or $$\Delta\omega_r(t) = (\sin\phi_2 - \sin\phi_1) A(t) - (\cos\phi_2 - \cos\phi_1) B(t)$$

where A(t) and B(t) are the coefficients of A_1 and B_1 in equation (5.17)

For angular step changes from

(a) -30^{o} to $+30^{o}$ and

(b) 120^{o} to 60^{o}, the corresponding speed changes are, respectively, given by

$$\Delta\omega_r(t) = (\sin(-30) - \sin 30)\, A(t) - (\cos(-30) - \cos 30)\, B(t)$$

$$= -A(t) \qquad \ldots (5.18)$$

and

$$\Delta\omega_r(t) = (\sin 120 - \sin 60)\, A(t) - (\cos 120 - \cos 60)\, B(t)$$

$$= B(t) \qquad \ldots (5.19)$$

5.8.2 Determination of the coefficient of mechanical damping when the angle between the control and reference voltages is 30°

The magnitude of the electromagnetic torque when the rated control voltage leads the reference voltage by an angle of $|\phi| < 90^\circ$ can be found from section (2.1.3) as

$$T_\varepsilon(\phi) = \frac{1}{2}\left(T_{Eb}(S)(1 + \sin\phi) - T_{Eb}(2 - S)(1 - \sin\phi)\right) \qquad \ldots (5.20)$$

where

$$T_{Eb}(S) = \frac{2}{\omega_s} |I_2|^2 \frac{R_2}{S}$$

is the torque obtained at a slip S with balanced supply voltages and $T_{Eb}(2 - S)$ is the torque obtained by replacing S by $(2 - S)$ in the expression for $T_{Eb}(S)$.

From the measured data of the machine, given in section (5.3.2), and the equivalent circuit of Fig. (4.1.c).

$$T_{Eb}(S) = \frac{S}{2.066\, S^2 + 6.926\, S + 8.964}\ N_m \qquad \ldots (5.21)$$

and

$$T_{Eb}(2 - S) = \frac{2 - S}{2.066\,(2 - S)^2 + 6.926\,(2 - S) + 8.964} \qquad \ldots (5.22)$$

Using equations (5.21), (5.22) and (5.20), the motor torques at speeds of -2000 r.p.m. and +2000 r.p.m., were calculated for a phase shift

of 30° as 0.040388 and 0.0058415 Nm respectively.

The corresponding coefficient of mechanical damping is

$$f = \frac{\Delta T_e}{\Delta \omega_r}$$

$$= \frac{0.0345465}{418.88}$$

$$= 8.24 \times 10^{-5} \text{ Nm/rad sec}^{-1}$$

from which the mechanical time constant follows as

$$T_m = J/f$$

$$= \frac{0.586 \times 10^{-5}}{8.24 \times 10^{-5}}$$

$$= 0.07112 \text{ secs}$$

Using equations (4.43) and (5.18) the speed response for a step change from -30° to $+30^{\circ}$ was computed, and was found to agree reasonably with the experimental result as shown in Fig. (5.13). (Computer programme is shown in Appendix (8.2b)).

5.8.3 Determination of the coefficient of mechanical damping when the angle between the control and reference voltages changes from 120° to 60°

For a step change in the angle from 120° to 60° the speed changes from an initial value of 2600 r.p.m. to a minimum of 2400 r.p.m. and then recovered to a final value of 2615 r.p.m.

Using equations (5.21), (5.22) and (5.20), the torque of the motor at speeds of 2600 r.p.m., 2400 r.p.m. and 2615 r.p.m. was calculated for a phase shift of 60° as 0.0082 Nm, 0.01359 Nm and 0.00778 Nm

respectively. The change in the magnitude of the torque for speeds 2600 r.p.m. and 2400 r.p.m. is 0.00539 Nm; and for the speeds 2400 r.p.m. and 2615 r.p.m. it is 0.00581 Nm. The total change in the torque between the initial and final states is:

$$\Delta T_\varepsilon = 0.00581 + 0.00539$$

$$= 0.0112 \text{ Nm}$$

and the change in speed, $\Delta\omega_r = 2615 - 2600 = 15$ r.p.m. Ideally, of course, ΔT_ε and $\Delta\omega_r$ should both be zero.

The corresponding coefficient of mechanical damping is

$$f = \frac{\Delta T_\varepsilon}{\Delta \omega_r}$$

$$= \frac{0.0112}{1.571}$$

$$= 713 \times 10^{-5} \text{ Nm/rad.sec}^{-1}$$

Following the same procedure, the motor torques at speeds of 2600 r.p.m., 2400 and 2615 r.p.m. were calculated for a phase shift of 75° as 0.0118665, 0.0177856 and 0.01164 Nm. It then follows that

$$\Delta T_\varepsilon = 0.01206591 \text{ Nm}$$

and that

$$f = \frac{\Delta T_\varepsilon}{\Delta \omega_r}$$

$$= \frac{0.01206591}{1.571}$$

$$= 768. \times 10^{-5} \text{ Nm/rad.sec}^{-1}$$

Taking the average mechanical damping as

$$f = 740.5 \times 10^{-5} \text{ Nm/rad sec}^{-1}$$

gives

$$T_m = \frac{J}{f}$$

$$= \frac{0.586 \times 10^{-5}}{740.5 \times 10^{-5}} = 0.00079 \text{ sec}$$

Using equations (4.43) and (5.19) the speed response for a step change from 120^{o} to 60^{o} was computed (computer programme shown in Appendix 8.2.b). The computed speed change decreases to about 2400 r.p.m. in approximately 15 msecs and increases to the steady state as shown in Fig. (5.14). Experimentally obtained results are also shown in this figure, and it is clear that a quite close prediction of these has been achieved.

5.9 Speed response following step changes in torque at various control voltages.

To obtain a torque on the motor, known weights were suspended on a thin string wrapped once round the shaft in a direction opposed to the rotation. The upper end of the string was attached to a spring balance. The reference winding of the motor was supplied with rated voltage and the control winding with 20% of the rated voltage, and the motor was allowed to reach steady state speed. Various step changes of torque were then applied at the shaft, and the corresponding speed response was obtained from the tachogenerator. The experiment was repeated with the control voltage raised in steps of 20% to rated voltage.

5.9.1 Computation of speed/time curves following step changes in torque at various control voltages:

Equation (4.45) was utilized to find theoretical changes in speed following step changes in the load torque, with the motor initially running at steady state speed and on no load. Thus, the required speed response can be written

$$\omega_r(t) = \omega_i - \frac{T_{MI}}{f}\left(1 - e^{-\frac{1}{T_m} \cdot t}\right) \qquad \ldots (5.23)$$

where

ω_i = initial steady-state no load speed at a certain control voltage.

T_{MI} = step input torque

f = mechanical damping

Speed/time curves calculated from equation (5.23) are given in Fig. (5.15) for several different values of T_{MI} with rated voltage applied to both stator windings. The figure for the mechanical damping(f)was obtained from the torque/speed characteristics of Fig. (5.5), as the slope of the straight line joining the operating points between the initial no load speed and the final step input torque. Because of the experimental difficulties it was not possible to obtain a full experimental response for comparison with these results, although the steady-state values added to Fig. (5.15) are in quite close agreement. Steady-state speeds for various step torques at different control voltages are tabulated together with the corresponding experimental results (Table (5.2)). No previous workers have investigated, either theoretically or experimentally this form of speed response.

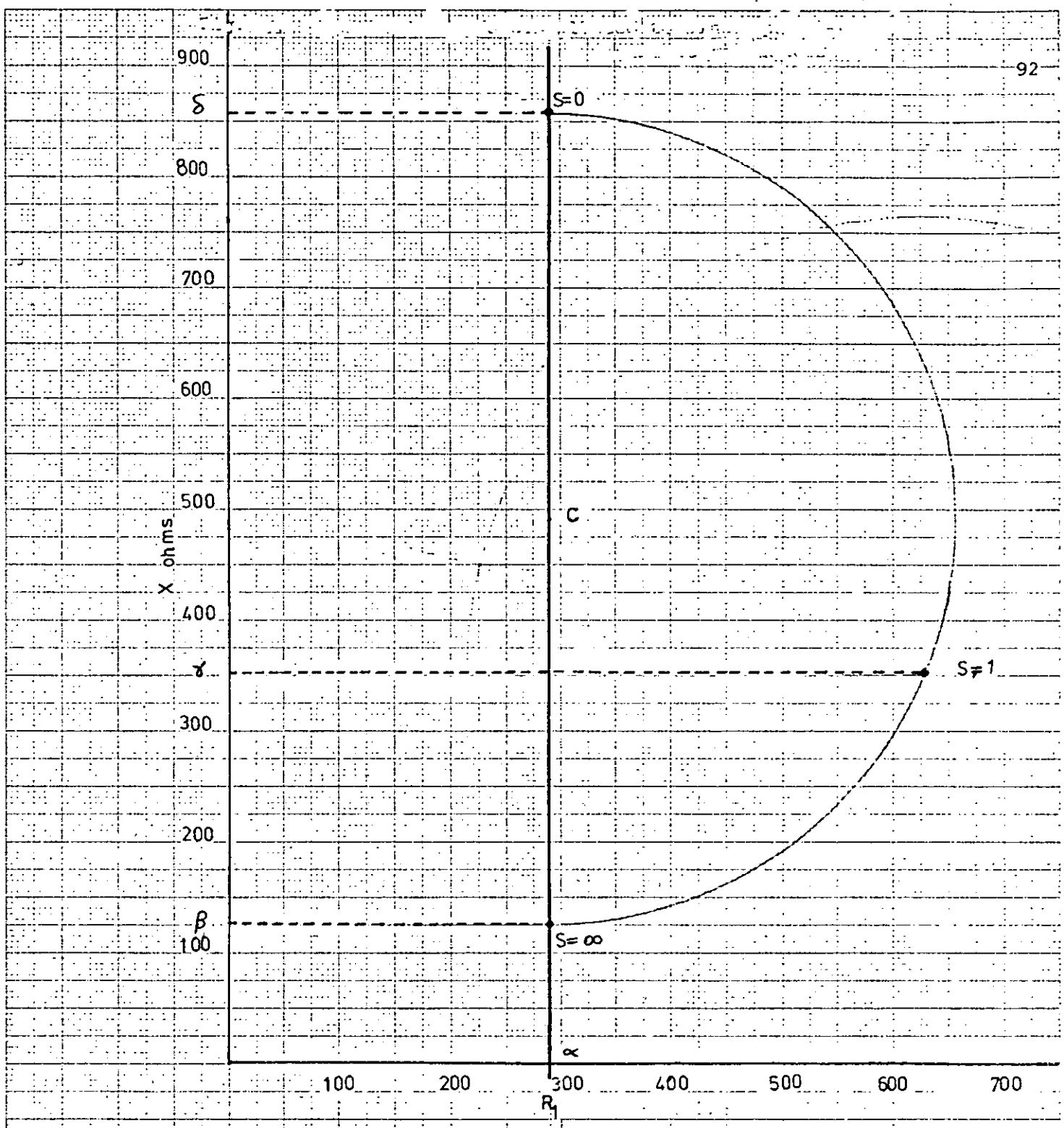

Fig. 5.1 Measured impedances plotted to find equivalent circuit impedances

Fig. 5.2 No load speed characteristics

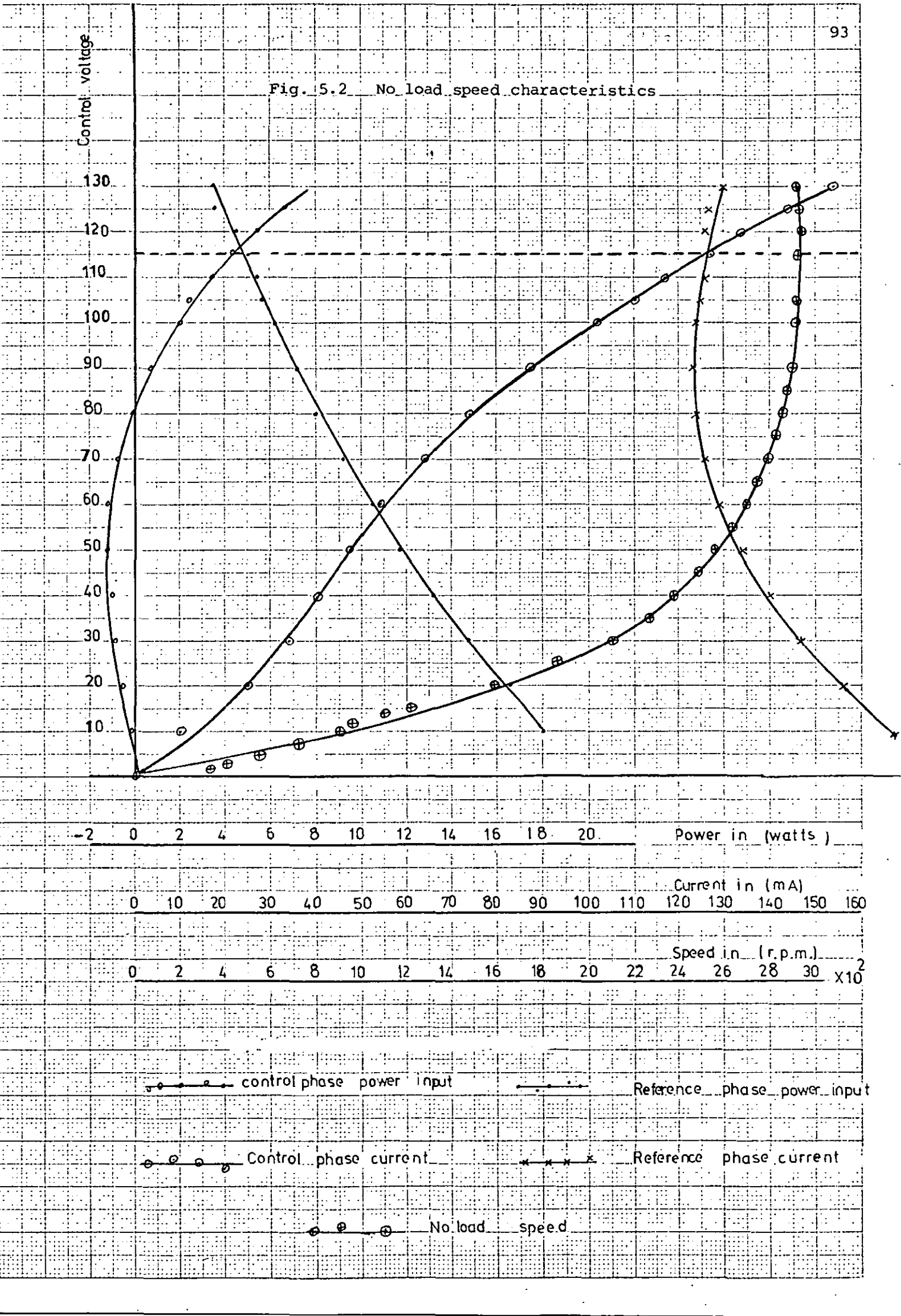

Fig. 5.3 Locked rotor characteristics

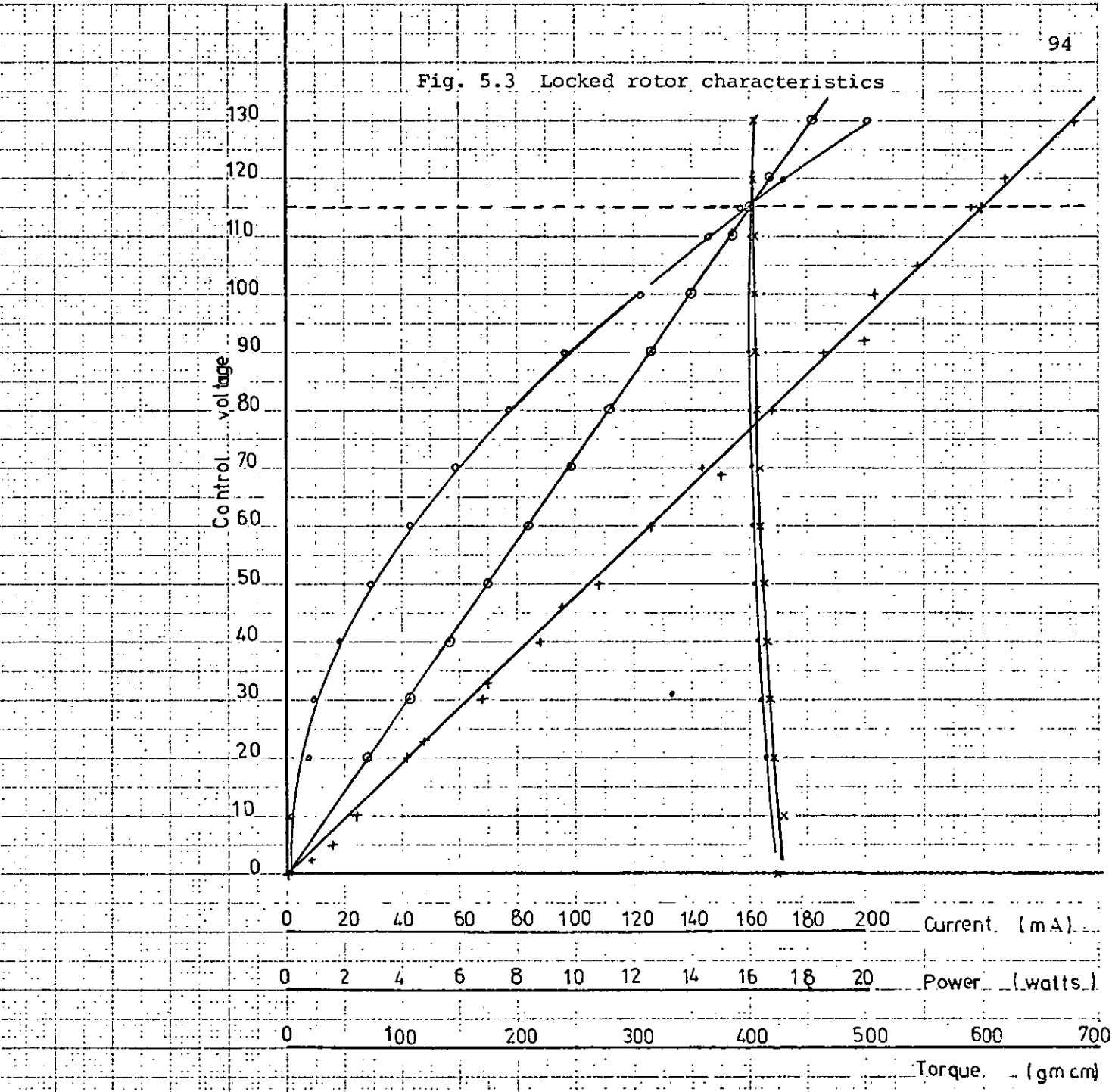

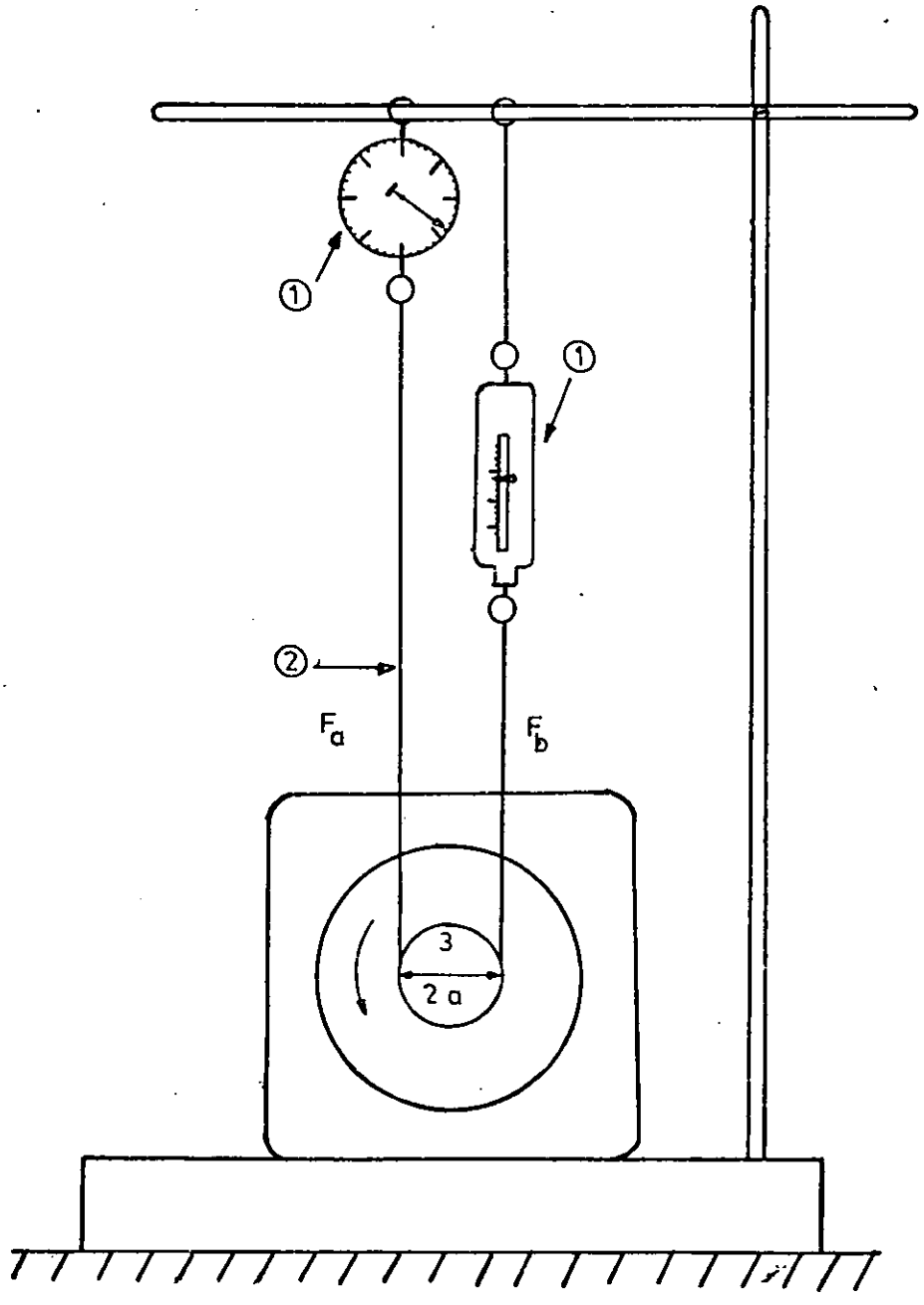

Fig. 5.4 Measurement of torque/speed characteristics of 2-phase servomotor

① Spring balance

② String

③ Servomotor shaft

Torque = $a(F_a - F_b)$

where F_a and F_b are tensions in the string

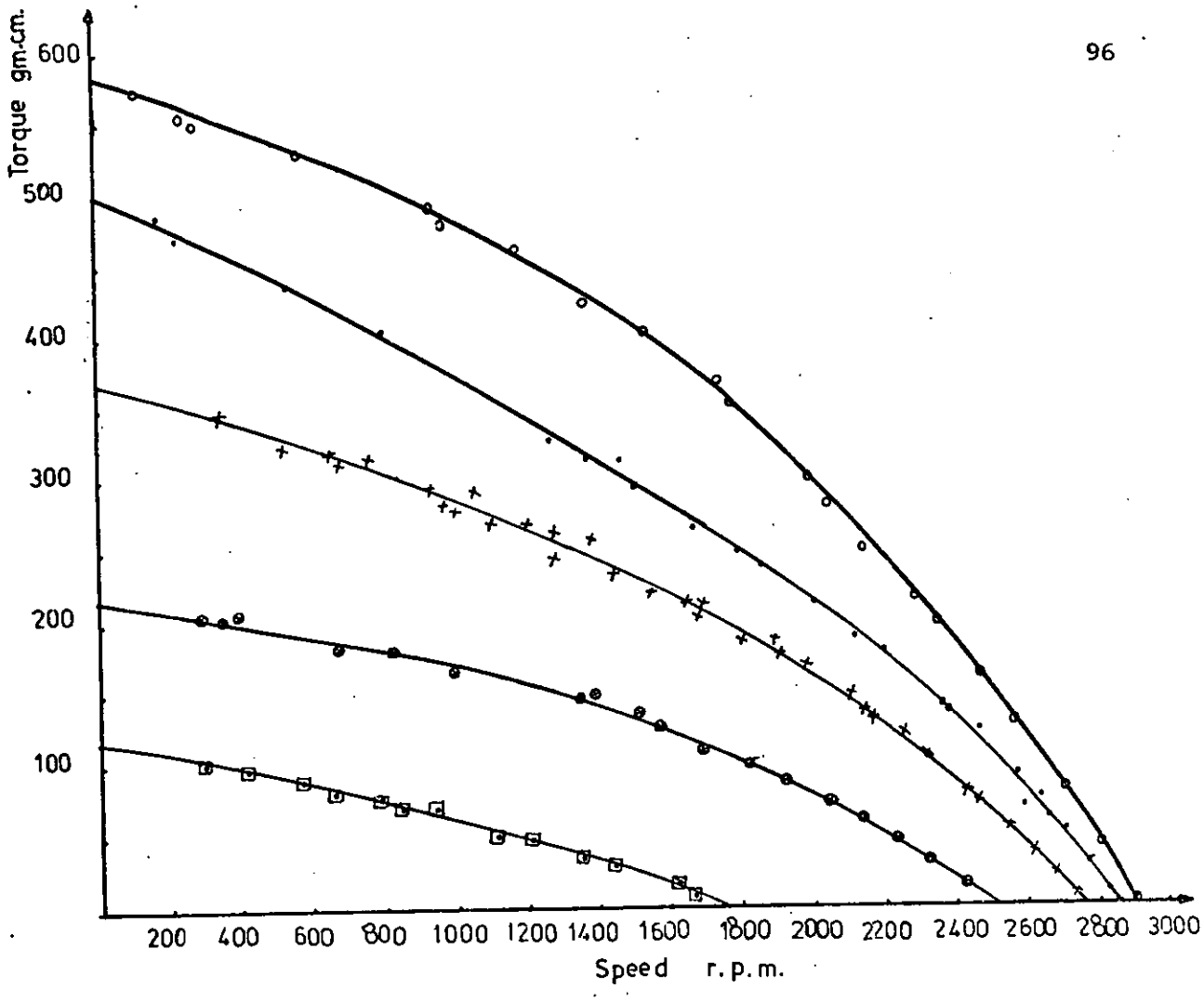

Fig. 5.5 Torque / speed characteristics at different values of control voltage and rated reference voltage

100% control voltage
80% control voltage
60% control voltage
40% control voltage
20% control voltage

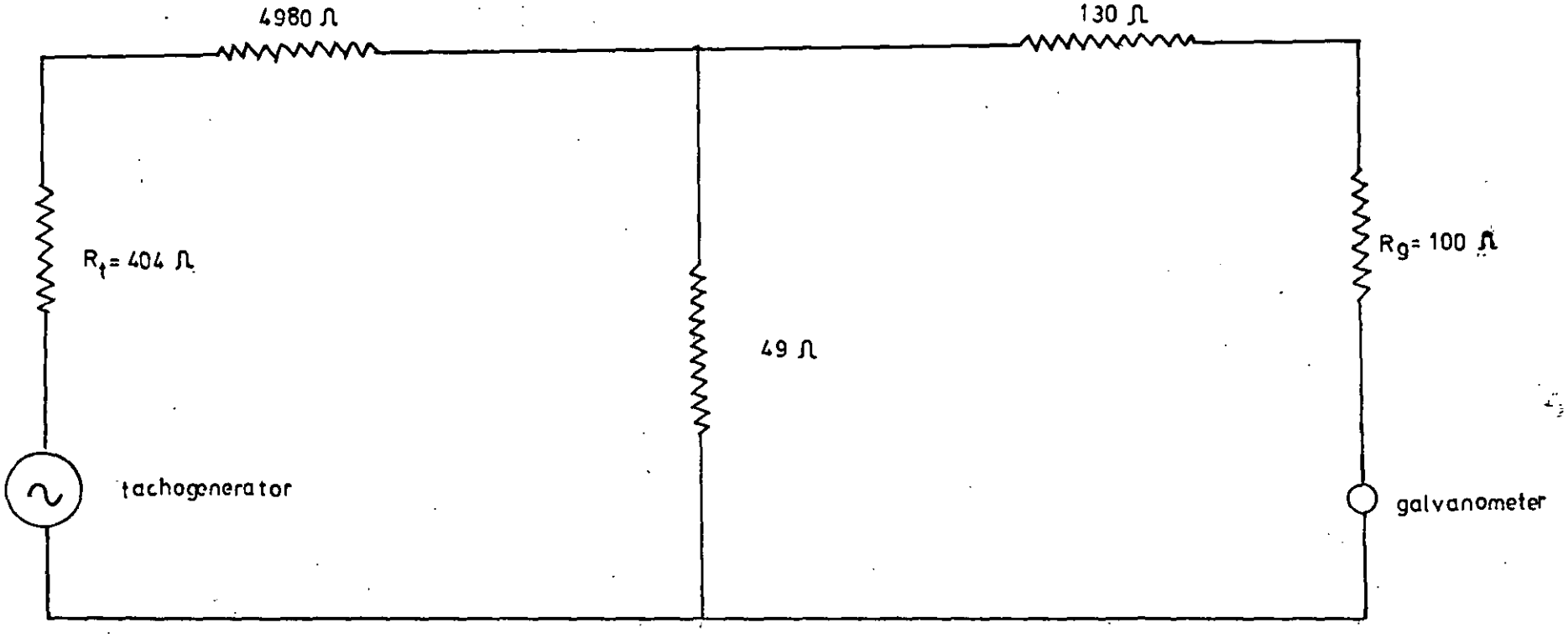

Fig. 5.6 Complex matching circuit for U. V. recorder galvanometer

R_t = tachogenerator output phase resistance R_g = galvanometer resistance
Galvanometer damping resistance ≃ 179 Ω

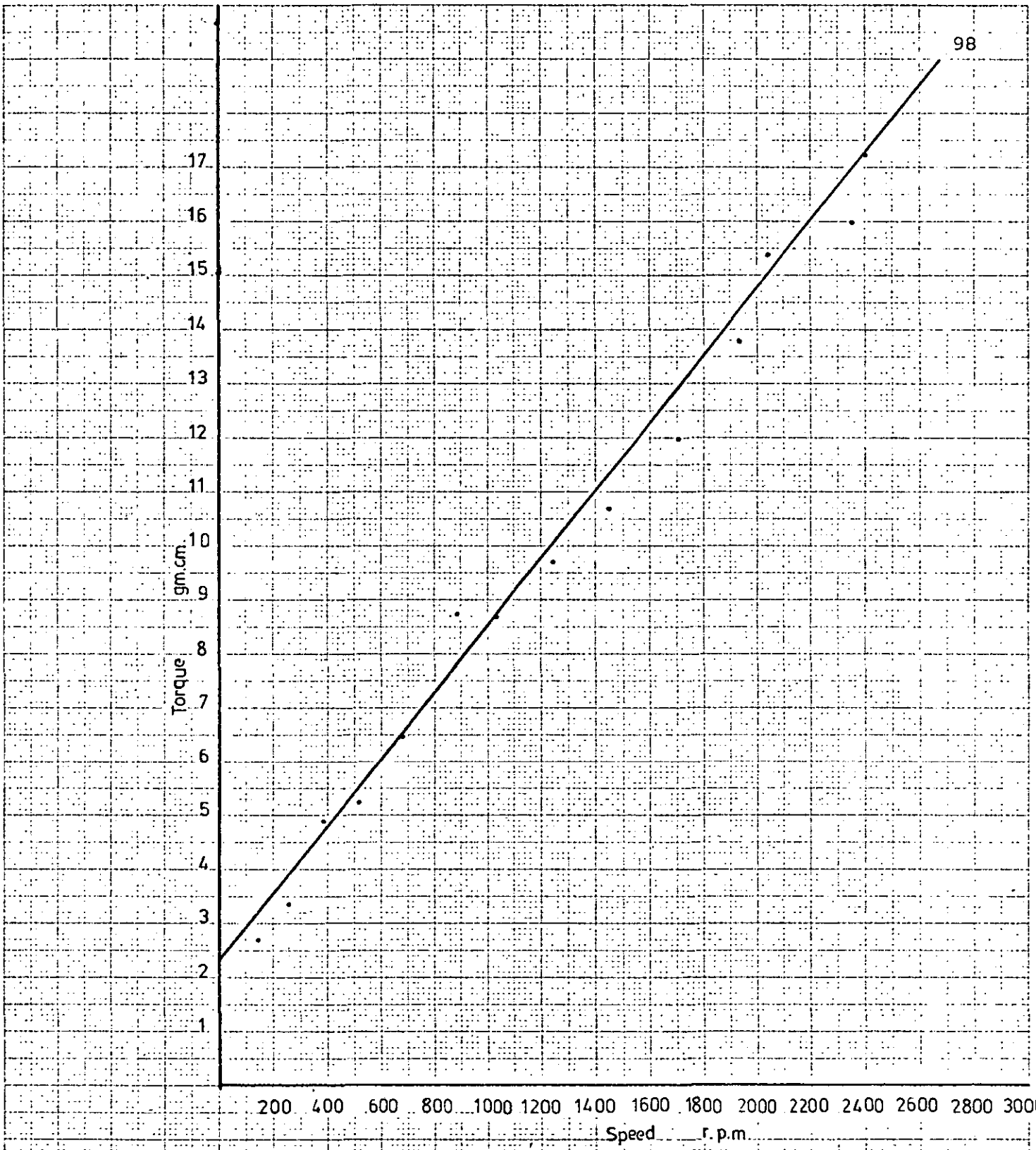

Fig. 5.7 Frictional torque vs speed

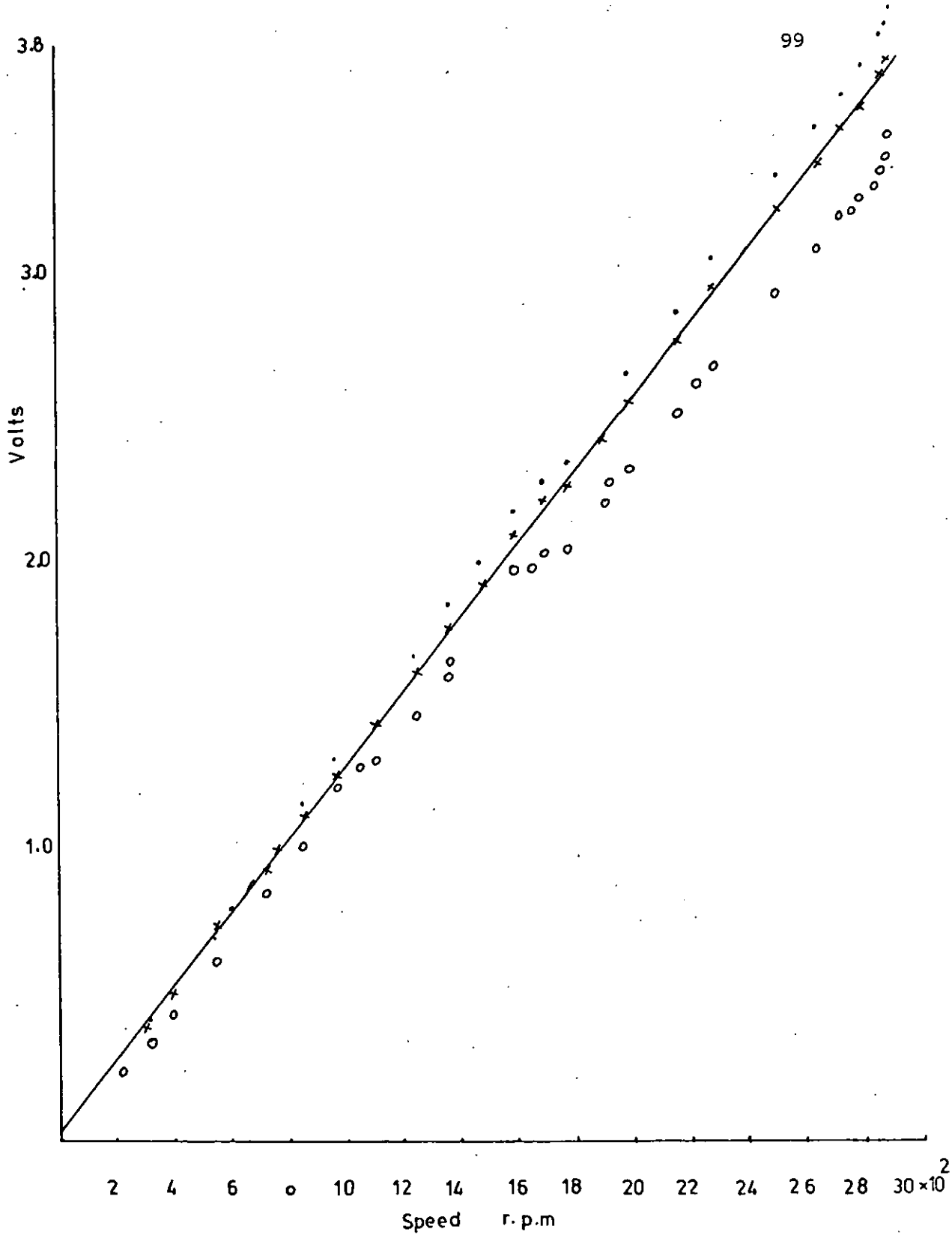

Fig.5.8 Voltage/speed characteristics of the tachogenerator terminated in

(a) 2 KΩ o o o

(b) 5 KΩ × × ×

(c) 10 KΩ . . .

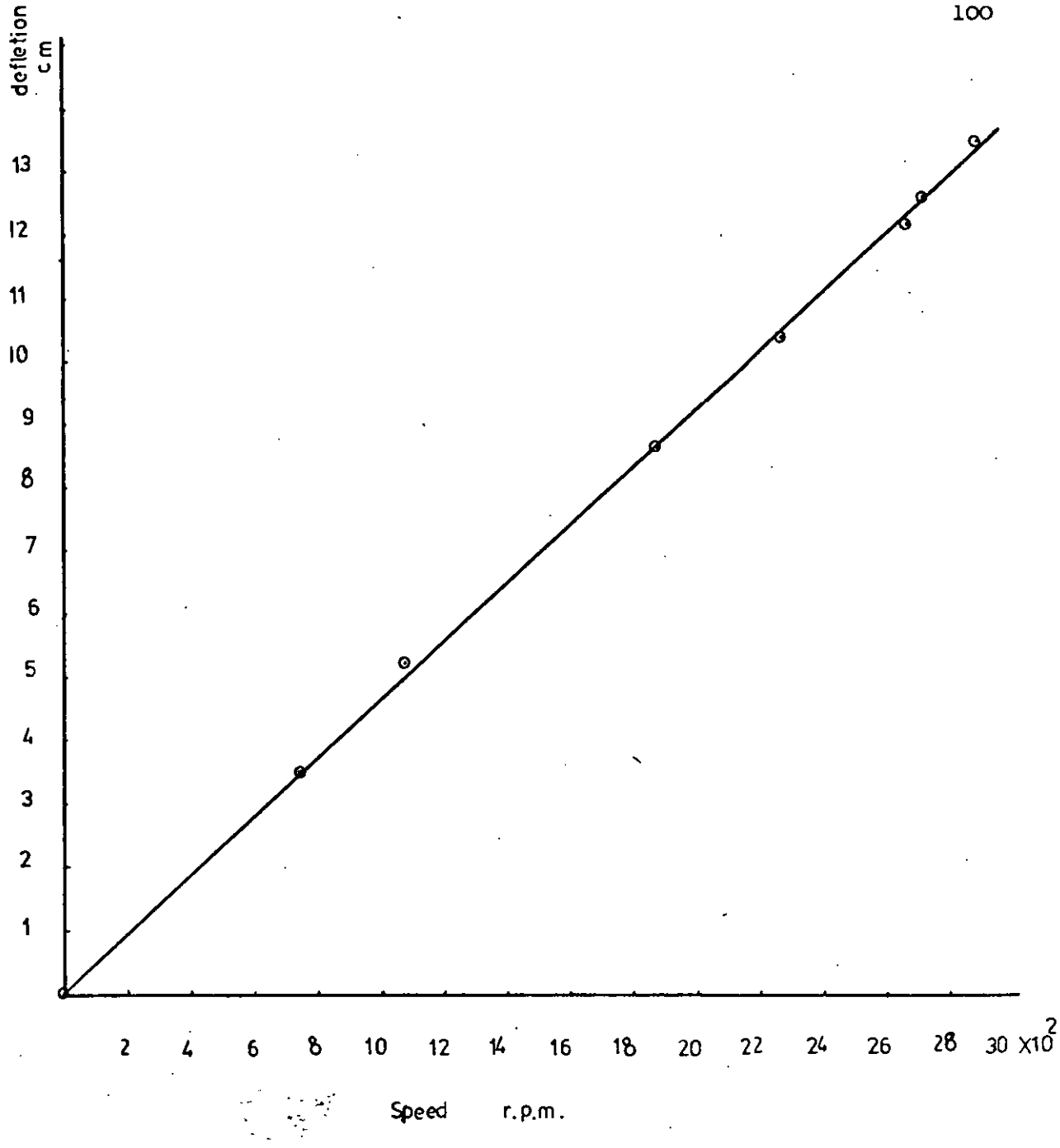

Fig.5.9 Determination of overall (galvo. & tacho) sensitivity

Fig 5.10 Experimental and theoretical speed / time curves following step changes in the control voltage

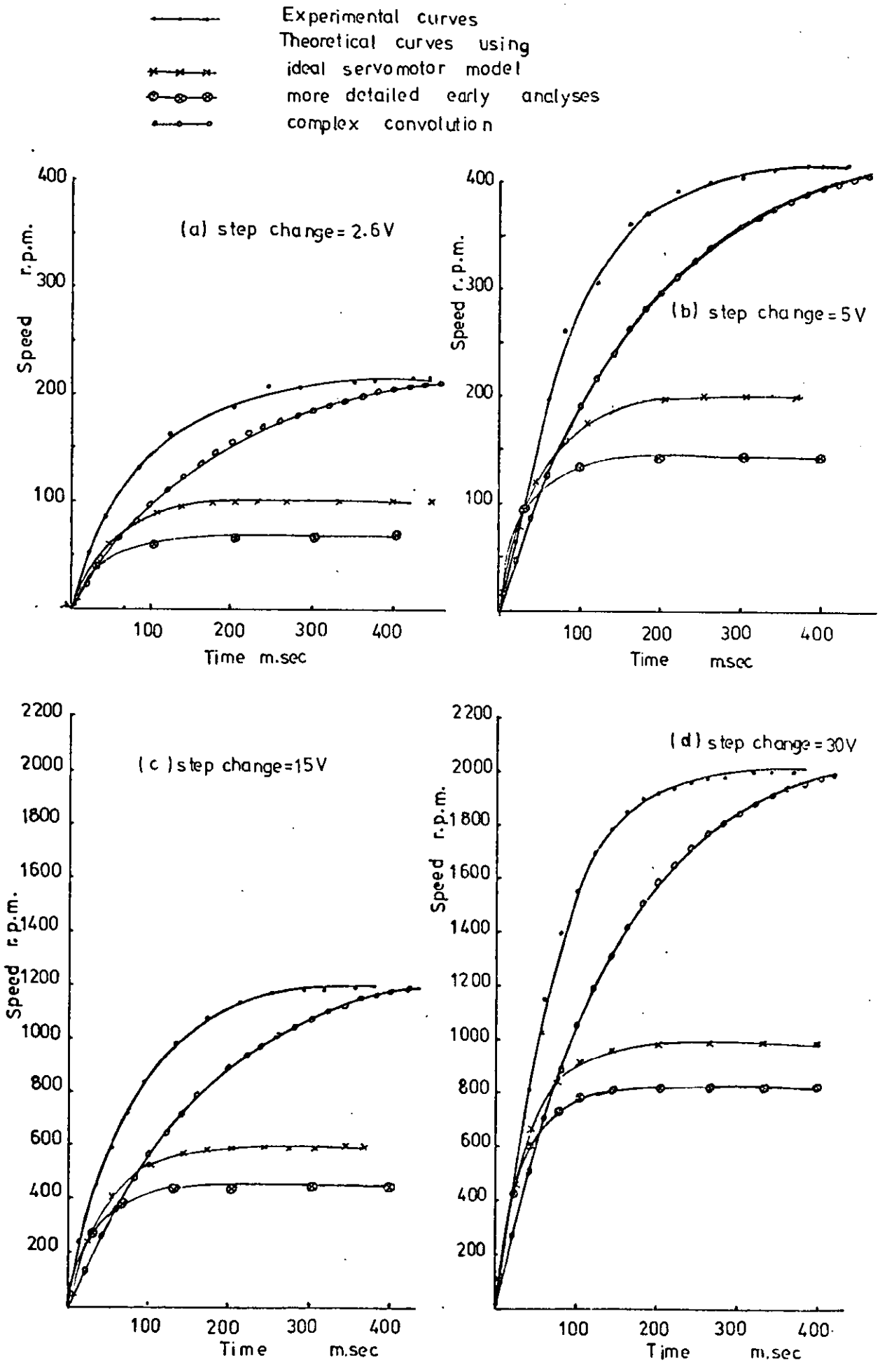

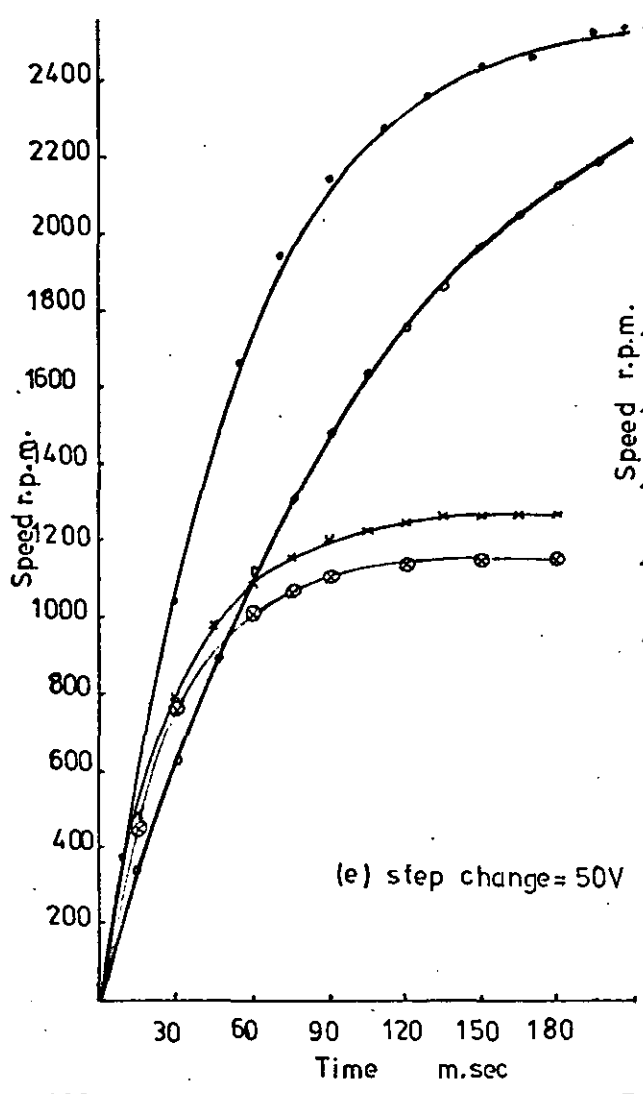
Speed r.p.m.
2400
2200
2000
1800
1600
1400
1200
1000
800
600
400
200
30
60
90
120
150
180
Time m.sec
(e) step change= 50V

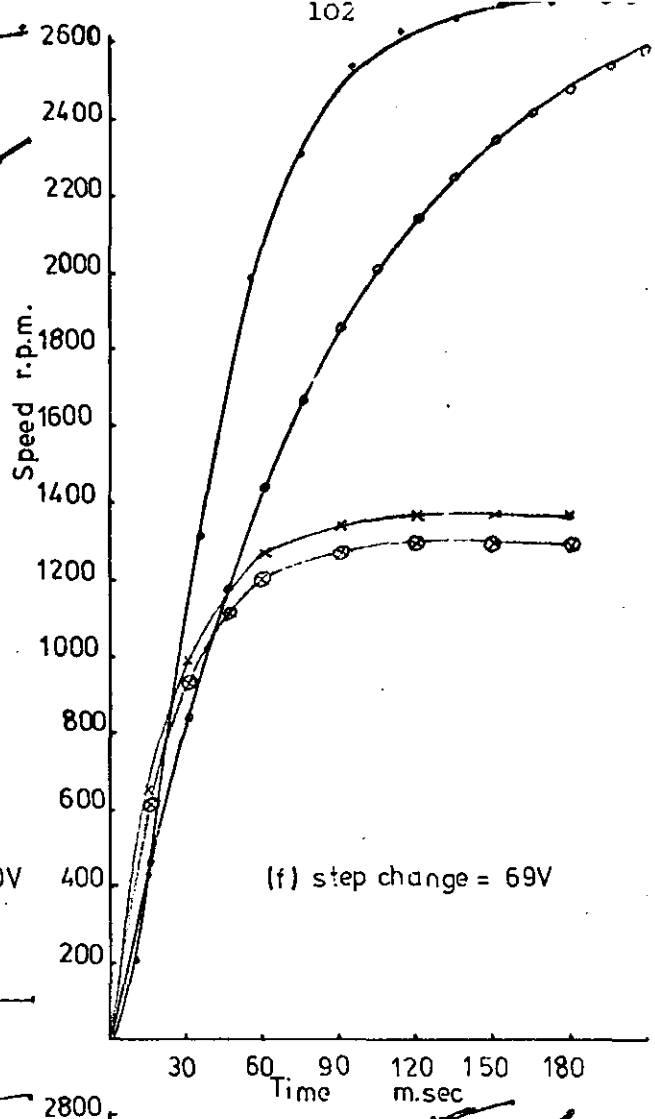
Speed r.p.m.
2600
2400
2200
2000
1800
1600
1400
1200
1000
800
600
400
200
30
60
90
120
150
180
Time m.sec
(f) step change = 69V

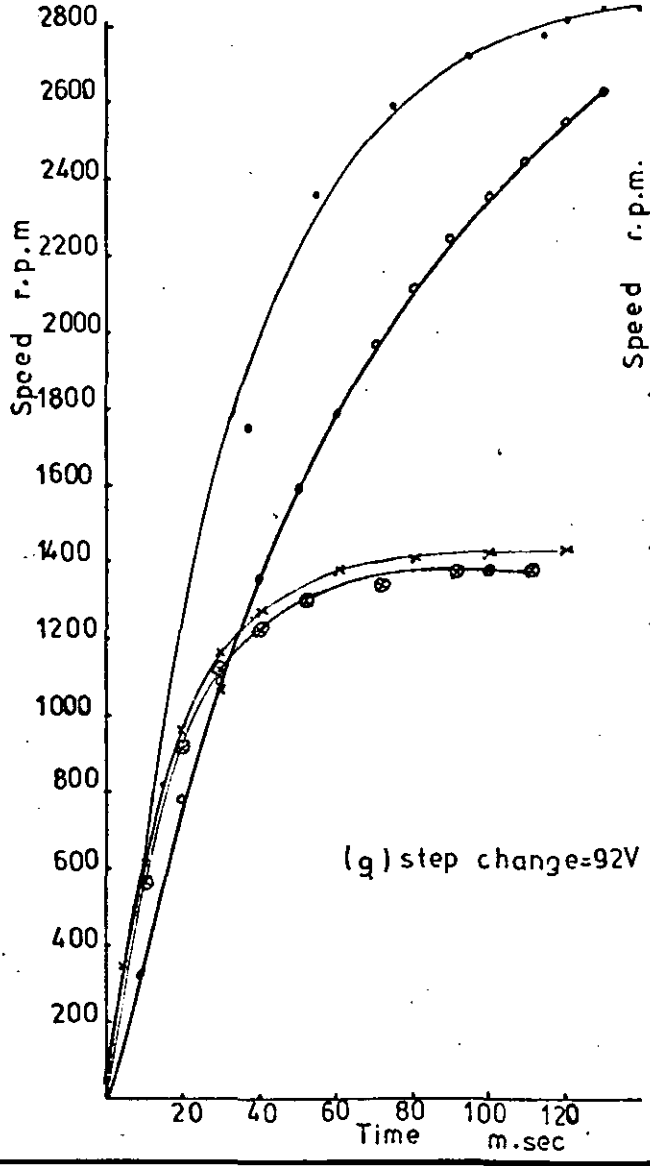
Speed r.p.m
2800
2600
2400
2200
2000
1800
1600
1400
1200
1000
800
600
400
200
20
40
60
80
100
120
Time m.sec
(g) step change=92V

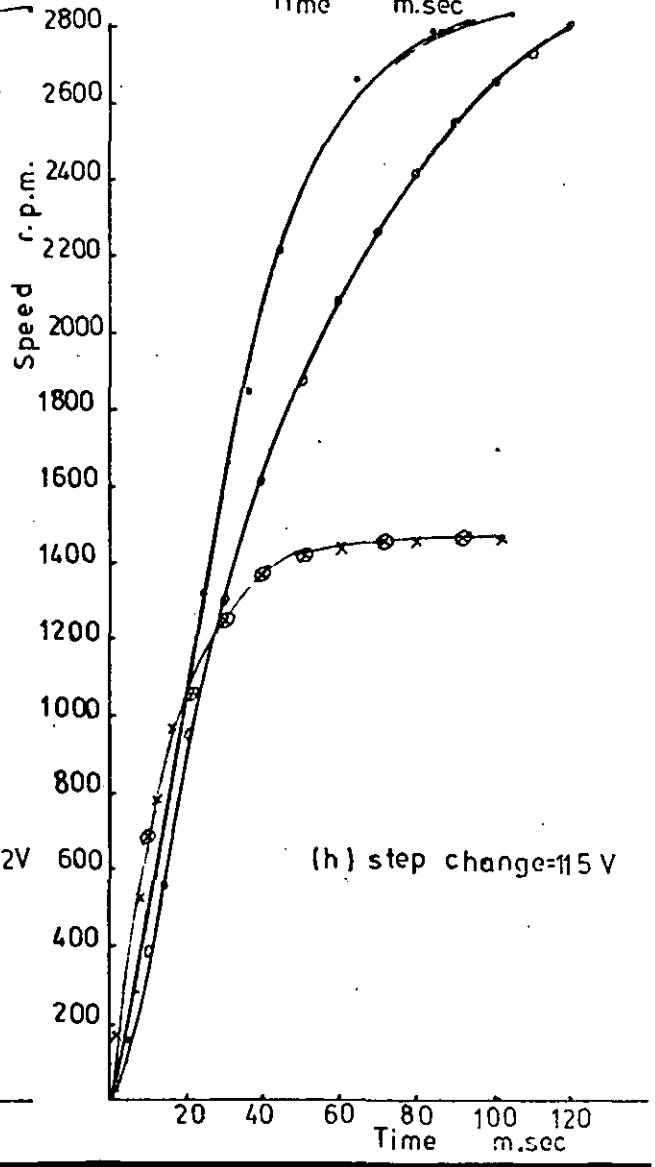
Speed r.p.m.
2800
2600
2400
2200
2000
1800
1600
1400
1200
1000
800
600
400
200
20
40
60
80
100
120
Time m.sec
(h) step change=115 V

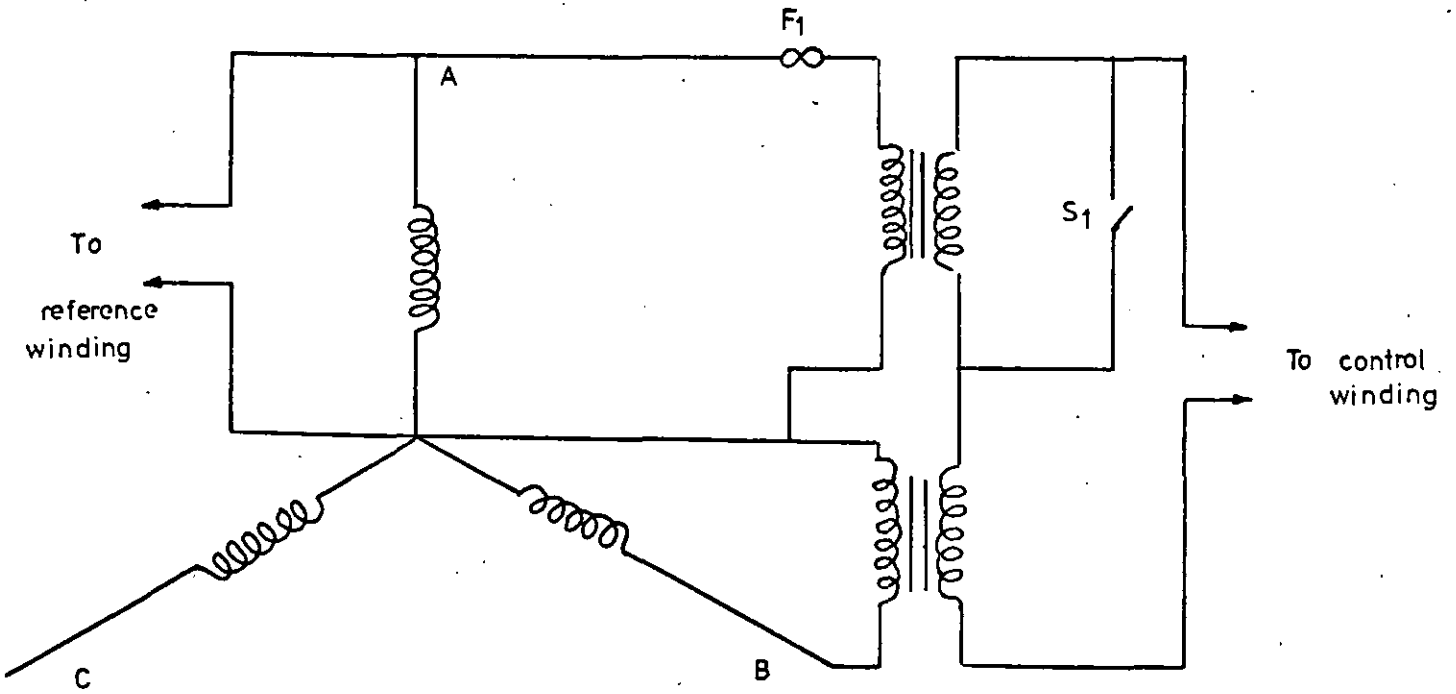

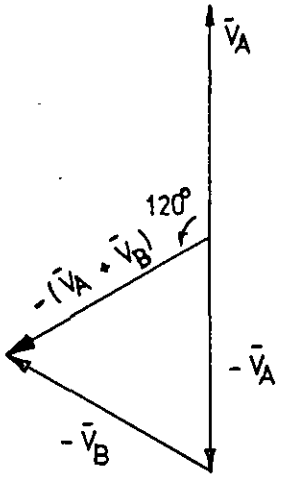

before closing switch S_1

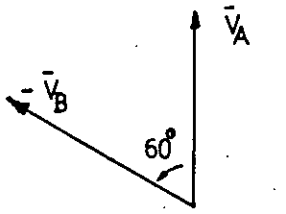

after closing switch S_1

Voltage vector diagrams

Fig. 5.11 Skematic circuit diagram to obtain 60° step change in the phase of control winding voltage (from 120° to 60°)

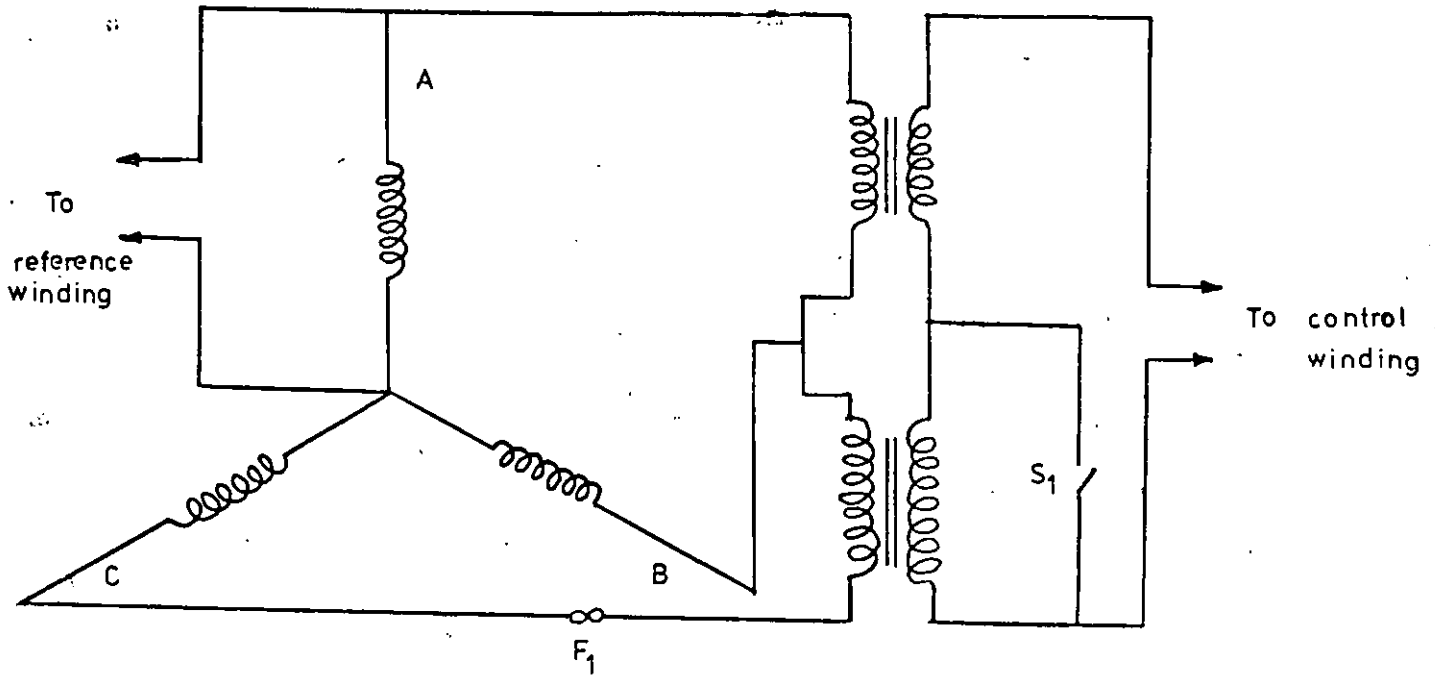

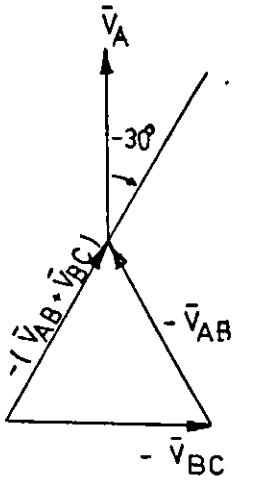

before closing switch S_1

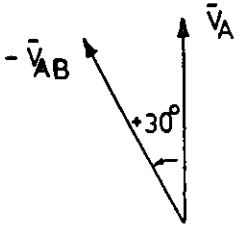

after closing switch S_1

Fig. 5.12 Skematic circuit diagram to obtain 60° step change in the phase of control winding voltage (from -30° to +30°)

Voltage vector diagrams

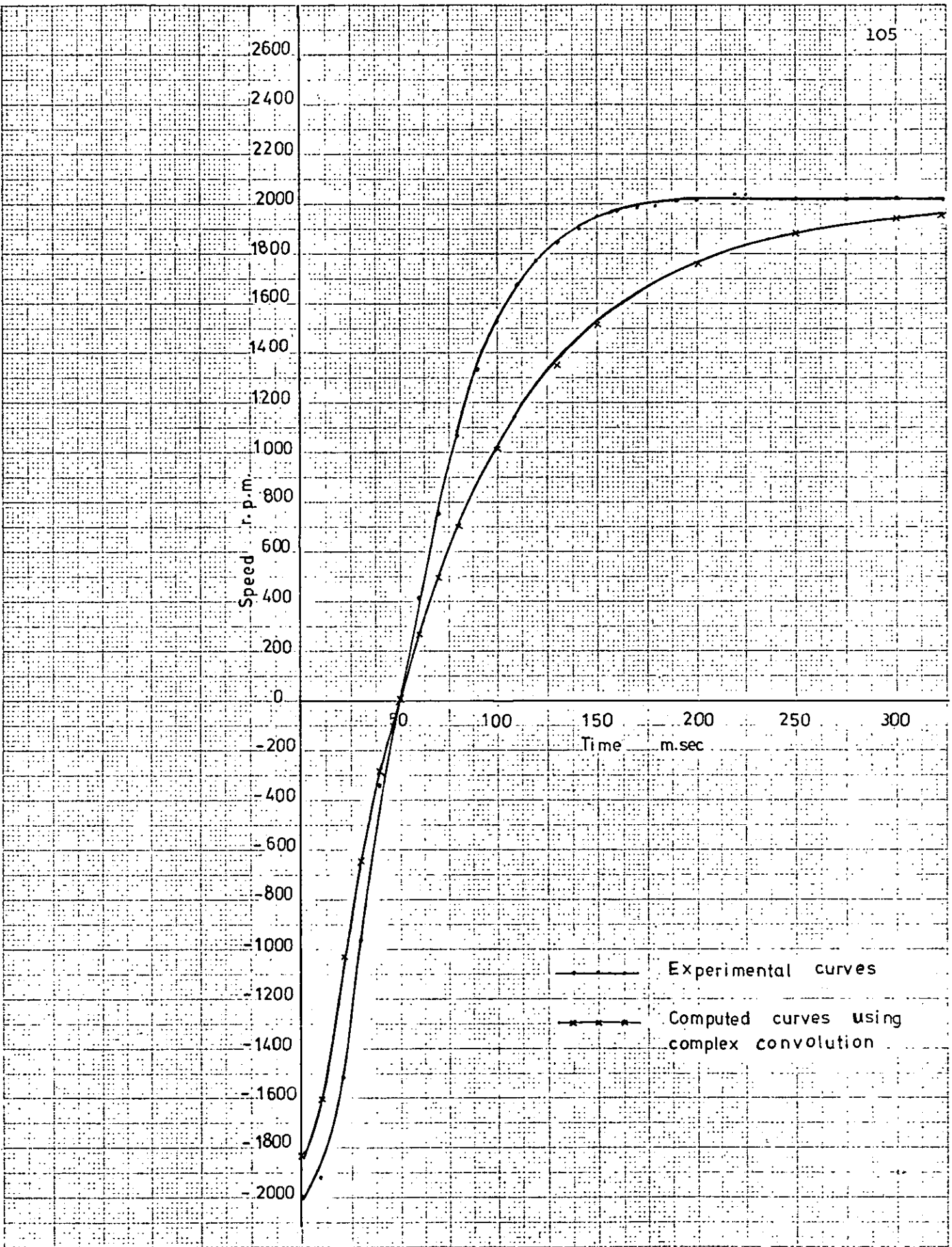

Fig.5.13 Experimental and theoretical speed / time curves following step changes in the phase angle of control voltage

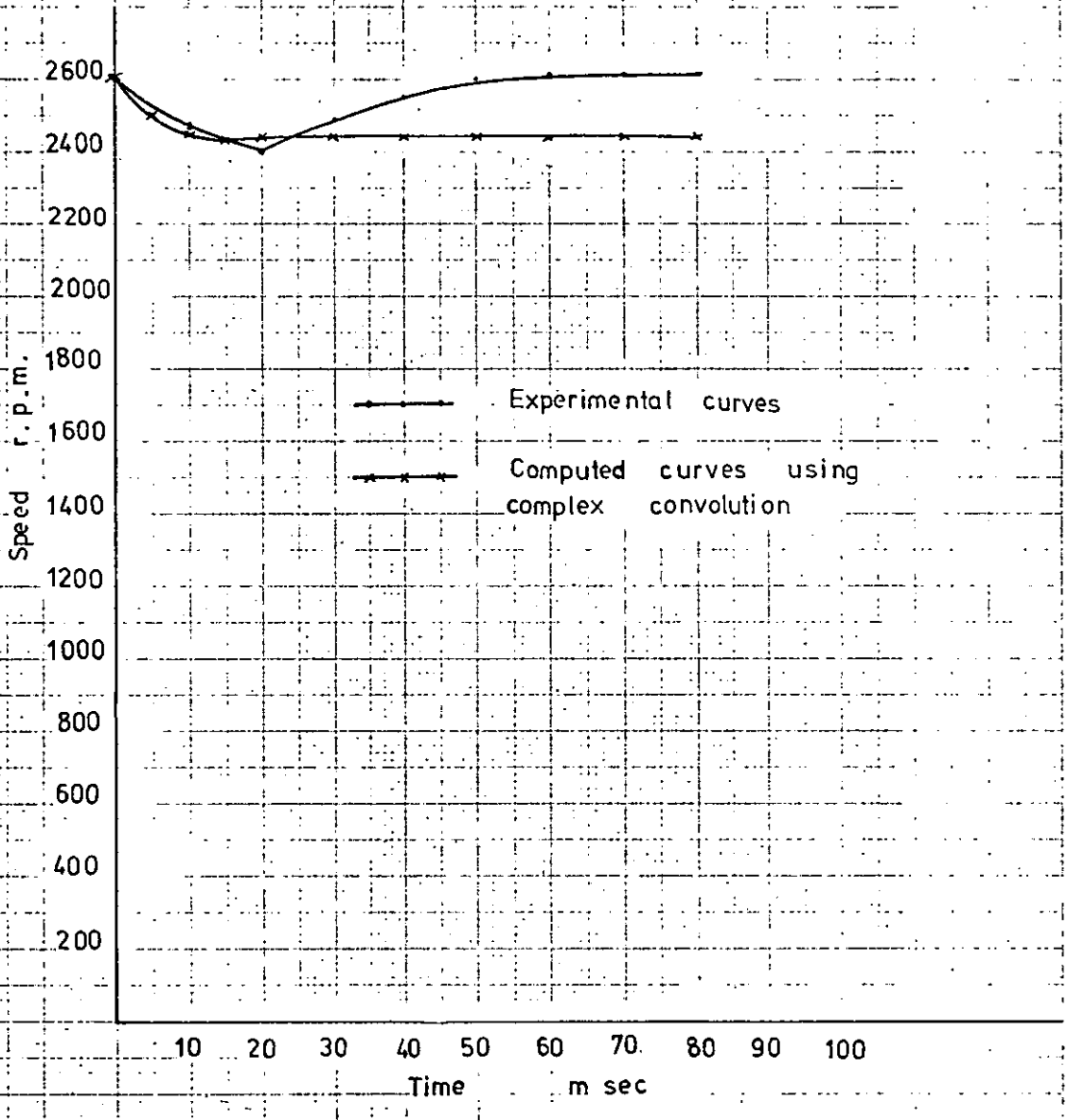

Fig.5.14 Experimental and theoretical speed/time curves following step changes in the phase angle of control voltage

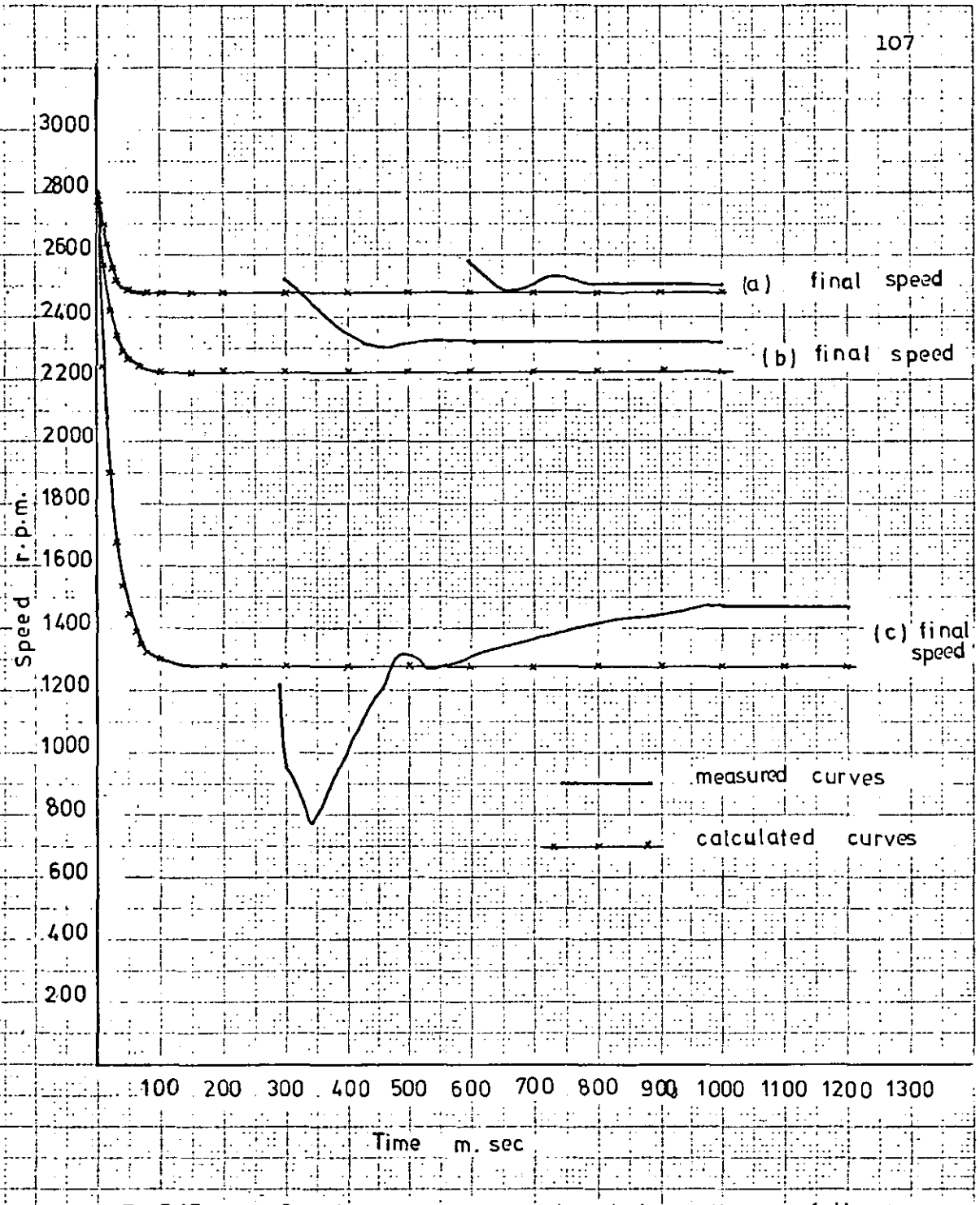

Fig.5.15 Speed/ time curves at rated voltage following step changes in load torque of:
(a) 122 gm.cm.
(b) 205 gm.cm.
(c) 417 gm.cm.

Control voltage V_D r.m.s.	stall torque T_s gm.cm	T_s' gm.cm.	Average damping fa x 10^5 Nm/rad.sec^{-1}	Steady-state speed with damping fa (r.p.m.)	Effective damping fe x 10^{+5} Nm/rad. sec^{-1}	Steady-state speed with damping fe (r.p.m.)	Experimental steady-state speed (r.p.m.)
115	585	740	18.64	1765	10.28	3200	2940
92	500	656	16.4	1619	8.6	2990	2860
69	370	475	12.6	1568	7.018	2818	2760
50	260	331	9.55	1494	5.48	2613	2550
46	225	280	8.4	1569	5.138	2566	2500
30	155	199	7.26	1184	4.04	2126	2000
23	115	151	6.12	1077	3.23	2041	1760
15	77.5	101	6.04	702	3.23	1330	1200
5	25	33	5.8	234	3.23	444	404
2.6	12.5	16	5.66	122	3.23	230	207

Table (5.1)

Control voltage V_D r.m.s.	Step torque T_{MI} gm.cm.	Experimental steady state speeds		f mechanical damping gm.cm/r.p.m.	Theoretical results	
		Initial ω_i r.p.m.	Final r.p.m.		T_{MI}/f r.p.m.	Final steady speed $\omega_i - T_{MI}/f$ r.p.m.
115	417	2816	1470	0.278	1500	1316
115	205	2784	2318	0.35	586	2198
115	122	2784	2513	0.4	305	2479
92	325	2806	1320	0.21	1548	1258
92	214	2828	2123	0.26	823	2005
92	120	2795	2448	0.3	397	2398
69	255	2756	1430	0.18	1416	1340
69	203	2763	1970	0.214	948	1815
69	122	2791	2275	0.221	552	2239
46	142	2492	1430	0.135	1052	1440
46	118	2405	1612	0.1355	871	1534
46	62	2288	1990	0.167	371	1917
23	75	1660	823	0.078	962	698
23	34	1625	1257	0.072	472	1153
23	26	1635	1387	0.1	260	1375

Table (5.2)

CHAPTER 6. Comments and Conclusions

From the theoretical and experimental work recorded in this thesis, the following comments and conclusions can be drawn:

(i) Previous theoretical studies of the performance of 2-phase servomotors have been confined largely to calculations of the steady-state torque/speed characteristics, often using symmetrical component analysis. When calculated curves were compared with measured results, close agreement was generally obtained.

Previous attempts to establish transfer functions for the 2-phase servomotor can be classified into either elementary analyses based on ideal machine models, assuming linear torque/speed characteristics and requiring quite drastic simplifying assumptions, or more detailed analyses in which some of these assumptions were lifted. However, since all the analyses neglected electrical transients and assumed the transient and steady-state torques to be equal, transfer functions of the same general form but with different gain and time constants were obtained. These investigations were almost entirely mathematical, without any significant attempt at justification from practical results.

The establishment of a correct transfer function for a servomotor necessitates consideration of the stator and rotor time constants, as well as that of the mechanical system. This more detailed machine modelling leads to differential equations which contain a product-of-variable type nonlinearity, and in this thesis complex convolution techniques are employed to provide from these equations transfer functions for different transient conditions. A servomotor usually operates at speeds much below synchronous, but even though it is then entirely reasonable to neglect rotational voltage terms, quite complicated results are obtained.

(ii) The transfer functions obtained relating the speed to a step change in either the magnitude or the phase of the control voltage, have poles which are functions of either the mechanical time constant, the stator time constant or the rotor time constant, and as they are all first-order poles, a special form of complex convolution is utilised. Furthermore, the poles that are functions of the stator and rotor time constants occur as conjugate pairs, the only difference between the poles being the replacement of the stator time constant with the rotor time constant. It can be seen from the speed response expressions of sections (4.2.1) and (4.3.1) that, after obtaining the constant coefficients of the exponential time functions associated with poles that are functions of the stator time constant, the corresponding rotor coefficients are obtained simply by interchanging the stator and rotor time constants. This leads to considerable simplification when time expressions for the transfer function are being established.

(iii) The speed response results, following a step change in the magnitude of the control voltage, as calculated using any of the early transfer function expressions are nearly the same. In these expressions, the mechanical viscous-friction damping of the servomotor is defined as the slope of the line joining zero speed to zero torque. When the same values of mechanical damping is used in the calculation of the steady-state speeds from the complex convolution approach (see Table(5.1)), the results are much closer to the experimental results, despite the low speed restriction in the analysis. When the damping coefficients are corrected to the stalled value (i.e. the values of the coefficients given in Table (5.1)), the results obtained from the complex convolution approach agree very much more closely with the measured values than

those using the early analyses approaches. This is especially true when the control voltage is low, validating the simplification made in the analysis by considering low speed conditions only. Both early analyses gave almost the same results confirming that the assumptions made in these cases are basically the same.

(iv) The complex convolution technique was also used in the establishment of transfer functions relating the speed change to a step change in the phase angle between the control and reference voltages. Computations of the speed response following a step change were found to agree reasonably well with measured results when the mechanical damping coefficients were obtained using the final steady-state angle between the voltages and covering the whole speed change. No previous work has been recorded in this area.

(v) The speed response following a step change in torque for various control voltages does not involve complex convolution and although the theoretical analysis is simple, considerable experimental difficulties arise. However, when the measured steady-state speeds are compared with the corresponding calculated values, close agreement is obtained, as indicated by Table (5.2).

(vi) In practice, servomotors are often supplied with nonsinusoidal signals, usually rectangular in form. Such a waveform can be analysed into its sinusoidal components in the form of a Fourier series and, using complex convolution technique, a transfer function can be established for each pair of sinusoidal signals of the same frequency supplied to the control and reference windings. Summing these individual results will give the overall transfer function for the machine, although a very considerable amount of work would be involved.

7 REFERENCES

1. S. A. Davis and J. Spector, "Application factors for 2-phase servomotor". Electrotechnology, Vol. 55, 1955, pp 76-84.
2. S. A. Davis, "Dynamic load characteristics of electric motors", Electromechanical Components and System Design, Vol. 2, Jan. 1958, pp. 56-63.
3. "A.C. instrument servomotors", Components Digest 1, Electro-mechanical Components and System Design, Vol. 2, Oct. 1958, pp 33-47.
4. Bruce, A. Chubb, Modern Analytical Design of Instrument Servo-mechanism, (book), Addison Wesley, New York, 1967.
5. S. A. Davis, "Rotating components for automatic control", Product Engineering, Vol. 24, Nov. 1953, pp 147-153.
6. Davis and Legwood, Electromechanical Components for Servomechanisms, (book), McGraw-Hill, London, 1961.
7. J. E. Gibson and F. B. Tuteur, Control System Components (book) McGraw-Hill, London, 1958
8. R.J.W. Koopman, "Operating characteristics of 2-phase servomotor", A.I.E.E. Transactions, Vol. 68, 1949, pp 319-329.
9. V. del Toto, Electromechanical Devices for Energy Conversion and Control Systems, (book), Prentice-Hall, New Jersey 1968.
10. F. W. Suhr, "Symmetrical components as applied to single phase induction motors", A.I.E.E. Transactions, Vol. 64, Sept. 1945, pp 651-6.
11. F. Harashima and Z. Sawai, "On the operating characteristics of 2-phase servomotors and driving circuits". Report of the Institute of Science, University of Tokyo, Vol. 21, No. 2, June 1971, pp 30-91.

12. L. Balmer and C.P. Lewis, Solution of Problems in Control Engineering, (book), Vol. 1, 1970.

13. G. S. Brown and D. P. Campbell, Principles of Servomechanisms, New York: Wiley 1950.

14. L. O. Brown, Jr., "Transfer functions for a 2-phase induction motor", A.I.E.E. Transactions, Vol. 70, Pt. 2, 1951, pp 1890-1893.

15. A. M. Hopkins, "Transient response of small 2-phase induction motors", A.I.E.E. Transactions, Vol. 70, Pt. 1, 1951, pp 881-886.

16. V. G. Kutvinov, "On the transfer function of an asynchronous 2-phase motor", Automatic and Remote Control, Vol. 20, July 1959, pp. 902-912.

17. N. P. Vlasov, "A method for obtaining transfer functions of automatic control systems on alternating current", Automatic and Remote Control, Vol. 21, June 1960, pp. 538-543.

18. S. M. Mikhail and G. H. Fett, "Transfer functions of 2-phase servomotors" A.I.E.E. Trans., Apparatus and Industry, Vol. 77, May 1958, pp. 97-99.

19. D. R. Wilson, "Methods of obtaining the transfer function of a 2-phase servomotor", I.E.E.E. Transactions on Power Apparatus and Systems, Vol. PAS 87, No. 1, Jan. 1968, pp. 257-265.

20. J. Ton, Modern Control Theory, (book), McGraw-Hill, London, 1964.

21. Györgyfodor, Laplace Transforms in Engineering (book), Akademiai Kiado, Budapest, 1965.

22. J. L. Douce, An Introduction to the Mathematics of Servomechanisms, (book) London, Hazell Watson and Viney, Ltd., 1963.

23. M. F. Gardener and J. L. Barnes, Transients in Linear Systems Studied by the Laplace Transformation, (book) Wiley and Sons, New York, 1942.

24. D. C. White and H. H. Woodson, Electromechanical Energy Conversion, (book), New York: Wiley 1959.

25. D. K. Cheng, Analysis of Linear Systems, (book) Addison Wesley, Reading1959

26. M. G.Rekoffjr, "Test yield equivalent circuits of 2-phase servo-motor", Control Engineering, Vol. 10, Aug. 1963, pp. 79-80.

27. A. E. Fitzgerald and C. Kingsley, Electric Machinery, Second edition, McGraw-Hill, New York, 1961, pp 521.

28. F. M. Hughes, Transient characteristics and simulation of induction motors, Proc. I.E.E., Vol. 111, No. 12, Dec. 1964, pp. 2041-2050.

Similarly, the time integral of the function which is identical with the convolution of the function and of a unit step I(t) is

$$I(t)* f(t) = \int_o^t I(t-\tau) \cdot f(\tau)\, d\tau$$

$$= \int_o^t f(\tau) d\tau$$

since $I(t-\tau) = 1$ for $0 < \tau < t$

8.1.2 Laplace Transform of the Convolution

If two functions $f_1(t)$ and $f_2(t)$ are Laplace transformable, and have respectively the transforms $F_1(s)$ and $F_2(s)$, then

$$L \left(\int_o^t f_1(\tau) \cdot f_2(t-\tau) d\tau \right) = F_1(s) \cdot F_2(s)$$

which shows that the Laplace transform of the convolution of two functions is the product of the respective transforms of these two functions. That is to say, convolution in the time domain changes to multiplication in the complex s domain. A proof of the above result may be found in several text books.[21-25]

8.1.3 Laplace Transform of the product of two time functions

If the two functions have abscissae of absolute convergence σ_{a1} and σ_{a2} respectively, then if

$$F(s) = L(f_1(t) \cdot f_2(t))$$

$$= \int_o^\infty f_1(t) \cdot f_2(t)\, e^{-st}\, dt \qquad \ldots\ (8.1)$$

provided that the maxima of σ_{a1}, σ_{a2} and $\sigma_{a1} + \sigma_{a2}$ are all $< \sigma$, where σ is the real part of s.

8. Appendices

Appendix 8.1 Complex Convolution

8.1.1 The Concept of Convolution

The convolution of two time-varying functions $f_1(t)$ and $f_2(t)$ is defined by

$$f_1(t)* f_2(t) = \int_o^t f_1(\tau).\ f_2(t - \tau)\ d\tau$$

where τ is the variable of integration. Introducing a new integration variable , such that $(t - \tau) = x$, it can be shown that convolution is a commutative process, that is

$$f_1(t)* f_2(t) = -\int_t^o f_1(t - x).\ f_2(x)dx$$

$$= \int_o^t f_2(\tau).\ f_1(t - \tau)d\tau$$

$$= f_2(t)* f_1(t)$$

In a similar way it can be shown that convolution is also an associative process,that is

$$(f_1(t)* f_2(t))* f_3(t) = f_1(t)* (f_2(t)* f_3(t))$$

An impulse of unit intensity and very short duration is called a Dirac impulse, and is normally denoted by $\delta(t)$. Any function can be written as the convolution of itself and the Dirac impulse, that is

$$\delta(t)* f(t) = \int_o^t \delta(\tau).\ f(t - \tau)\ d\tau$$

Using the mean value theorem of the integral calculus, the above integral may be evaluated as

$$= \left[f(t - \tau) \right] \tau = o$$

$$= f(t)$$

By substituting for $f_2(t)$ its integral representation in terms of $F_2(\omega)$, where ω is any complex variable, that is

$$F_2(\omega) = \frac{1}{2\pi j} \int_{c_2 - j\infty}^{c_2 - j\infty} F_2(\omega)\, e^{t\omega} d\omega \qquad \ldots\ (8.2)$$

where c_2 is a real constant such that $\sigma a_2 < c_2$, and max $(\sigma_{a1}, \sigma_{a2}, \sigma_{a1} + \sigma_{a2}) < \sigma$ it follows that

$$F(s) = \int_o^\infty f_1(t) \cdot \frac{1}{2\pi j} \int_{c_2 - j\infty}^{c_2 + j\infty} F_2(\omega)\, e^{t\omega} d\omega e^{-st}\, dt$$

Integration is to be carried out first with respect to the complex variable ω and then with respect to t, but since the functions are Laplace transformable it is permissible to change the order of integration. Thus

$$F(s) = \frac{1}{2\pi j} \int_{c_2 - j\infty}^{c_2 + j\infty} F_2(\omega) \int_o^\infty f_1(t) \cdot e^{-(s - \omega)t}\, dt\, d\omega$$

subject to the same restriction as equation 8.2.

Since, by definition

$$\int_o^\infty f_1(t)\, e^{-(s - \omega)t}\, dt = F_1(s - \omega)$$

provided that $R_e(\omega) < \sigma - \sigma_{a1}$, it follows that

$$F(s) = L(f_1(t) \cdot f_2(t)) = \frac{1}{2\pi j} \int_{c_2 - j\infty}^{c_2 + j\infty} F_1(s - \omega)\, F_2(\omega)\, d\omega \qquad \ldots(8.3)$$

The process expressed by the integral 8.3 is called "Convolution in the Complex domain" or, more briefly, "Complex Convolution". The functions

$F_1(s)$ and $F_2(s)$ are said to be convolved. The theorem, as expressed by equation (8.3), states that the Laplace transform of the product of two functions of the real variable is found by convolving the Laplace transforms of these two functions. Thus multiplication in the real domain becomes complex convolution in the complex domain. The integral indicates folding, translation, multiplication and integration. In the complex ω plane, the function $F_1(\omega)$, and hence the geometric pattern of its singularities and zeros is first folded about the imaginary axis and then translated by the complex variable s. Since the translations are limited to those which keep $\sigma_{a2} < c_2 < \sigma - \sigma_{a1}$, the path of integration from $c_2 - j\infty$ to $c_2 + j\infty$ lies in an analytic strip.

The idea of complex convolution can be used in certain special forms which do not require complex integration. Generally there are two forms

a. A form in which at least one transform factor has first order poles only

b. A form in which at least one transform factor has multiple order poles.

Different forms of the transfer function expressions for a 2-phase servomotor will have poles which are functions of one of the mechanical time constant, the stator time constant or the rotor time constant. The poles are therefore of the first order, and only form 'a' above will be considered.

8.1.4 Forms of Complex Convolution utilized in establishing 2-phase servomotor transfer functions

In the general rational algebraic fraction of the form

$$F(s) = \frac{A(s)}{B(s)} \qquad \ldots\ (8.4)$$

let A(s) be a polynomial of the order p in s, and with constant nonzero coefficients. Similarly, let B(s) be another polynomial with constant nonzero coefficients of the order q, both p and q being positive integers. Generally there are two possible cases.

1. $p \geq q$ when $\frac{A(s)}{B(s)} = K_o + K_1 s + \frac{A_1(s)}{B(s)}$.

2. $p < q$ when F(s) is a proper fraction. Two cases may arise

   a. the poles of F(s) are all first order

   b. some or all of the poles may be of higher order.

All the transfer functions arising in this thesis fall into type 2(a).

The poles of equation(8.4) are found by putting B(s) = 0, and if the roots are $s_1, s_2, \ldots s_q$, then none are repeated. When $A(s_K) \neq 0$, for K = 1, 2, ... q, F(s) has q poles and not less. It may be shown that

$$L^{-1} \frac{A(s)}{B(s)} = \sum_{k=1}^{k=q} \frac{A(s_K)}{B'(s_K)} e^{s_K t} \quad 0 \leq t \quad \ldots\ (8.5)$$

where $B'(s_K) = \left| \frac{d}{ds} B(s) \right|_{s = s_K}$

$$= (s_K - s_1)(s_K - s_2) \ldots (s_K - s_{K-1})(s_K - s_{K+1}) \ldots (s_K - s_q)$$

and if one of the poles lies at the origin

$$L^{-1} \left(\frac{A(s)}{s\, B_1(s)} \right) = \frac{A(o)}{B_1(o)} + \sum_{K=2}^{K=q} \frac{A(s_K)}{s_K\, B_1'(s_K)} e^{s_K t} \qquad 0 \leq t$$

$$\ldots\ (8.6)$$

where $B_1'(s_k) = \left| \frac{dB_1(s)}{ds} \right|_{s = s_K}$

$$= (s_K - s_2) \ldots (s_K - s_{K-1}) (s_K - s_{K+1}) \cdots (s_K - s_q)$$

Finally, the complex convolution theorem that can be used if at least one transform factor has first-order poles only, can be stated as:

If $f_1(t)$ and $f_2(t)$ are Laplace transformable functions, having the Laplace transforms $F_1(s)$ and $F_2(s)$, respectively, and if $F_1(s) = \frac{A(s)}{B(s)}$ is a rational algebraic fraction having q first order poles and no others then

$$L\ (f_1(t).\ f_2(t)) = \sum_{k=1}^{k=q} \frac{A(s_K)}{B'(s_K)}\ F_2(s - s_K) \qquad \ldots\ (8.7)$$

APPENDIX 8.2 COMPUTER PROGRAMS

In this appendix, documentation is presented for the computation of

(a) the speed response following step changes in the control voltage, as presented in section (4.2.1), equation (4.35)

(b) the speed response following step changes in the phase angle, as described in section (4.3.1), equation (4.43) and section (5.8.1), equations (5.17), (5.18) and (5.19).

Appendix 8.2.a

PROGRAMME FOR THE SPEED RESPONSE FOLLOWING STEP CHANGES IN THE CONTROL VOLTAGE

T1= STATOR WINDINGS TIME CONSTANT AT STALL
T2= ROTOR TIME CONSTANT
TM= MECHANICAL TIME CONSTANT
OMEGA=ANGULAR SUPPLY FREQUENCY (RAD./SEC.)
VD=STEP CHANGE IN CONTROL VOLTAGE
J=H (GIVEN IN SECTION(4.2.1),EQUATION(4.27))
TMIN=MINIMUM TIME
TINC=TIME INCREMENT
TMAX=MAXIMUM TIME
OMEGAR= ROTOR SPEED IN R.P.M.

```
      MASTER MAIN
      REAL J
      DATA OMEGA/314.15926536/
    3 READ(1,900)VD,TM,T1,T2
      IF(TM.LE.0.0)GOTO4
      PI=4.0*ATAN(1.0)
      J=149.75/(T1*T1*T2*T2)
      OMEGA2=OMEGA*OMEGA
  900 FORMAT(4F10.6)
      A=(T1-T2)/(T1+T2)
      X1=2.0*A*OMEGA2*(2.0*((T1-TM)/(T1*T1*TM)+OMEGA2)-A*(T1
     1-2.0*TM)/(T1*TM))
      Y1=2.0*OMEGA*A*(2.0*OMEGA2*(T1-2.0*TM)/(T1*TM)+A*((T1-
     1TM)/(T1*T1*TM)+OMEGA2))
      A=-A
      X2=2.0*A*OMEGA2*(2.0*((T2-TM)/(T2*T2*TM)+OMEGA2)-A*(T2
     1-2.0*TM)/(T2*TM))
      Y2=2.0*OMEGA*A*(2.0*OMEGA2*(T2-2.0*TM)/(T2*TM)+A*((T2-
     1TM)/(T2*T2*TM)+OMEGA2))
      TTOT=T1+T2
      WRITE(2,901)
  901 FORMAT(1X,10X,14HRESULTS SO FAR)
      READ(1,903)TMIN,TINC,TMAX
  903 FORMAT(3F10.6)
      B=2.0*(1.0-OMEGA2*T1*T2)
      LAMDA=B-TTOT/T1
      LAMDAD=B-TTOT/T2
      C=B*TM*T2*T2*T1*T1/((1.0+OMEGA2*T1*T1)*(1.0+OMEGA2*T2*T2))
      D=((TM-T1)**2+OMEGA2*T1*T1*TM*TM)*((TM-T2)**2+OMEGA2*T
     12*T2*TM*TM)
      E=(B-(T1+T2)/TM)*T1*T1*T2*T2*TM**5
      D=E/D
      E=(X1*LAMDA-OMEGA*TTOT*Y1)
      F=(Y1*LAMDA+OMEGA*TTOT*X1)
      G=(X2*LAMDAD-OMEGA*TTOT*Y2)
```

```
      H=(Y2*LAMDAD*OMEGA*TTOT*X2)
      T=TMIN
    1 E=2.0/(X1*X1*Y1*Y1)*EXP((-1.0/T1*T))*(E*COS((OMEGA*T))
     1-F*SIN((OMEGA*T)))
      F=2.0/(X2*X2*Y2*Y2)*EXP((-1.0/T2*T))*(G*COS((OMEGA*T))
     1-H*SIN((OMEGA*T)))
      OMEGAR=VD*J*(C-D*EXP((-1.0/TM*T))+E+F)*60/(2.0*PI)
      WRITE(2,904)OMEGAR,T,VD,TM
  904 FORMAT(1X,10X,7HOMEGAR=,F12.4,5X,2HT=,F5.3,5X,3HVD=,
     1F5.1,3HTM=,F8.5)
      IF(T.GE.TMAX)GOTO3
      T=T+TINC
      GOTO1
    4 CONTINUE
      STOP
      END
      FINISH
```

Appendix 8.2.b

PROGRAMME FOR THE SPEED RESPONSE FOLLOWING STEP CHANGES IN THE PHASE ANGLE

```
T1= STATOR WINDINGS TIME CONSTANT AT STALL
T2= ROTOR TIME CONSTANT
TM= MECHANICAL TIME CONSTANT
J=H (GIVEN IN SECTION(4.2.1),EQUATION(4.27))
OMEGA=ANGULAR SUPPLY FREQUENCY (RAD./SEC.)
WI=INITIAL STEADY STATE SPEED
W= INITIAL PHASE ANGLE
A1 AND B1 ARE GIVEN IN SECTION (5.8.1)
TMIN=MINIMUM TIME
TINC=TIME INCREMENT
TMAX=MAXIMUM TIME
OMEGAR= ROTOR SPEED IN R.P.M.


      MASTER MAIN
      REAL J,K,L
      DATA OMEGA,VD/314.15926536,115.0/
    3 READ(1,900)A1,B1,W,TM,T1,T2,WI
      IF(TM.LE.0.0)GOTO4
  900 FORMAT(7F0.0)
      OMEGA2=OMEGA*OMEGA
      T1S=T1*T1
      T2S=T2*T2
      TMS=TM*TM
      PI=4.0*ATAN(1.0)
      J=149.75/(T1S*T2S)
      S=2.0*(T1+T2)*TM*T1S*T2S*OMEGA2
      P=TMS*T1S*T2S*(-T1*T2+TM*(T1+T2)-TMS*(3.0*OMEGA2*T1*T2
     1+1.0)+2.0*TMS*OMEGA2*(T1+T2)*TM)
      S1=(1.0+OMEGA2*T1S)*(1.0+OMEGA2*T2S)
      S2=S/S1
      A3=OMEGA2*(T1+T2)
      B3=OMEGA*(1.0-2.0*OMEGA2*T1*T2-T2/T1)
      B5=OMEGA*(1.0-2.0*OMEGA2*T1*T2-T1/T2)
      A=(T1-T2)/(T1+T2)
      X1=2.0*A*OMEGA2*(2.0*((T1-TM)/(T1*T1*TM)+OMEGA2)-A*(T1
     1-2.0*TM)/(T1*TM))
      Y1=2.0*OMEGA*A*(2.0*OMEGA2*(T1-2.0*TM)/(T1*TM)+A*((T1-
     1TM)/(T1S*TM)+OMEGA2))
      A=-A
      X2=2.0*A*OMEGA2*(2.0*((T2-TM)/(T2*T2*TM)+OMEGA2)-A*(T2
     1-2.0*TM)/(T2*TM))
      Y2=2.0*OMEGA*A*(2.0*OMEGA2*(T2-2.0*TM)/(T2*TM)+A*((T2-
     1TM)/(T2S*TM)+OMEGA2))
      TTOT=T1+T2
      B=2.0*(1-OMEGA2*T1*T2)
      LAMDA=B-TTOT/T1
```

```
      LAMDAD=B-TTOT/T2
      C=B*TM*T2S*T1S/((1.0+OMEGA2*T1S)*(1.0+OMEGA2*T2S))
      D=((TM-T1)**2+OMEGA2*T1S*TMS)*((TM-T2)**2+OMEGA2*T2S*TMS)
      E=(B-(T1+T2)/TM)*T1*T1*T2*T2*TM**5
      R=E/D
      E=(X1*LAMDA-OMEGA*TTOT*Y1)
      F=(Y1*LAMDA+OMEGA*TTOT*X1)
      G=(X2*LAMDAD-OMEGA*TTOT*Y2)
      H=(Y2*LAMDAD+OMEGA*TTOT*X2)
      WRITE(2,901)
  901 FORMAT(1X,10X,14HRESULTS SO FAR)
      READ(1,903)TMIN,TINC,TMAX
  903 FORMAT(3F10.6)
      T=TMIN
    1 E=2.0/(X1*X1+Y1*Y1)*EXP((-1.0/T1*T))*(E*COS((OMEGA*T))
     1-F*SIN((OMEGA*T)))
      F=2.0/(X2*X2+Y2*Y2)*EXP((-1.0/T2*T))*(G*COS((OMEGA*T))
     1-H*SIN((OMEGA*T)))
      Z1=(A3*X1+B3*Y1)/(X1*X1+Y1*Y1)*EXP((-1.0/T1*T))
      Z2=(A3*X2+B5*Y2)/(X2*X2+Y2*Y2)*EXP((-1.0/T2*T))
      Z3=(B3*X1-A3*Y1)/(X1*X1+Y1*Y1)*EXP((-1.0/T1*T))
      Z4=(B5*X2-A3*Y2)/(X2*X2+Y2*Y2)*EXP((-1.0/T2*T))
      K=2.0*(Z1+Z2)*COS((OMEGA*T))
      L=2.0*(Z3+Z4)*SIN((OMEGA*T))
      A6T=VD*J*(C-R*EXP((-1.0/TM*T))+E+F)*60/(2.0*PI)
      B6T=VD*J*(S2-P/D*EXP((-1.0/TM*T))+K+L)*60/(2.0*PI*OMEGA)
      OMEGAR=WI-(A1*A6T+B1*B6T)
      WRITE(2,904)OMEGAR,T,TM
  904 FORMAT(1X,10X,7HOMEGAR=,F12.4,5X,2HT=,F5.3,5X,3HTM=,F8.6)
      IF(T.GE.TMAX)GOTO3
      T=T+TINC
      GOTO1
    4 CONTINUE
      STOP
      END
      FINISH
```